Max Planck Institut für Molekulare Pflanzenphysiologie
Molecular Plant Nutrition Group

Characterization of Ammoniumtransporters in *Arabidopsis thaliana*

Dissertation
zur Erlangung des akademischen Grades
„doctor rerum naturalium“
(Dr. rer. nat.)
in der Wissenschaftsdiziplin „Molekulare Pflanzenphysiologie“

eingereicht an der
Mathematisch-Naturwissenschaftlichen Fakultät
der Universität Potsdam

von
Arne Schäfer

Potsdam, den 27.06. 2005

„Nicht Kunst und Wissenschaft allein,
Geduld will bei dem Werke sein.
Ein stiller Geist ist jahrelang geschäftig;
Die Zeit erst macht die feine Gärung kräftig.“

Goethe, Faust

Table of Contents

I. Introduction page

1. Nitrogen in the Biosphere 7
2. Chemical Properties of Ammonium 8
3. Sources of Ammonium for Plants 9
4. Physiology of Ammonium Assimilation 10
5. Ammonium Transporters 11
6. The structure of *E. coli* AmtB and the mechanism of transport 13
7. Aims of the Thesis 15

II. Material and Methods

II.1. Material

1.1. Enzymes, Chemicals and Equipment 16
1.2. *AMT* Gene Names and Idenfification Numbers 18
1.3. Synthetic Oligonucleotides 19
1.4. Plasmids 21
1.5. Bacterial Strains 21
1.6. *Arabidopsis thaliana* lines
1.6.1. Wildtype Variety 21
1.6.2. T-DNA Lines 22
1.6.3. RNAi-Lines 22
1.7. Media
1.7.1. Bacterial Growth Media 22
1.7.2. Plant Growth Media 23
1.8. Soils and Fertilizers
1.8.1. *Arabidposis*-soils 24
1.8.2. 10µM NH_4Cl – Fertilizer 24
1.9. Solutions and Buffers
1.9.1. LC Q-TOF Mass Spectrometry 25
1.9.2. GUS activity assay 25

II.2. Methods

2.1. DNA Manipulations and Analysis 26
2.1.1. Construction of the GATEWAY™ *AMT1.1*-RNAi Destination Vector 26
2.1.2. Cloning of the *AMT 1 and AMT2* Family Promoters into pUC19 27
2.2.3. Cloning of the *AMT 1 and AMT2* Family Promoters into pBI 101.3 27

2.2. Transformations
2.2.1. Transformation of Bacteria 28
2.2.2. Transformation of Plants 28

2.3. Transcript Analysis
2.3.1. Preparation of RNA for Reverse Transcription 28
2.3.2. Reverse Transcription 28
2.3.3. Determination of Transcript Levels 30

2.4. Cultivation of Plant Material
2.4.1. Growth in Sterile Liquid Medium 31
2.4.2. Growth on Soils 31
2.4.3. Hydroponic Growth 32
2.4.4. Growth on Sterile Solid Medium 32

2.5. Physiological Analysis
2.5.1. ^{14}C-Methylammonium Uptake Studies 32
2.5.2. Ammonium Uptake Studies 33
2.5.3. ^{15}N-Ammonium Uptake Studies 35
2.5.4. HPLC Measurements of Amino Acids 36
2.5.5. Histochemical Analysis of *AMT*-Promoter-GUS expression in plants 36

2.7. Morphological Characterization of Plants
2.7.1. Characterization of Root Growth 37
2.7.2. Characterization of Shoot Growth 37

2.8. Creation of Double Mutants 38

2.9. Segregation Analysis 39

III. Results

1. Sequence Analysis of Ammonium Transporters in *Arabidopsis thaliana* 40
2. Quantification of *AtAMT* Transcript Levels in *Arabidopsis thaliana*
2.1. *AtAMTs* Expression Patterns on Whole Plant Level 41
2.2. *AtAMTs* Expression Patterns in Roots, Shoots and Flowers 43

3. Spatial Expression Profiles of *AtAMT* Genes in *Arabidopsis thaliana*

3.1. *pAMT1.1-GUS* expression 46

3.2. *pAMT1.2-GUS* expression 48

3.3. *pAMT1.3-GUS* expression 49

3.4. *pAMT1.4-GUS* expression 50

3.5. *pAMT1.5-GUS* expression 51

3.6. *pAMT2.1-GUS* expression 52

4. Characterization of *AtAMT* –T-DNA Insertion Lines

4.1. Insertion Sites of the T-DNA into the *AtAMT* Genes 53

4.2. Developmental and Morphological Characterization of the T-DNA Lines 54

4.2.1. Root growth of *AMT* T-DNA Lines Under Different Nutritional Conditions 55

4.2.2. Inforescence Development of *AtAMT*-T-DNA Lines 58

4.3. Quantification of *AtAMT* Transcript Levels in *AtAMT* T-DNA Lines 60

4.4. ^{14}C-Methylammonia Uptake Kinetics of *AtAMT* T-DNA Lines 61

4.5. Creation of Doublemutants of the T-DNA Lines 62

5. Characterization of *AMT1.1*RNAi lines in *Arabidopsis thaliana* *64*

5.1. Creation of single insert *AtAMT1.1RNAi* Lines 66

5.2. Quantification of *AtAMT* Transcript Levels in *AtAMT1.1RNAi* T_2-Plants 69

5.3. ^{14}C-Methylammonium Uptake Kinetics of *AtAMT1.1*RNAi Lines

5.3.1. ^{14}C-MA uptake in *AtAMT1.1*-RNAi T_2-Plants 69

5.3.2. ^{14}C-MA and ^{15}N-NH_4^+ Uptake of Selected Single Insert Lines in the T_3 71

5.3.3. ^{14}C-MA Uptake of Selected Single Insert Lines in the T_4-Generation 72

5.3.4. Time Courses of MA Depletion at Various Concentrations 73

5.4. Quantification of *AtAMT* Transcript Levels in *AtAMT1.1RNAi* Lines 75

5.5. Ammonia Uptake Kinetics of *AtAMT1.1RNAi* Lines 77

5.6. Developmental and Morphological Characterization of *AtAMT1.1RNAi* Plants 79

IV. Discussion

Summary 82

1. Expression Analysis of *AtAMT* Genes in *Arabidopsis thaliana*

1.1. General Expression of *AMT* Genes in *Arabidopsis thaliana* 83

1.2. Specific Expression and Possible Physiological Roles of AMTs in Roots 84

1.3. Expression and Possible Physiological Roles of AMTs in Leaves 86

1.4. Expression and Possible Physiological Roles of AMTs in Flowers 89

2. Analysis of *AMT* T-DNA Insertion Lines

2.1. *AMT* T-DNA Insertion Lines: Initial Analysis 91

2.2. Effects of the T-DNA Integration on *AtAMT*-Gene Expression 93

2.3. Phenotypical and Developmental Effects of the *AMT*-T-DNA Integrations 93
2.4. ^{14}C-MA Uptake of the T-DNA Insertion Lines 94

3. Analysis of *AMT1.1*RNAi Lines 95
3.1. Quantification of *AtAMT* Transcript Levels in *AtAMT1.1RNAi* Lines 95
3.2. Analysis of Ammonium Uptake Kinetics of *AMT1.1RNAi* Lines 97
3.3. Growth Analysis of the *AtAMT1.1*RNAi Lines 98

References 101

Table of Abbreviations CXII

Appendix CXIII

I. Introduction

1. Nitrogen in the Biosphere

Nitrogen is an integral component of all plant and animal proteins and amino acids. In the atmosphere it is the predominant molecule (N_2) where it comprises over 78 %. Chemically, nitrogen is considerably inert which prevents plants from directly assimilating the ubiquitous element nitrogen from the air. Instead, plants rely entirely on nitrogen containing molecules such as nitrate and ammonia/ammonium which are assimilated directly from their environment (the term ammonium will be used to denote both, NH_3 and NH_4^+. The chemical symbols are only used for distinction when specifity is required.). These nitrogen components are deposited at relatively low concentrations in the soil and in water, and, since the demand for nitrogen during protein biosynthesis exedes any other mineral nutrient (Fried *et al*., 1965; Clarkson *et al*., 1986), the supply of this molecule is often growth limiting. Therefore, plants have evolved a number of different strategies to acquire nitrogen from their environment. These primarily include root systems that are developmentally plastic and can explore the soil for nitrogen, together with high and low affinity transporters for inorganic and organic nitrogen, which enable the root cells to take up nitrogen compounds from the soil. Additionally, specialists have evolved symbioses with N_2 fixing bacteria, that provide the plant with nitrogen in a process called nitrogen fixation.

The atmospherically abundant N_2 is incorported in various processes into compounds, which can be directly converted by the plants. Ammonium and nitrate are believed to be the principal sources of nitrogen for plants in most natural environments. Ammonium and nitrate are rarely available in equal amounts in the soil and their concentrations can vary over several orders of magnitude, from micromolar to hundreds of millimolar (Marschner, 1995). However, ammonium is the preferred form for root uptake due to the reduced state of the nitrogen whereas extra energy must be expended in reducing nitrate to ammonium before it can be incorporated into organic compounds (Bloom *et al*., 1999). However, because excess uptake of ammonium can also cause toxicity due to increased acidity, nitrate is simultaneously taken up with ammonium under normal conditions.

In the biosphere, nitrogen is primarily fixated by bacteria, either free-living or symbiotic. This process makes up 90 % of all naturally fixated molecular nitrogen. Minor contributions to the natural fixation of molecular nitrogen are provided by atmospheric reactions of O_2, N_2, and H_2 into HNO_3 catalysed by lightning (8 %) and photochemical reactions in the stratosphere that produce nitric oxide, NO (2 %). In total, the natural fixation of molecular nitrogen fixes 190 x 10^6 tonnes of nitrogen per year (Taiz and Zeiger, 1991). In comparison, worldwide industrial processes fix 87 x 10^6 tonnes of nitrogen per year (Tilman *et al*., 2001).

Molecular nitrogen is continuously taken from the air and passed back. The totality of these processes is called the nitrogen cycle. The organic nitrogen cycle (figure 1.) begins with the assimilation of nitrate and ammonium by plants and other autotrophes. In plants, mineral nitrogen is transported into the cytoplasm of the cells, where nitrate is enzymatically reduced into ammonium by Nitrate Reductase. Cytoplasmic ammonium, either derived from nitrate or imported directly from the soil, is subsequently incorporated into glutamine by Glutamine Synthetase and further into glutamate by Glutamate Synthase. Glutamate serves as amino donor for the

production of all other amino acids which serve as the building blocks for proteins. Via consumption of proteins or nucleic acids by other organisms, the nitrogen moves further through the nitrogen cycle.

The cycle is reversed by the excretion of $OC(NH_2)$ by animals, or upon the death of the organisms. During the decay of organic matter through microorganisms, proteins and nucleic acids are cleaved into aminonitrogen. The conversion of organic nitrogen into ammonium is called ammonification. The ammonium is either recycled as a nitrogen source by microorganisms and plants, or it can be oxidised via nitrite to nitrate in a process called nitrification which is performed by bacteria (primarily *Nitrosomonas* and *Nitrobacter*). In the form of nitrate, the nitrogen is completely oxidized. The further conversion of nitrate into molecular nitrogen is called denitrification.

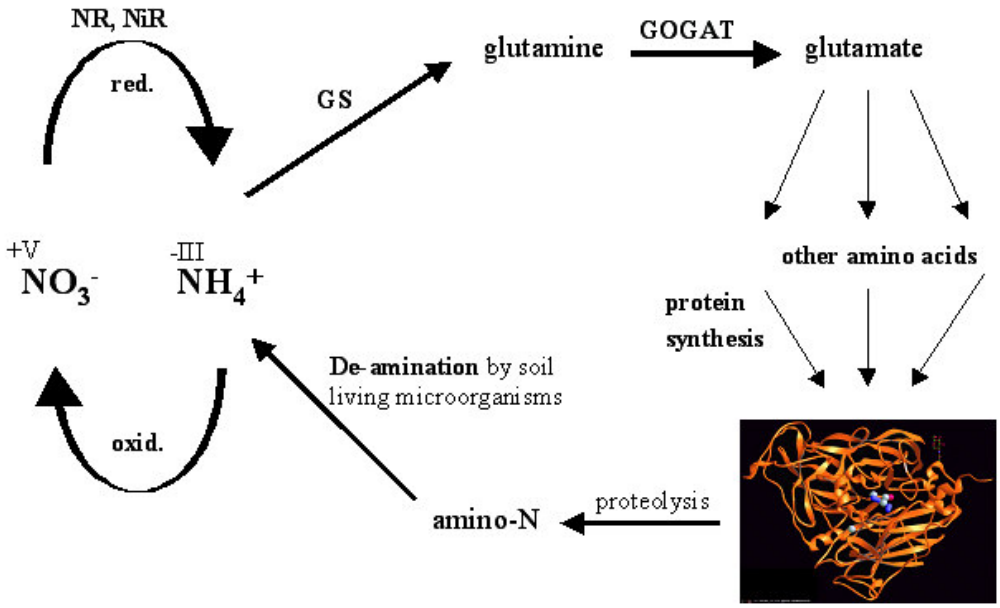

Fig. 1. Organic Nitrogen Cycle. Nitrate is reduced by Nitrate Reductase (NR) and Nitrite Reductase (NiR) to ammonium, which is incorporated into glutamine and glutamate via Glutamine Synthase (GS) and Glutamate Synthase (GOGAT), respectively. Glutamate is the origin for the synthesis of other amino acids which eventually form proteins. The proteins of decaying organic matter are proteolysed into amino acids which are deaminated to ammonium and, depending on environmental circumstances, can subsequently be oxidised into nitrate.

2. Chemical Properties of Ammonium

Ammonium in solution exists as an equilibrium between NH_3 and NH_4^+. NH_3 is a weak base, with a pKa of 9.25. Thus, at the neutral pH typical of the plant cell cytosol, approximately 99 % of ammonium is present in the cationic form NH_4^+ (Fig. 1.).

The neutral species NH_3 and H_20 have similar sizes and molecular dipole moments (1.47 D and 1.85 D). Both are able to form hydrogen bonds with other molecules. The cation NH_4^+ has a similar ionic radius to K^+ but is larger than H_3O^+, Li^+ and Na^+, and smaller than Cs^+ and Rb^+. The similarities between NH_4^+ and K^+, and between NH_3 and H_2O, as they relate to ammonium transport, will be discussed below (Section 4). Finally, the neutral molecule NH_3 dissolves much more readily in organic

solvents than its ionic counterpart, NH_4^+. Consequently, the permeability of NH_3 across lipid bilayers is three orders of magnitude greater than that of NH_4^+ (P.S. Nobel, 1983). Hence, whilst diffusion of NH_3 across the lipid portion of membranes is believed to be of biological significance, diffusion of NH_4^+ is not.

Ammonium is the preferred nitrogen source for plants instead of other mineral compounds because it is an immediate precursor for amino acid biosynthesis, and because no extra energy must be invested by the plants prior to amino acid biosynthesis as is required for the use of nitrate and nitrite

3. Sources of Ammonium for Plants

In nature, ammonium and nitrate are rarely available in equal amounts and ammonium concentrations are often 10 to 1000 times lower than those of nitrate in well-aerated soil (Marschner, *et al*. 1995). In general, the prevailing concentrations of ammonium and nitrate depend on different biotic and abiotic factors such as the microorganism composition, pH, and the water contents of the soil. Nitrate, in contrast to ammonium, is easily leached from the soil because it does not adhere to the negatively charged soil particles. Hence, ammonium plays an essential role in plant nutrition in waterlogged and acidic soils. If ammonium and nitrate are provided to plants at similar concentrations, ammonium is generally taken up more rapidly than nitrate (Macdu, *et al*. 1991). This preference for ammonium over nitrate is mainly explained by the extra energy the plant must expend in reducing nitrate to ammonium before it can be incorporated into organic compounds (Bloom, *et al*. 1992). Nonetheless, other imperatives such as the need to maintain pH homeostasis during nitrogen assimilation (Smith, *et al*. 1979) result in the simultaneous utilisation of ammonium and nitrate under normal conditions.

The soil and atmosphere are primary sources of ammonium for nitrogen assimilation, and ammonium uptake from the environment is faciliated by specific ammonium transporters in the plasma membrane of root and shoot cells, as describrd in more detail below.

In addition, large amounts of ammonium are produced in the mitochondria of leaves of C_3-plants during photorespiration. In fact, ammonium fluxes resulting from photorespiration can be 10 times higher than the net uptake of nitrogen from the soil (Stitt, 1999). Another source of ammonium in plants is the release of ammonium during biochemical processes such as protein catabolism, amino acid deamination and amino acid synthesis (e.g. methionine and isoleucine), and other more specific biosynthetic reactions such as the biosynthesis of lignin. The release of ammonium in these processes can be very high, especially during germination, senescence, and the break down of storage proteins. The ammonium released in these processes is assimilated into glutamine and glutamate as described above, and both of which can serve as long distance transport forms of nitrogen in plants (Lam *et al*., 1996).

Symbiotic nitrogen fixation is another important source of ammonium for some plant species. In fact, legumes and the few non-legumes that establish symbioses with nitrogen-fixing bacteria can obtain most, if not all of their nitrogen via reduction of molecular nitrogen to ammonium. Most of this ammonium is transferred to the plant cytoplasm where it is assimilated into glutamine (Ireland and Lea, 1999).

4. Physiology of Ammonium Assimilation

Biphasic uptake kinetics for ammonium in higher plant roots (Ireland and Lea, 1999; Ullrich *et al*., 1984; Wang *et al*., 1993; Mäck and Tischner, 1994) and leaves (J.R. Raven, G.D. Farquhardt, 1981) have shown that there are two distinct transport systems for ammonium: a high and a low-affinity system. The high-affinity transport system (HATS) in roots is predominant at low (submillimolar) external ammonium concentrations and is saturable. Estimations of the K_m-values for ammonium are typically below 100 µM (Wang *et al*., 1993; Kronzucker *et al*., 1996) The HATS is dependent on metabolism for its activity (Glass *et al*., 1997) and is regulated by the nitrogen status of the plants (Gazzarrini *et al*., 1999; Rawatt *et al*., 1999; Ryan and Walker, 1994; Kronzucker *et al*., 1998). In general, conditions of nitrogen deprivation lead to an increase of the HATS activity, while high concentrations of ammonium or its assimilation products (e.g. glutamine) lead to a repression of the HATS activity. Electrophysiological studies have shown that the substrate of the HATS is NH_4^+, and that the membrane electrical potential is the driving force for ammonium uptake at low concentrations of the ion (Walker *et al*., 1979; Ullrich *et al*., 1984; Wang *et al*., 1993; Ayling *et al*., 1993; Wang *et al*., 1994; Shelden *et al*. 2001).

The low-affinity ammonium transport system (LATS) becomes significant at high external ammonium concentrations (> 1mM). It exhibits a linear increase in activity in response to increases in ammonium concentrations and is non-saturable. Additionally, the LATS is expressed constitutively and is insensitive to nitrogen regulation (von Wiren *et al*., 1994). Despite the fact that it is much less sensitive to inhibition by membrane uncouplers, it was suggested that the LATS, like the HATS, may represent a broad-specifity cation channel that can transport NH_4^+ (White *et al*., 1996). However, this is not the case with the LATS in leaves, which appears to transport NH_3 by diffusion across the plasma membrane, as a consequence of pH changes (Kronzucker *et al*., 1996).

Ammonium that enters the cell through one of the described transport systems in the plasma membrane of root cells (Forde and Clarkson, 1999) and leaf cells (Yin *et al*., 1996) is assimilated either in the cytoplasm or in the plastids. Ammonium is incorporated into glutamine in a reaction catalysed by Glutamine Synthase (Figure 4.) present in the cytoplasm and the plastids (Glass *et al.*, 1997; Forde and Clarkson, 1999; Schjoerring *et al.*, 1999; Howitt and Udvardi, 2000; vonWiren *et al.*, 2000a). Although the GS has a cytoplasmic and plastidic form and both forms share a high affinity for ammonium, with a K_m ranging from 10 to 20 µM (Stewardt and Mann, 1980), the incorporation of ammonium into glutamine in roots appears to occur mainly via cytoplasmic GS, although the gene that encodes the plastidic GS is also expressed (Ireland and Lea, 1999).

In leaves, the chloroplastic isoenzyme is the predominant form and it appears to play an important role in the recovery of ammonium derived from photorespiration (Lamm *et al*., 1996) Glutamine is further processed in a reaction catalysed by the Glutamate Synthase (glutamate oxoglutatate aminotransferase-GOGAT) which converts glutamine plus α-ketoglutaric acid into two molecules of glutamate (Marschner *et al*., 1995; Lam *et al*., 1996).

In this context, it has been suggested that a second enzyme, Glutamate Dehydrogenase (GDH) which is present in mitochondria, may also play a role in ammonium assimilation, particularly for the recovery of ammonium obtained during photorespiration in leaf cells (Yamaha and Oaks, 1987). Although GDH has

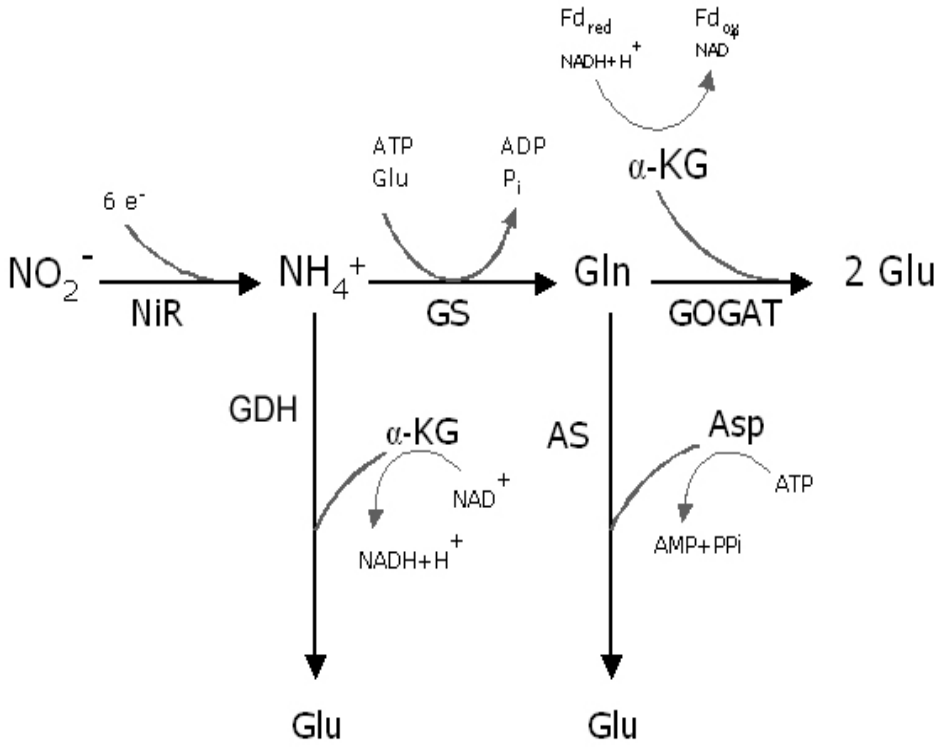

Fig. 4. Enzymatic pathways for the assimilation of inorganic nitrogen into organic compounds.NR-nitrate reductase, NiR-nitrate reductase, GDH-glutamate dehydrogenase, GOGAT-glutamine oxoglutarate aminotransferase, GS-glutamine synthetase, AS-asparagine synthetase.

a much lower affinity for ammonium than GS (Km 10-80 mM; Stewart *et al*. 1980), which argues against a role for GDH in ammonium assimilation in plants (Lam *et al*., 1996), the concentrations of ammonium in leaf cell mitochondria may be as high as 5 mM, which is sufficient for assimilation of ammonium into glutamate. However, recent research shows that direct assimilation of ammonium does not take place in mitochondria, and that most of the ammonium generated in mitochondria during photorespiration is transported to the chloroplasts where it is assimilated by GS. Strong support for this conclusion came from studies with photorespiratory mutants that lack plastidic GS and show the classic symptoms of N-starvation (Wallsgrove *et al*., 1987; Blackwell *et al*., 1988).

In addition to GS and GDH, Asparagine Synthase (AS) was proposed to be used in ammonium assimilation in plants. Although the normal substrate for AS is glutamine, it has been shown that at high concentrations, ammonium can also serve as substrate for AS (Lam *et al*., 2004)

5. Ammonium Transporters

The first ammonium transporters (AMT) to be isolated from any organism were two related high-affinity ammonium transporters from yeast (MEP1; Marini *et al*., 1994) and *Arabidopsis* (AMT1; Ninnemann *et al*., 1994). Related proteins have since been identified in bacteria (Siewe *et al*., 1996; Montesinos *et al*., 1998; Soupene *et al*., 1998), yeast (MEP2/MEP3; Marini *et al*., 1997, Lorentz and Heitmann,

1998), other higher plants like tomato, rice and soy bean (LeAMT1.1; Lauter *et al*., 1997), and animals (Marini *et al.,* 1994; Ninnemann *et al*., 1994).

Two related families of ammonium transporters have been identified and partially characterised in plants in *Arabidopsis*; the AMT1 and AMT2 family. The larger family, AMT1 includes five members, named At*AMT1.1* to At*AMT1.5*. all of which share more than 70 % identity with *AtAMT1.1* at the amino acid level (Howitt and Udvardi, 2000). Similar multigene families exist in other plant species, including tomato (Lauter *et al.*, 1996; von Wiren *et al.*, 2000b) *Lotus japonicus* (Simon-Rosin *et al*., 2003) and rice (von Wiren *et al.*, 1997).

The *AMT1* gene family encodes transporter proteins that are specific for ammonium and methylammonium as heterologous expression studies in yeast using *Arabidopsis* and tomato homologs have demonstrated (Gazzarini *et al*., 1999; von Wiren *et al*., 2000). All *AMT1* family members appear to be saturable, high-affinity ammonium transporters except for *AtAMT1.2* which exhibits in addition to a saturable, high-affinity component, a non-saturable component (Shelden *et al*., 2001).

The biochemical properties of AtAMT1.1 have been studied in yeast (Ninnemann, 1996). Yeast cells expressing AtAMT1.1 were able to take up the ammonium analogue ^{14}C-methylammonium (MA) in an energy-dependent manner. The K_m of ATAMT1.1 for MA is 65 WM and the uptake was competitively inhibited by ammonium with a Ki of 5-10 µM. Furthermore, AtAMT1.1 was found to be relatively specific for (methyl)ammonium over a wide range of concentrations, with other monovalent cations such as K^+ and Cs^+ having little effect on the uptake (Gazzarini *et al*., 1999). Recently, the kinetic properties of *Arabidopsis* AtAMT1.1, AtAMT1.2, and AtAMT1.3 were compared in yeast (Loque and van Wiren, 2004). The values for AtAMT1.1 were significantly lower than those reported earlier. Interestingly, the affinity of these transporters for ammonium ranged over two orders of magnitude. Despite these differences, it is likely that all AMT1 homologues share a similar transport mechanism, as discussed above. Similar to the situation in yeast, multiple AMT1 family members with different but complementary affinities in an

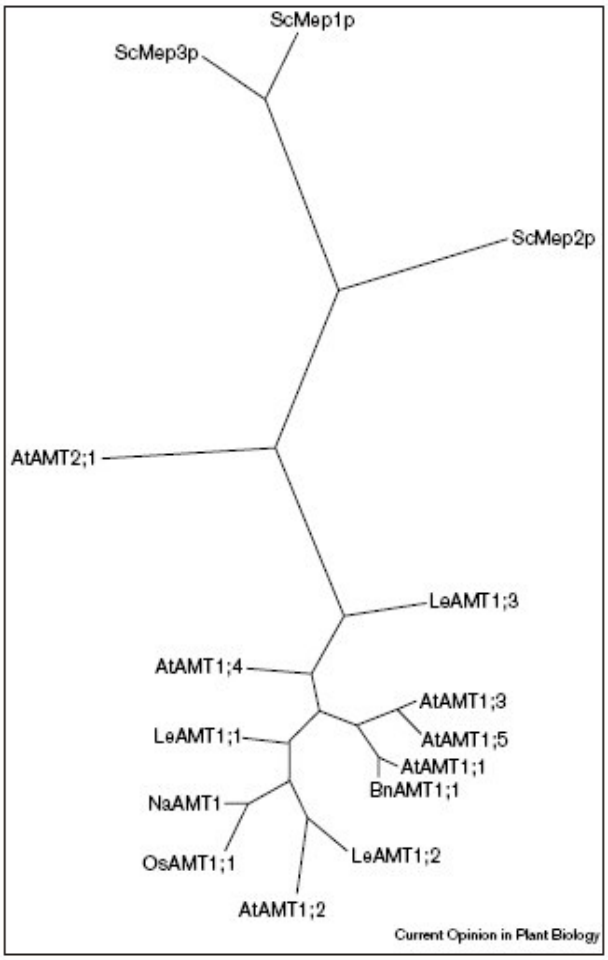

Fig. 5. Phylogenetic tree of ammonium transporters of the AMT/MEP gene family in yeast (*Saccharomyces cerevisiae* [*Sc*]) and plants (*Arabidopsis thaliana* [*At*], *Lycopersicon esculentum* [*Le*], *Oryza sativa* [*Os*], *Brassica napus* [*Bn*] and *Nepenthes alata* [*Na*]). Parsimony analysis and heuristic tree search was performed using PAUP 4d65 (Swofford, 1997) (taken from van Wiren. 2001).

organism may allow the organism to react appropriately to a wide range of ammonium concentrations in the environment.

AMT-GFP-fusion studies showed that ammonium transporters in *Arabidopsis* are located at the plasma membrane of plant cells where they presumably catalyse ammonium uptake from the apoplast (Simon-Rosin, 2001; Sohlenkamp, 2002).

The AMT1-family members are likely to to play complementary roles in ammonium uptake into roots (Gazzarrini *et al.*, 1999; von Wiren *et al.*, 2000b; Shelden *et al*., 2001) and expression of some *AtAMT1* genes in shoots also suggests that the encoded proteins are likely to play important roles there, although the nature of those roles have largely remained unknown (Ninnemann *et al*., 1994; Gazzarrini *et al*., 1999; Sohlenkamp *et al*., 2000).

The multiple forms of *AMT1* probably allow greater regulatory flexibility and organelle-, cell-, tissue- or organ- specialisation, in addition to enabling cells to take up NH_4^+ over a wide range of concentrations.

The *AtAMT2* family contains only one member, *AtAMT2.1* (Sohlenkamp *et al*., 2002). Sequencing projects have uncovered other members of the *AMT2* family in several plant species, including *Lotus japonicus* (Simon-Rosin *et al*., 2001), *Medicago truncatula*, and rice (*Oryza sativa*). AtAMT2.1 is a functional plant ammonium transporter but the amino acid sequence shares less than 25 % identity with AMT1 family proteins (Howitt and Udvardi *et al*., 2001). This transporter is more closely related to some bacterial ammonium transporters (Altschul *et al*., 1999), as shown in Figure 5. AtAMT2.1 is most probably located at the plasma membrane of the cells (Sohlenkamp *et al*., 2002). Like members of the AMT1 family, AtAMT2.1 is a high-affinity ammonium transporter, with a *K*m for NH_4^+ of approximately 15 to 25 µm, which is similar to AtAMT1.1. The V_{max}, however, is at least an order of magnitude less than that exhibited by AtAMT1.1 (Sohlenkamp *et al*., 2002). The form of ammonium transported by AtAMT2 is not clear but the *K*m for ammonium uptake at various pH indicates that NH_4^+ is likely to be the substrate instead of NH_3. One specific feature of AtAMT2.1 is that unlike the other ammonium transporters, AMT2.1 is unable to transport ^{14}C-MA (Sohlenkamp *et al*., 2000).

6. The structure of *E. coli* AmtB and the mechanism of transport

Although AMTs from all kingdoms have been functionally expressed and partially characterised in recent years, the transport mechanism and the identity of the substrate, NH_3 or NH_4^+, has remained unclear. Recent studies however, have now resolved the crystallographic structure of the bacterial inner membrane ammonia transport channel AmtB of *E. coli* (Khademi *et al*., 2004). These studies showed that the crystallised AmtB had the same structure in both, the absence and presence of ammonia, which suggests that AmtB is a channel rather than a transporter due to the lack of observation of flexible elements which would normally had to be involved in the translocation of the substrate.

Structural details of the AmtB ammonium transport channel were determined and showed that a trimer of channel-containing proteins span the membrane 11 times (Figure 6.). The 11 transmembrane-spanning α-helices (M1 to M11) were shown to form a right-handed helical bundle thus generating a vestibule on each surface around each channel. Residues from M1 and M6-M9 of one monomer were seen to interact with the first three helices of the neighbouring monomer.

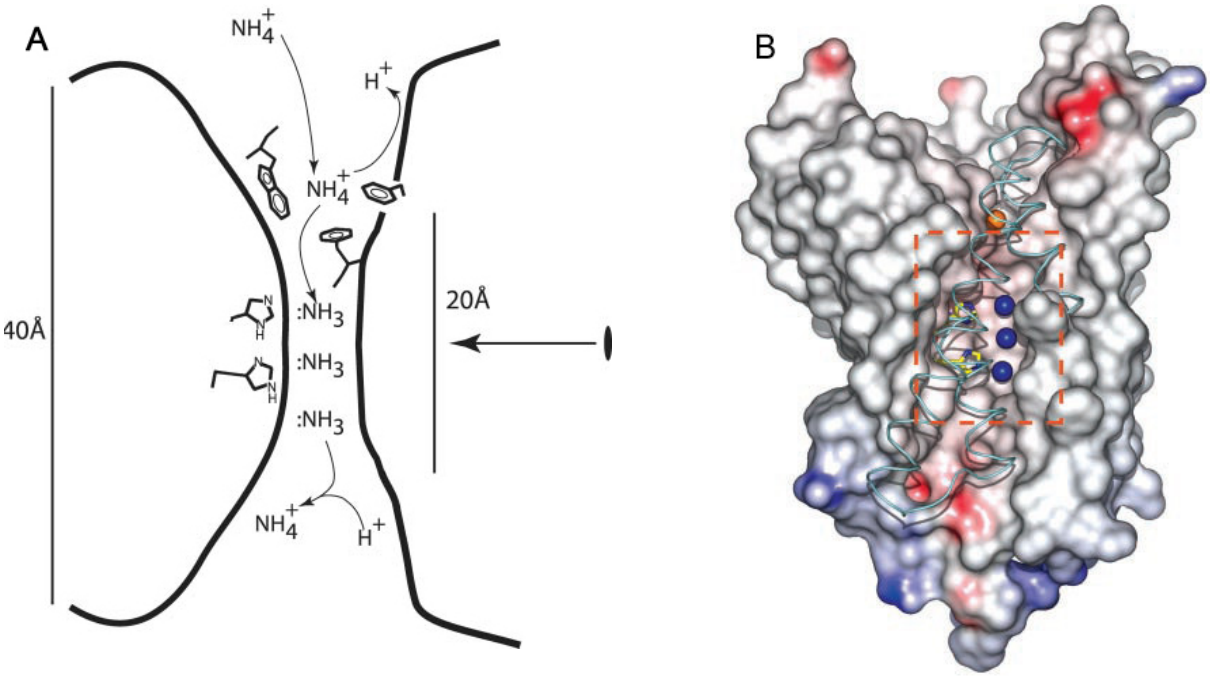

Fig. 6. The ammonia-conducting channel in AmtB. (**A**) Supposed mechanism of conductance. The low electron density for NH_3 may represent the substitutional interchange or relative freedom of NH_3 within the hydrophobic channel. NH_3 normally undergoes rapid inversion. (**B**) Three dimensional structure of AmtB. The surface of the lumen of the ammonia channel is colored according to electrostatic potential, after removal of the surface helices (whose helical backbones are indicated by the cyan line). Two narrow hydrophobic regions through the channel lie above and below the NH_3 positions (the zone within a dashed rectangle). The orange sphere represents an ammonium ion, the blue spheres represent ammonia ions (taken from Khademi *et al*., 2004).

At the extracellular side, the threefold axis is protected by three copies of M1 monomers that seal the central axis against passage. At the cytoplasmic side, the three M1 monomers are moved aside from the threefold axis, forming an open pocket together with the M6 monomer. The amino acid residues that line the pore of this outer vestibule stabilize ammonium.

The structure of the inside of the channel, mediated by the amino acid composition, eases the passage of electron acceptors, - NH_3 but not NH_4^+. NH_4^+ becomes less basic in the channel as it becomes progressively desolvated during passage, until it is deprotonated and becomes uncharged (the pK_a is lowered to below 6 and NH_4^+ gives up its proton leaving it predominantly on the side of entry.) Now the molecule is being transported in the form of NH_3. Cation-attracting amino acid residues (Phe, Tyr and Val) surround the cytoplasmic constriction and asparagine, acting as a helix cap close to where the exit approaching NH_3 reacquires a proton to become NH_4^+. Thus, after having left the narrow passage, the ammonia is able to return to equilibrium as ammonium in the widened inner vestibule of the cytoplasmic side of the pore. Apart from blocking the monovalent NH_4^+ ion, the narrow passage of the channel also prevents the monovalent K^+ ion from crossing the inner membrane. Thus, this study also deduced that AmtB is an ammonia channel which does not mediate the net transfer of protons and does not directly alter the membrane potential (Khademi *et al*., 2004.

7. Aims of the Thesis

Prior to this thesis, phylogenetic studies indicated the presence of six putative high-affinity transport systems (HATS) for NH_4^+ in *Arabidopsis* and the functions of several AMTs were investigated in yeast, bacteria, and higher plants. Furthermore, *AtAMT1.1* (Gazarrini *et al*. 1999, Glass and Kaiser 2002), *AtAMT1.3* (Gazzarrini *et al*. 1999) and *AtAMT2.1* (Sohlenkamp *et al*. 2002) were analysed by gene expression studies and biochemical studies of transport properties in mutants and heterologous expression systems prior to this thesis. However, these methods were not sufficient to assign precise physiological functions to the individual transporters and *AMT1.4* and *AMT1.5* had not been studied. Given this background, it was considered desirable to acquire a deeper knowledge of the physiological functions of the six *Arabidopsis* ammonium transporters and to create a link between the molecular biology of AtAMTs and the probable function of these proteins to transport ammonium in plants.

To this end, tissue specific expression profiles of the individual wildtype *AMT* genes should be acquired by quantitative real time PCR (qRT-PCR) and promoter-GUS expression. T-DNA insertional mutants of *AtAMT* genes should be isolated and the effects of the insertions on ammonium transport capacity and on possible growth phenotypes should be analysed. Further, double mutants of these plants should be created and studied. To supplement the data going to be obtained by these approaches, RNAi should be used to reduce the mRNA level of the whole *AtAMT1* gene family in parallel and to analyse the possible resulting effects on the capacity of ammonium transport. Pysiological and growth phenotypes of these lines should be analysed.

Thus, knowledge of the roles of high affinity ammonium transporters in plants should be broadened and the contributions of individual proteins to ammonium transport in *A. thaliana* should be elucidated to some extent.

II. Material and Methods

II.1. Material

1.1 Enzymes, chemicals, kits and equipment

Amersham Pharmacia Biotech, Little Chalfont, UK; RediPrime Random Labelling Kit

Applied Biosystems, Foster City, California, USA; SDS 5700 Real-Time PCR machine, 2x SYBR Green Master Mix, 96 well PCR plates optical grade

Bachofer, Reutlingen, Germany; Vakuumpumpe Vacumat 100

BD Biosciences Clonetech, California, USA; Advantage HF2 PCR-Kit

Beckmann Coulter Instruments Inc., Fullerton, USA; Avanti j30I centrifuge, LS 6500 Scintillation Counter, Ready Safe Liquid Scintillation Cocktail

Biometra, Göttingen, Germany: UNO II PCR machine

Bio-Rad, Richmond, USA; Gene Pulser II, ethidiumbromide, Smart Spec^{TM}, Chemi Doc

Boehringer Mannheim, Mannheim, Germany; Restriction endonucleases, T4 DNA ligase

Chromasolv, Riedel de Haen (SAF), Seelze, Germany; Ammonium acetate, acetic acid, acetonitrile

CIDtech Research Inc., Cambridge, Canada; 24-Epibrassinolide

CTC Analytics, Zwingen, Switzerland; HTS PAL autosampler

Duchefa, Haarlem, Netherlands; X-GlcA, Vitamins, 10x conc., Murashige & Skoog Medium 6-Benzylaminopurine, Kinetin, Indole-3-acetic acid, jasmonic acid, abscisic acid, gibberellic acid

Eppendorf, Hamburg, Germany; Microcentrifuges 5417, 5417C; 5417R, Pipettes, Thermomicer 5436, vacuum concentrator 5301

Eurogentec, 96 well qPCR Natural Plates with Caps, Smart DNA-ladder

Flux Instruments AB, Karlskoga, Sweden; Rheos 2000 pump

GFL, Wunstorf, Germany, Schüttler 3005

Heidolph, Kelheim, Germany; Mixer RZR1

Hoechst, Frankfurt a.M., Germany; BASTA

Hoefer Scientific Instruments, San Francisco, USA; vacuum container XR-1000

ICN, Irvine, USA; α-^{32}P-dCTP,

Kodak Eastman, Rochester, USA; developer, fixative, X-OMAT-AR films

Kontron Instruments, Watford herts, UK; HPLC Pump 422, HPLC Autosampler 465, SFM25

Invitrogen, Paisley, UK; Topo TA Cloning Kit, 50 bp DNA ladder, 1 kb DNA ladder, Trizol, oligonucleotides, Superscript III RNAse H$^-$, Taq DNA Polymerase

Leica, Heidelberg, Germany; Leica MZ 125

Machery-Nagel, Düren, Germany; Porablot NY amp nylon membranes, Porablot NY amp Plus nylon membranes, Nucleospin extraction columns, Nucleobond AX plasmid purification kit

Merck, Darmstadt, Germany; other chemicals

NEN life science products, Boston, USA; ^{14}Methylammoniumchloride,

New England Biolabs, Beverly, USA; Restriction endonucleases

PolyLC Inc., MA, USA; PolyHYDROXYETYL columns

Qiagen, Hilden, Germany; Qiaquick Gel Extraction Kit

Retsch Technology GmbH, Haan, Germany; Retsch mill MM200

Roth, Karlsruhe, Germany; Phenol-Chloroform

Sartorius AG, Göttingen, Germany; Waage BP1L1S

Sigma Chemical Company, St. Louis, USA; Methylammonium, DNAse I, DEPC,

Antibiotics, IPTG, X-gal

Stratagene, Heidelberg, Germany; *Pfu* DNA polymerase, UV-crosslinker

Syngenta U.S. Corporate - Torrey Mesa Research Institute, San Diego, USA; Biological Material (T-DNA Insertion Lines (Sy.-*AMT*s)

ThermoFinnigan, San Jose, CA, USA; Finnigan LCQ DECA mass spectrometer, Xcalibur software version 1.3

TIB Molbiol, Berlin, Germany; oligonucleotides

Whatman, Maidstone, UK, Glass Microfiber Filter

1.2. *AMT* Gene Names and Identification Numbers

Table 1.2 *AMT* gene identification informations

Gene	Description	Gene ID-number	gi-number
AMT1.1	*Arabidopsis thaliana* ammonium transporter 1, member 1	At4g13510	gi|30682507|
AMT1.2	*Arabidopsis thaliana* ammonium transporter 1, member 2	At1g64780	gi|30697099
AMT1.3	*Arabidopsis thaliana* ammonium transporter 1, member 3	At3g24300	gi|30687442
AMT1.4	*Arabidopsis thaliana* ammonium transporter, putative	At4g28700	gi|18417246
AMT1.5	*Arabidopsis thaliana* ammonium transporter, putative	At3g24290	gi|822017
AMT2.1	*Arabidopsis thaliana* ammonium transporter 2	At2g38290	gi|42571120

1.3 Synthetic Oligonucleotides

For screening of the Syngenta T-DNA insertion lines for homozygosity the following oligonucleotides were used:

Syngenta T-DNA insertion line *AMT 1.1*
oAMT 1.1 fwd: 5' CTg AAC ACACAg ATC TTA TCT TCA CCg A 3'
oAMT 1.1 rev: 5' gCA TTA ggA CCC AAC Agg AC

Syngenta T-DNA insertion line *AMT 1.2*
oAMT 1.2 fwd: 5' AgT ACC gCA ACT TTT TgT gAT gTA ACG 3'
oAMT 1.2 rev: 5' ggC ATA AgT TgT gTC ggA gAg TTT gT 3'

Syngenta T-DNA insertion line *AMT 1.4*
oAMT 1.4 fwd: 5' ATG AgC AgT AAg TAC gTT TAA ggA ggA gA 3'
oAMT 1.4 rev: 5' TCA gAg gCA gAg CAA gAg AgA g 3'

Syngenta T-DNA insertion line *AMT 2.1*
oAMT 2.1 fwd: 5' ACC TVCg AAg ACT TTT CTC CAT CAA AA 3'
oAMT 2.1 rev: 5' CTg gCA TAC TCT gTA gAC CAA CCA gA 3'

For the determination of mRNA cDNA level using quantitative real-time PCR (qRT-PCR) the following oligonucleotides were used:

oAMT 1.1 fwd: 5'gCT TAg gAg AgT TgA gCC ACg 3'
oAMT 1.1 rev: 5' CAA ATC AAA CCg gAg TAg gTg 3'

oAMT 1.2 fwd: 5' ATg gAg gAT TTg CTT ACg CA 3'
oAMT 1.2 rev: 5' CCA Tgg TTT AgT CgA CAC gTC g 3'

oAMT 1.3 fwd: 5' TCA Cgg Tgg CTT TgC TTA T 3'
oAMT 1.3 rev: 5' CCA ggA TCC ACT CTA TgA gA 3'

oAMT 1.4 fwd: 5' Tgg TgA TAA TgA TCC CAA TgT Ag 3'
oAMT 1.4 rev: 5' gCA AAA gCT ACg AAA gAg TA 3'

oAMT 1.5 fwd: 5' TgA TgA TTC CAT Tgg AgT gCC T 3'
oAMT 1.5 rev: 5' CTT gAA AAT CAA ACg gCT gg 3'

oAMT 2.1 fwd: 5' CCA AAA CgC AgA GAT CAg g 3'
oAMT 2.1 rev: 5' ggT ggA TgA TAC ATT AgC ggT 3'

For reverse transcription of mRNA into cDNA, a primer designed to anneal at the polyA terminus of mRNA was used:

odT: 5’ TTT TTT TTT TTT TTT TTT 3’

For standardisation of transcript levels of the various *AMT*-genes the following oligonucleotides were used:

oUBIQ-10 fwd: 5’ CAC ACT CCA CTT ggT CTT gCg T 3’
oUBIQ-10 rev: 5’ Tgg TCT TTC Cgg TgA gAg TCT TCA 3’

oELFα fwd: 5’ TgA gCA CgC TCT TCT TgC TTT CA 3’
oELFα rev: 5’ ggT ggT ggC ATC CAT CTT gTT ACA 3’

For the PCR amplification of the promoters of the different ammonium transporters the following oligonucleotides were used:

oAMT 1.1 fwd: 5’ Acg TCT gCA gTT TCT TCA ATC ACA ATT gCA TG 3’
oAMT 1.1 rev: 5’ Acg TCC Cgg gTT gAg AgT TTA gAg AAg AAg ATg 3’

oAMT 1.2 fwd: 5’ ACg TCT gCA gTT TAT TCT CTA ATA CgT AgT gC 3’
oAMT 1.2 rev: 5’ ACg TCC Cgg gTg gAg Agg gAg ggA ggg AgA g 3’

oAMT 1.3 fwd: 5’ ACg TCT gCA gAT ggC TTg gCA CAA ACT gAg Ag 3’
oAMT 1.3 rev: 5’ ACg TCC Cgg ggT TTg AgA gAg CTg AgA gAg AgA AAg 3’

oAMT 1.4 fwd: 5’ ACg TCT gCA gTg TAg ATA TCC TAA CAT AAT TgT Ag 3’
oAMT 1.4 rev: 5’ ACg TCC Cgg gTg TTg CAA AgA TTA AgA gAg ATT TTg 3’

oAMT 1.5 fwd: 5’ ACg TCT gCA gTA TTC TCC TTC gTA CgT ATA TAT TC 3’
oAMT 1.5 rev: 5’ ACg TCC Cgg gTT TTA gAg ACT TgA gAg Agg AAC CAC 3’

oAMT 2.1 fwd: 5’ ACg TCT gCA gAA CAT gAA TCT TAT TgA ATC TCT AA 3’
oAMT 2.1 rev: 5’ ACg TCC Cgg gTT TgT TAT TCT ATC TTT CCC ggA g 3’

1.4. Plasmids

Table 1.4 Plasmid names, references and characteristics

Plasmid	Reference	Features	Length
pJawohl8-RNAi	B. Ülker, V. Lipka, Th. Rademacher, I. Somssich; MPI für Züchtungsforschung, Köln	GATEWAY™ compatible binary vector for gene silencing in plants Ampicillin, Carbenicillin, Kanamycin, Gentamycin resistance	9.016 kb
pUC19	Yanisch-Perron *et al*. 1985	*E. coli* transformation vector LacZα gene, Ampicillin resistance	3.9 kb
pBI 101.3	Jefferson *et al*., 1987 Bevan, 1984	Binary plant transformation vector for GUS expression in the backbone of pBIN19, Kanamycin resistance	12 kb

1.5. Bacterial Strains

Table 1.5. Bacterial strains and references

Bacteria	Strains	Reference
Escherichia coli	DH5α sup E44 ΔlacU169 (φ80lacZΔ)	Gibco-BRL, Gaithersburg, USA; unpublished
Agrobacterium tumefaciens	GV3101.pMP90	Koncz and Schell, 1986

1.6 *Arabidopsis thaliana* lines

1.6.1 Wildtype varieties

For WT controls in all experiments *Col-0* was used.

1.6.2. T-DNA Insertion Lines

Table 1.6.2. T-DNA lines, transformation vectors, accession and identification numbers and gene annotations

Garlic Seed Line	binary vector used for transformation	GenBank Accession Number	AGI number	Annotation	Name
garlic 283 E12.b.1a.LB3Fa	CSA 110	AL161536.2	At4g13510	AtAMT1.1	Sy-AMT1.1
garlic 97 E09.b.1a.Lb3Fa	CSA 110	AF110771	At1g64780	AtAMT1.2	Sy-AMT1.2
garlic 628 E08.b.1a.Lb3Fa	pDAP101	AI035353.1	At4g28700	AtAMT1.4	Sy-AMT1.4
garlic 1233 E 06.b.1a.Lb3Fa	pDAP101	AF182039	At2g38290	AtAMT2.1	Sy-AMT2.1
garlic 422 Ao6.b.1a.Lb3Fa	CSA 110	AF182039	At2g38290	AtAMT2.1	not used

The genetic background of the T-DNA insertion lines was *A. thaliana* var. *Col-0*.

1.6.3 RNAi-Lines

The RNAi construct was transformed into the genetic background of *A. thaliana* var. *Col-0*.

1.7 Media

1.7.1 Bacterial growth media

Escherichia coli was grown in/on LB media (Sambrook *et a*l., 1989).

For transformation experiments *E. coli* was grown in SOC Media.

Agrobacterium tumefaciens was grown in YEB medium (Vervliet *et al*., 1975), for growth on solid media 1.5 % agar was added.

1.7.1. Components of Growth Media

LB-Medium	SOC-Medium	YEB-Medium
2 % Bactotryptone	2 % Bactotryptone	0.5 % Bactotryptone
0.5 % Yeast extract	0.5 % Yeast extract	0.1 % Yeast extract
10 mM NaCl	10 mM NaCl	0.1 % Bacto-pepton
1.5 % Agar (for plates)	2.5 mM KCl	0.5 % sucrose
	10 mM MgCl2	2 % $MgSO_4$
	10 mM MgSO4	50 mM $MgCl_2$
	1.5 % Agar (for plates)	
	20 mM Glucose	

Antibiotics were added in the following concentrations:

Kanamycin: 50 µg/ml

Ampicillin: 100 µg/ml

Rifampicin: 100 µg/ml
Gentamycin: 125 µg/ml

For the screening of transformed colonies for the disruption of the LacZα reading frame IPTG and X-gal was added in the following concentrations:
IPTG: 100mg/ml
X-gal: 40mg/ml

1.7.2. Plant growth media

1.7.2.1 Solid Sterile Culture Medium

Table 1.7.2.1. Solid Sterile Culture Medium Components

Concentrations of compounds	Makros	Mikros	Additives
5.0 % Makros	0.88 % $CaCl_2$	0.124 % Boric Acid	Fe-EDTA (20mM): 7.46g/l
0.5 % Mikros	0.74 % $MgSO_4$	0.338 % ManganII-sulfate-Monohydrate	Titriplex III 5.57 g/l FeII-sulfate-heptahydrate
0.5 % Vitamines (1:1000)	Heptahydrat		
0.5 % 20M Fe-EDTA	0.34 % H_2PO_4	0.0166 % Kaliumjodid	
0.2 % MES	2.8 %KCl (0,38M)		Vitamines:
2.0 % saccharose		0.005 % Molybdic Acid	0.1 g/l Nicotinic Acid
0.6 % agar			0.1 g/l Pyrodoxine
		0.0005% Copper(II)-sulfate-pentahydrate	0.02 g/l Thiamine
pH 5.7 – 5.8			20 g/l myo-Inosite
		0.0005 % Cobaltchloride	

For the selection of *Agrobacterium* transformed plants, seedlings were germinated on MS-medium (Murashige and Skoog, 1962), containing 1 % sucrose and 0.8% agar.
Antibiotics were added at the following concentration:
Kanamycin: 50 µg/ml

1.7.2.2 Liquid Sterile Culture Medium

1.7.2.2.1. Liquid Sterile Culture Medium Components

Concentrations of compounds	Oligoelements (2500x)	Additives (after autoclaving)
1 mM KNO3	2g NaFeEDTA	1x Gambourg Vitamines (1000x)
0,5 mM NH4Cl	150 mM H3BO3	1 mM Glutamine
3.5 mM KCl	35 mM MnSO4	
3 mM K_2HPO_4 (pH5.7)	2.5 mM ZnSO4	
4 mM K_2SO_4	1.5 mM CuSO4	
4 mM $CaCl_2$	1 mM NiSO4	
1 mM $MgSO_4$	0.75 mM HMoO4	
3 mM MESS	50µM CoCl2	
1x oligoelements (2500x)		
0.5% sucrose		

For no Nitrogen containing media, KNO_3, NH_4Cl and Glutamine were omitted.

1.7.2.2.2. Hydroponic Culture Medium

Tab. 1.7.2.2.2. Hydroponic Culture Medium Components

Concentrations of compounds	Oligoelements (2500x)	Additives (after autoclaving)
72µM FeEDTA	150 mM H3BO3	1x Gambourg Vitamines (1000x)
1,25 mM KNO3	35 mM MnSO4	1 mM Glutamine
0,5 mM NH4Cl	2.5 mM ZnSO4	
3.5 mM KCl	1.5 mM CuSO4	
0,5 mM K_2HPO_4 (pH5.7)	1 mM NiSO4	
4 mM K_2SO_4	0.75 mM HMoO4	
1,25 mM Ca $(NO_3)_2$	50µM CoCl2	
1 mM $MgSO_4$		
1000x micros		
1x oligoelements (2500x)		
0.5% sucrose		

1.8. Soils and Fertilizers

1.8.1. *Arabidposis*-soils

Soil containing all nutrients: GS 90 soil : Vermiculit (1:1volume ratio)

Nutrient deprived soil: type-0 (Einheitserde®, Werkverband e.V.)

1.8.2. 10µM NH_4Cl – Fertilizer

For plant culturing on nutrient deprived soils the following nitrogen-free fertilizer was used:

KCl	0.50 mM
KH_2PO_4	0.25 mM
K_2HPO_4	0.25 mM
$MgSO_4$	1.00 mM
Fe EDTA	0.05 mM
Trace Elements	0.50 mM
$CaCl_2$	0.50 mM

adjusted to 10 µM NH_4Cl

1.9. Solutions and Buffers

1.9.1. LC Q-TOF Mass Spectrometry:

Pre-mix: 30 µl Ribitol* (0.2 mg/ml; dissolved in 100% Methanol)
30 µl d4-Alanine (1mg/ml dissolved in water dest.)
30 µl isoascorbate (0.5 mg/ml dissolved in water dest.)
quantitative internal standard for the polar phase

1.9.2 GUS activity assay:

GUS - Staining Buffer: 50 mM sodium phosphate buffer, pH 7.2
10 mM EDTA
Triton X-100, 0.1 %
Tween 20, 0.1 %
210 mg/l $K_4(Fe(CN)_6) \times 3H_20$
166 mg/l $K_3(Fe(CN)_6)$
0.5 mg/ml X-Gluc

II.2. Methods

2.1. DNA Manipulations and Analysis

Standard DNA manipulations like plasmid mini preparation, restriction digestions and gel electrophoresis were performed as described in Sambrook *et al*. (1989).

DNA sequencing was performed by AGOWA (Berlin, Germany) using Big Dye™ chemistry on a Perkin Elmer ABI 377 HT sequencer.

2.1.1. Construction of the GATEWAY™ *AMT1.1*-RNAi Destination Vector

The GATEWAY™ conversion technology (Invitrogen, Gaithersburg, USA) is based on the site-specific recombination reaction mediated by phage λ. By this technology, DNA fragments flanked by recombination sites (*att*) can be transferred into vectors that contain compatible recombination sites (*att*B x *att*P or *att*L x *att*R) in a reaction mediated by the GATEWAY™ BP Clonase™ Enzyme Mix. These Entry Clones, which can be considered as donor plasmids, are made by recombining the DNA fragment of interest containing the flanking *att*B sites into the *att*P site pDONR201, in a reaction mediated by the GATEWAY™ BP Clonase™ Enzyme Mix. Subsequently, the fragment in the entry clone can be transferred to a destination vector that contains the *att*R sites by mixing both plasmids and by using the GATEWAY™ LR Clonase™ Enzyme Mix (Depicker A., 2002; GibcoBRL GATEWAY™ Cloning Technology, Instruction Manual; 1999-2001 Invitrogen Corporation).

To make the RNAi-silencing cassette, the *AMT 1.1*cDNA (bp1-800 of the 5'end) was flanked with the *att*-sites in sense and anitsense orientation in the course of a PCR reaction with attB-modified GATEWAY primers (GibcoBRL® Life Technologies, 2002).

The attB-flanked PCR products (the attB Expression Clone) were transferred in the BP Reaction in the attL-flanked Entry Clone through a recombination reaction with the Donor Vector (pDONR™; GibcoBRL®), mediated by the BP Clonase Enzyme Mix (Figure 2.1.1).

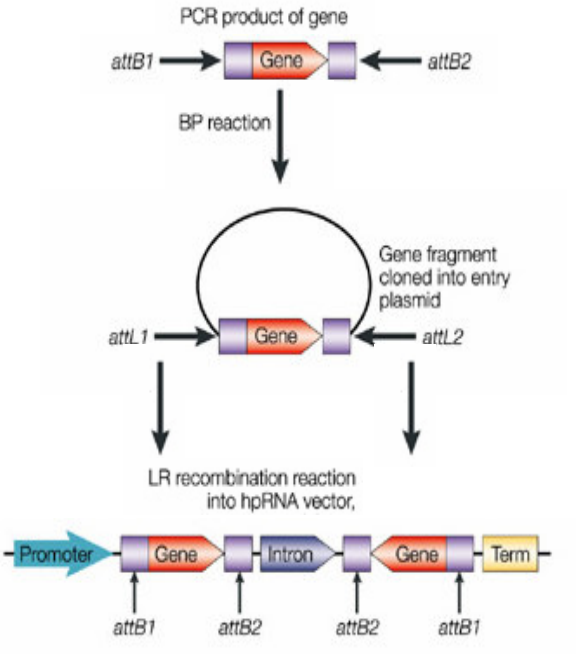

Fig. 2.1.1 Construction of a GATEWAY™ hpRNA destination vector for RNAi (picture taken from Waterhouse and Helliwell, 2003; slightly modified).

The resulting Entry Plasmid contained the *AMT 1.1*cDNA. To create the pJawohl13-RNAi destination vector with the hpRNAi *AtAMT1.1* fragment, the *AMT 1.1*cDNA was cut at both sides by the recombination enyzmes within the attL sites of the Entry Vector in the course of the LR recombination reaction. Subsequently, it was ligated to the corresponding attR site in the Destination Vector. The result was the expression vector for the hpRNAi *AtAMT1.1* construct (For comprehensive details of the reaction protocols and of the components of the used reaction mixes and chemicals see the Instruction Manual of the GATEWAY™ Cloning Technology; GibcoBRL®, Life Technologies, 2002).

2.1.2 Cloning of the *AMT1 and AMT2* Family Promoters into pUC19 vector

PCR using the proof reading *Pfu* polymerase was employed to amplify bp –1 to –1000 of each promoter. For the PCR reactions the respective oligonucleotides given in 2.1.3 were used as primers.

Table 2.1.2 PCR program for the amplification of the promoter fragments

step	time (seconds)	temperature (˚C)
1	180	95
2	60	95
3	60	55
4*	60	72
5	180	72

* step 2 to 4 were repeated 29 times.

The PCR products were purifid and cloned into pUC19 using the restricition sites of SmaI and Pst I in PUC19. Positive clones were selected by ampicillin resistance.

2.1.3 Cloning of the *AMT 1 and AMT2* Family Promoters into pBI101.3

For the cloning of the *AMT* promoters into pBI101.3 the restriction enzymes given in Table 2.1.3 were used. Positive clones were selected on Kanamycin. Clones with correct orientation were selected using the restriction enzymes given in Table 2.1.4.

Table 2.1.3 Restriction enzymes used for the cloning of *AMT* promoters into pBI101.3

AMT1.1	***AMT1.2***	***AMT1.3***	***AMT1.4***	***AMT1.5***	***AMT2.1***
Sma I	Sma I	Sma I	Sma I	Sma I	Sma I
PstI	HindIII	HindIII	HindIII	HindIII	PstI

Table 2.1.4 Restriction enzymes used for screening of the correct orientation of the promoters

AMT1.1	*AMT1.2*	*AMT1.3*	*AMT1.4*	*AMT1.5*	*AMT2.1*
	EcoRI	EcoRI	EcoRI	EcoRI	
HindIII	HindIII	HindIII	HindIII	HindIII	HindIII

2.2. Transformations

2.2.1. Transformation of Bacteria

Escherichia coli was transformed as described in Hanahn (1983).

Agrobacterium tumefaciens was transformed by elecroporation, according to the suppliers instructions (Gene Pulser II, Bio-Rad; Richmond, USA).

2.2.2. Transformation of Plants

Arabidopsis thaliana was transformed using *Agrobacterium tumefaciens*-mediated gene tranfer. A floral dip method was used as described in Clough *et al*. (1998).

2.3. Transcript Analysis

2.3.1 Preparation of RNA for Reverse Transcription

Total RNA was isolated from plant tissues using the Trizol™ RNA Extraction Protocol (Life Technologies; Rockville, USA). To test the quality of the extracted RNA it was run on a 1% agarose TBE gel at 90V for 20min (Figure 2.3.a). Subsequently, the RNA concentration of each sample was determined by comparison to a known amount of RNA (using Smart®-ladder) and by spectrometry (A260/A280 OD>1.8±0.2).

To remove residual genomic DNA the RNA was DNAse I treated according to the suppliers instructions (Invitrogen). Subsequently the DNAse I-treated RNA was purified of residual enzymes and nucleotides, precipitated and tested by PCR for the complete removal of genomic DNA (Figure 2.3.b).

The quality and the concentration of the RNA was again estimated on 1% agarose TBE gels run with Smart®-ladder (Figure 2.3.c).

2.3.2. Reverse Transcription

The pur genomic RNA was transcribed into cDNA using Superscript III RNAse H^- according to the suppliers instructions (Invitrogen). For priming, oligo dT-primers were used. To test the cDNA, a PCR was run with cDNA templates and the RT-PCR-Primers on the RT-PCR programme (Table 2.3.1; Figure 2.3.d).

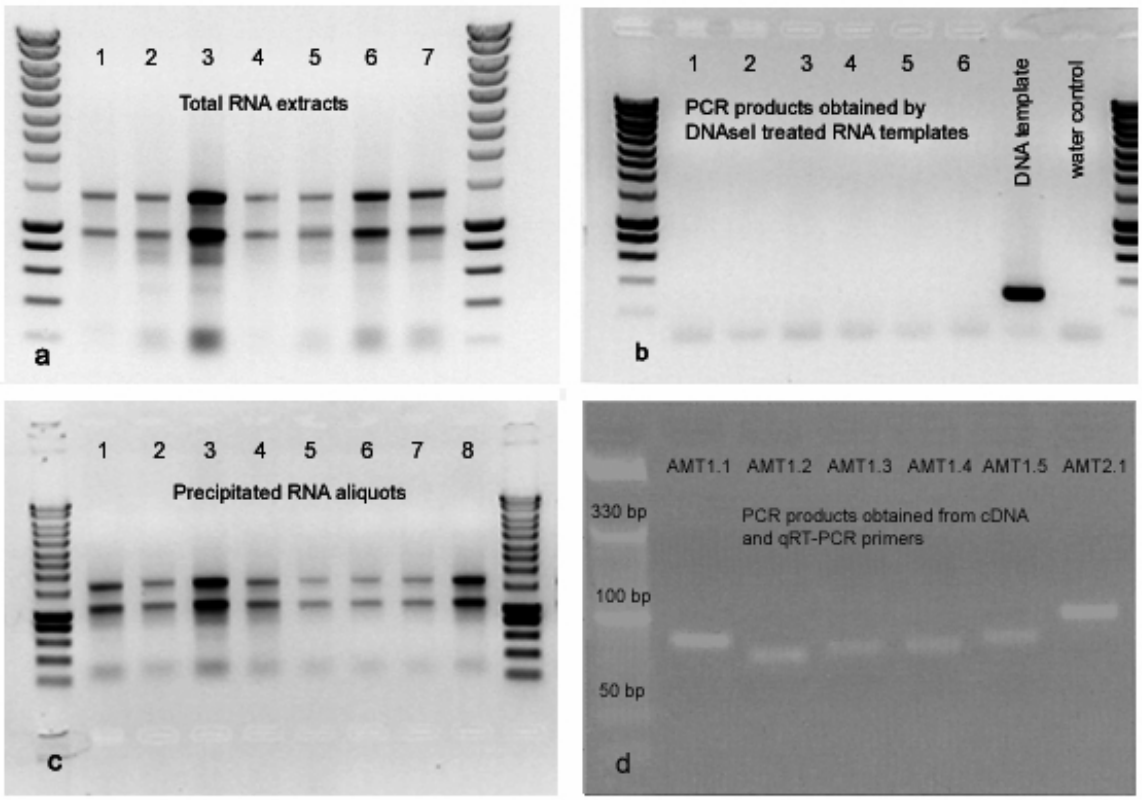

Figure 2.3. Gel electrophoresis for RNA and cDNA quality control.
(a) Clean, undegradaded RNA after extraction from leaves on an agarose TBE gel. The sharpness of ribosomal RNA double bands was used as an indication for RNA quality after extraction.
(b) Complete removal of DNA from the RNA sample was tested on agarose gels with PCR products obtained by PCR usingDNAse I treated RNA templates (2nd lane from the right: DNA template control, last lane from the right: no template control).
(c) After isopropanol precipitation RNA was again tested for degradation by running of aliquots on an agarose TBE gel.
(d) The quality of the cDNA after reverse transcription was tested on an agarose TBE-gel run with PCR products obtained from PCR with cDNA templates and qRT-PCR primers.

Solutions for RT-PCR were prepared as given in Table 2.3.1.

PCR reactions were performed in an optical 384-well plate with an ABI PRISM® 7900 HT Sequence Detection System (Applied Biosystems), using SYBR® Green to monitor dsDNA synthesis. Reactions contained 5 µL 2X SYBR® Green Master Mix reagent (Applied Biosystems), 1.0 ng cDNA and 200 nM of each gene-specific primer in a final volume of 10 µL (Table 2.3.1.).

RT-Primers were designed using the program Primer-Express™ (Applied Biosystems).

For every RT-PCR reaction three replicates were performed. Furthermore, three no template controls were included for each reaction to identify possible DNA contamination of samples.

Table 2.3.1. Pipetting scheme for a single reaction of RT-PCR

compound	volume
cDNA (1 ng)	0.5 µl
2x SYBR Green Master Mix	10 µl
Primer-mix fwd and rev (10 µM)	1 µl
H_20 dest.	8.5 µl

For the quantification of the mRNA transcipt levels the SDS 5700 sequence detection system (Applied Biosystems) was used and run with the program given in Table 2.3.2.

Table 2.3.2 PCR program for quantification of cDNA levels

step	time	temperature
1	2 min	50 ^{o}C
2	10 min	95 ^{o}C
3	15 s	95 ^{o}C
4	1 min	60 ^{o}C
5	back to step 3, 39x	
6	dissociation protocol*	

*

The dissociation protocol of step 6 monitors the reassociation kinetics of complementary single strand-DNA to double stranded DNA (by denaturing of the DNA for 5 minutes at 95 ^{o}C, subsequent cooling down to 60 ^{o}C.) By comparison of the dissociation curves of the triplicates it can be observed if unspecific products accumulated during a run.

2.3.3. Determination of Transcript Levels

Data were analysed using the SDS 2.1 software (Applied Biosystems). To generate a baseline-subtracted plot of the logarithmic increase in fluorescence signal (ΔR_n) versus cycle number, baseline data were collected between cycles 3 and 15. All amplification plots were analysed with an R_n threshold of 0.3 to obtain C_T (threshold cycle) values. In order to compare data from different PCR runs or cDNA samples, C_T values for all TF genes were normalised to the C_T value of *ubiquitin10* included in each PCR run (Ct, the threshold cycle, is the cycle number at which SYBR® Green fluorescence (ΔRn) in a real-time PCR, reaches an arbitrary value during the exponential phase of DNA amplification).

The number of cycles needed to reach a given fluorescence intensity depends not only on the amount of cDNA in the extract, but also on the amplification efficiency (E). In the ideal case, when the amount of cDNA is doubled in each reaction cycle, E equals one. The PCR efficiency was estimated in two ways. The first method of calculating efficiency utilised template dilutions and the equation $(1+E) = 10^{(-1/slope)}$, as described previously (Pfaffl et al., 2001). The second method made use of data obtained

from the exponential phase of each individual amplification plot and the equation $(1+E) = 10^{slope}$ (Ramakers et al., 2003).

Dissociation curves of the PCR products were analysed using SDS 2.1 software. Additionally, all RT-PCR products were resolved on 4% (w/v) agarose gels (3:1 HR agarose, Amresco, Solon, OH) run at 4 V cm^{-1} in TBE buffer, along with a 50 bp DNA-standard ladder (Invitrogen GmbH).

RT-PCR was performed for every individual cDNA with 3 replicates from the same cDNA sample. Than, the Ct-values were measured. In order to compare the transcript levels of each cDNA sample, the Ct-values for each gene were normalized to the constitutive gene *UBQ-10*. Of these 3 replicates the mean value and the standart error were taken for each sample. The mean values of the Ct-values were normalised relative to the transcript levels of the housekeeping gene *UBQ-10* (formula 2.2.3.3.1.).

formula 2.2.3.3.1.: $\Delta C_t = C_t$ (ammonium transporter) – C_t(UBQ-10)

In the case that the transcript levels of the expression of same ammonium transporter under different conditions were compared, the differences of the ΔC_t values of the two conditions were calculated (formula 2.2.3.3.2.)

formula 2.2.3.3.2.: $\Delta\Delta C_t = \Delta C_t$(condition x) – ΔC_t(condition y)

The ratios of the transcript levels relative to the endogenous control (the housekeeping gene) and relative to a calibrator were calculated using formula 2.2.3.3.3..

formula 2.2.3.3.3.: $1+E^{-\Delta\Delta Ct}$

2.4. Cultivation of Plant Material:

2.4.1. Growth in Sterile Liquid Medium:

Arabidopsis thaliana seeds were germinated and grown in liquid sterile culture medium (2.1.7.2.2) in constant light conditions at 20 ^{o}C in 50 ml Erlenmeyer flasks at constant rotation of 90rpm for 6 days. For nitrogen-deprivation treatment, plants were then transferred to fresh culture medium lacking N 24hours under the same environmental conditions: The plants were harvested after 7 days.

2.4.2. Growth on Soils

Arabidopsis thaliana seedlings were germinated on *Arabidopsis* GS 90 soil and grown in a phytotron with a diurnal rythm of 16h light (light intensity 145 µE (fluorescent tube, colour of light 183, 184), at 20℃, 75 % humidity) and 8 hours in darkness (6 ℃, 7 5 % humidity) for 7 days. Plants were transferred to 9cm pots containing either GS 90 soil : Vermiculit (1:1volume ratio) or soil type-0 (Einheitserde®, Werkverband e.V.) and grown in the greenhouse with a diurnal rythm of 16h light (light

intensity 250 µE at 20 °C, 80 % humidity) and 8 hours in darkness (18 °C, 50 % humidity). Plants were fertilized every 2nd day with 5ml 10 µM NH_4Cl-fertilizer (see 2.1.6.3.) and harvested after 2 weeks and immediately frozen in liquid nitrogen.

2.4.3. Hydroponic Growth

Seeds were sown on soil, germinated, and Basta selected. After 4 days growth, plants were washed and transferred to open 0.5ml black eppendorf tubes with the bottoms cut off. The tubes were placed into styropore plates, which were put into trays containing the respective hydroponic growth medium (see 2.1.7.2.3.). Plants were cultivated in hydroponic medium at a 16 hours light cycle at a light intensity in phytotrons until flowering. The hydroponic growth medium was replaced every 7 days. Before harvest, one subset of plants were deprived of nitrogen by incubation in nitrogen-free hydroponic growth medium for 24h. Roots, leaves, and flowers were harvested seperately, immediately frozen in liquid nitrogen, and stored at –80 degrees for further use.

2.4.4. Growth on Sterile Solid Medium

Seeds were sterilized and subsequently sown on sterile MS-plates. For selection of transformed plants, antibiotics were added to the MS-medium (for concentrations see 2.1.7.2.1.). The plants were grown in constant light conditions at 20 °. For root growth experiments, the plates were placed perpendicularly.

2.5 Physiological Analysis

2.5.1 ^{14}C-Methylammonium Uptake Studies

Arabidopsis thaliana seeds (10 - 20 seeds) were germinated and grown in 24-well microtiter plates containing 1 ml liquid sterile culture medium under constant light conditions at 20 °C with constant rotation at 80rpm. After 5 days the medium was removed and replaced with 1 ml fresh liquid sterile culture medium. After 7 days, the medium was removed and replaced with nitrogen-free medium.

After a further 24h, plants were harvested and the residual medium removed from the plants by gentle drying on glass microfiber filters on a vacuum manifold. Plants were pooled to obtain batches of similar mass and placed into a new 24-well microtiter plate containing 1ml nitrogen-free liquid culture medium. The medium was subsequently adjusted to different concentrations of methylammonium chloride which was followed by the addition of 2 µl ^{14}C-methylammonium chloride (^{14}C-MA). Plants were incubated on a temperature controlled shaker at 80 rpm and 20 °C for various amounts of time (see 4.2.). After incubation, plants were transferred to glass microfiber filters and immediately washed with 1 ml 1 mM $CaSO_4$ by means of the vacuum pump. In total, plants were washed three times.

After washing, plants were surface dried, transferred to 1.5 ml tubes, and homogenised using the mixer RZR1. Homogenised plants were suspended in 400 µl 1 mM $CaSO_4$ and the open tube placed into a 15 ml scintillation tube. 10 ml Ready Safe Liquid Scintillation Cocktail was then added.

Finally, radioactivity of each sample was counted in a scintillation counter for 1 minute.

During the two hours experiments, evaporation took place in the open 24 well 1 ml micro titer plates and lead to an increase of ^{14}C-MA concentration. The evaporation rate of 1 ml in the wells of a 24 well micro titer plate was analysed for two hours incubation (Fig. 2.5.1.). The scintillation counts (CPM) of each sample were calibrated to the evaporation rate.

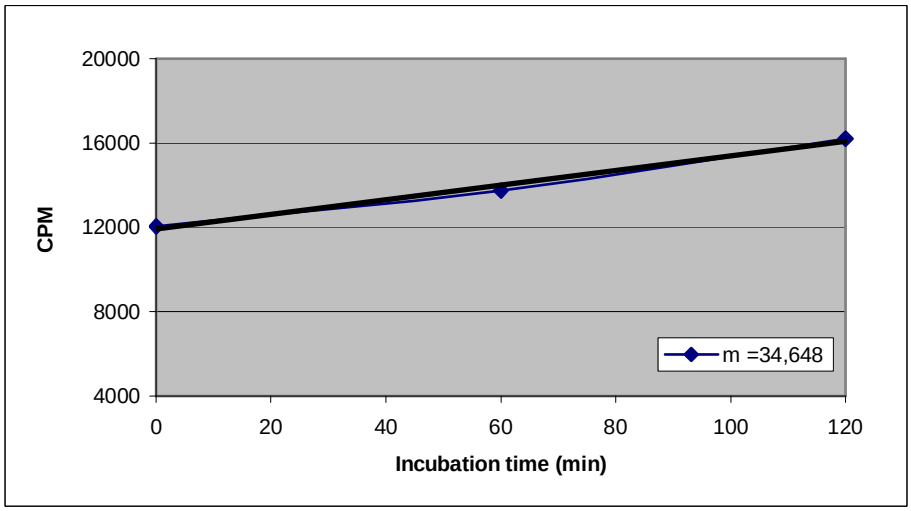

Fig. 2.5.1. Increase of the ^{14}C-MA concentration in 1 ml incubation medium in 2 hours, due to evaporation (m= 34,648 cpm/min).

2.5.2 Ammonium Uptake Studies

Plants were grown in liquid sterile culture medium as described in 2.4.1 for one week and deprived of nitrogen for 24 hours. Seedlings were then pooled, pools were adjusted to the same weight, and transferred to new 24-well plates. Each well contained 1ml fresh liquid culture medium lacking nitrogen. Immediately prior to the beginning of the uptake experiments, the medium was adjusted to the specific concentration of ammonium (e.g. 20 µM, 100 µM, 200 µM) and incubated on a shaker at room temperature for 120 min. Samples of 50 µl medium were taken every 5 minutes. The removed medium was replaced by the same volume of 50 µl nitrogen-free liquid culture medium.

To measure ammonium in liquid samples, 1 ml reagent A and 1ml reagent B (Table 2.5.2.) were added to each sample after incubation and samples were vortexed for 30 seconds. Samples were then incubated in the dark for 6 to 12 hours and the resulting ammonium absorbtion (A_{260}) measured in a spectrometer at 625 nmeters (nm). The optical densitiy (OD) of the samples was measured in a spectrometer at 625 nm. To refer the obtained OD of each sample to a specific ammonia concentration, a standard was made for each concentration generated by an ammonium addition series for each experiment from 0-200 µM in 20 µM steps from a 50 µM, 100 µM, and 200 µM ammonium stock solution (Fig. 2.5.2.).

Table 2.5.2: Contents of reagents A and B

Reagent A (g/L)	Reagent B (g/L)
10 g phenol 50 mg sodium nitroprusside	5 g NaOH 0.42 g $NaClO_2$ (equal to 3.5 ml of 12%v/v standard vommercial grade solution)

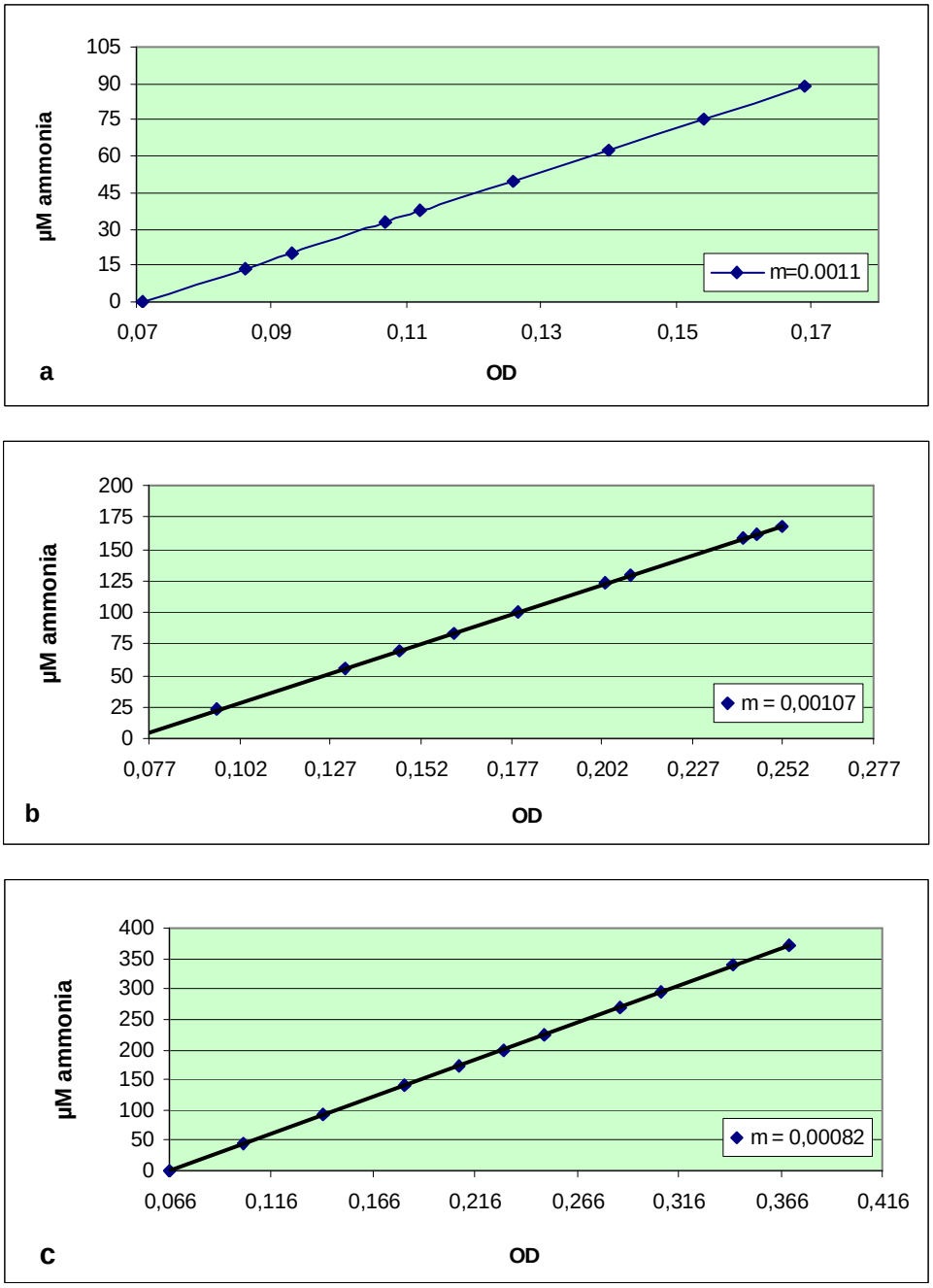

Fig. 2.5.2. Standard curves to refer the obtained OD of each sample to a specific ammonia concentration. The curves were generated by ammonium addition series in 20 µM steps from a 50 µM (a), 100 µM (b), and 200 µM (c) ammonium stock solution. The OD was measured at 625 nm.

2.5.3. ^{15}N-Ammonium Uptake Studies

Plants were grown as described in 2.4.1 and prepared as described in 2.5.1, except that they were incubated in ^{15}N-ammonium chloride instead of ^{14}C-methylammonium chloride. After ^{15}N-ammonium chloride incubation, surface dried plants were transferred into 2ml tubes and immediately frozen in liquid nitrogen.

60mg ± 3mg of each sample were homogenized using a Retsch Mill MM200 (Retsch Technology GmbH, Haan, Germany) for 2 min.

Metabolites were then extracted from homogenised plant material, using the protocol below (Table 2.5.3).

Table 2.5.3 Extraction protocol of plant metabolites for LC Q-TOF

step	add/take (to 60 mg hom. plant material)	treatment
1	+ 300 µl Methanol abs	precooled at –20 °C
2	+ 30 µl Chloroform	mix
3	- 30 µl Pre-Mix	shake for 15 min at 70 °C
4	+ 200 µl Chloroform	shake 5 min at 37 °C
5	+ 400 µl water	mix, centrifuge at 14000 rpm, 5 min
6	- two 80 µl aliquots from the polar phase	transfer to fresh 2 ml tubes
7	+100 µl QC-mix, 5 µl PC-mix polar, 5µl PC-Mix lipid (Qualitymix)	into a 2ml tube containing one aliquot; dry in vacuum centrifuge over night
8	+ 20 µl water dest	ready to use for injection

Mass spectrometry was performed on a LC/MS system consisted of a Finnigan LCQ DECA mass spectrometer, a Rheos 2000 pump, and an HTS PAL autosampler. The system was operated using Xcalibur™ software (Thermo electric corportion).

Nitrogen sheath gas pressure was set to 6 bars at a flow rate of 0.8 L/min. Spray voltage was set to 5 kV. The temperature of the heated transfer capillary was maintained at 200°C. Helium collision gas incoming pressure was 2.6 bar, and the ion gauge pressure was 0.89 x 10^{-5} L/min.

Full scan mass spectra were acquired from 100-1500 amu at unit mass resolution. For MS experiments, data dependent scan was chosen with the wideband activation turned off. The normalized collision energy was set to 35%, and the activation Q was 0.250 with the source fragmentation turned off. Analytical liquid chromatography was performed using LC-MS grade acetonitrile (A) and 6.5 mM ammonium acetate (pH 5.5, adjusted by acetic acid) (B) as the mobile phase at flow rates of 0.2 mL/min at ambient temperature. Ammonium acetate and acetic acid were HPLC grade.

LC/MS analysis was performed on PolyHYDROXYETYL A column, 100 x 2.1 mm, 3 µm particle size, 100 A pore size. After a 5 min isocratic run at 0% B, a gradient to 15% B was concluded at 8 minutes, then a gradient to 40% B was completed at 50 minutes. The injection volume was set to 7 µL. HPLC column was connected to the electrospray interface of the mass spectrometer without splitting.

2.5.4 HPLC-measurement of amino acids

Arabidopsis thaliana seeds of each homozygous T-DNA-Insertion line were germinated and grown in full liquid culture medium under constant light conditions at 20 °C in 50ml Erlenmeyer flasks with constant rotation at 90 rpm for 6 days. Plants were then transferred to nitrogen-free liquid sterile culture medium for 24 hours under the same environmental conditions. Plants were harvested after 7 days and immediately frozen in liquid nitrogene. WT and RNAi-lines were grown hydroponically and harvested as described in 2.2.4.3.

10-20 mg of ground plant tissue was collected in a 1.5 ml tube and the soluble metabolites extracted following the protocol below (Table 2.5.5).

Table 2.5.5 Extraction protocoll for determination of amino acids by HPLC

step	add (to 10-20 mg ground tissue)	treatment
1	250 µl 80 % ethanol	shake 20 min at 80 °C
2		centrifuge 5 min at 14000 rpm
3		transfer supernatant to a fresh tube, store on ice
4	to pellet: 150 µl 80 % ethanol	shake 20 min at 80 °C
5		centrifuge 5 min at 14000 rpm
6		transfer supernatant to tube from step 3, store on ice
7	to pellet: 250 µl 50 % ethanol	shake 20 min at 80 °C
8		centrifuge 5 min at 14000 rpm
9		transfer supernatant to tube from step 3, store on ice
10		tube of step 9 can be used for analysis of amino acids
11		pellet of step 8 can be used for the determination of proteins

2.6 Histochemical Analysis of *AMT*-Promoter-GUS expression in plants

Approximately 1kb of the promoter sequences upstream of the ATG of each AMT gene was cloned into the binary vector pBI 1.3 and transformed into *Arabidopsis thaliana* v. Col-0 as described in 2.1.3. and 2.2.2 (For the promoter length of each gene that was fused to the GUS gene see Table 1.6).

Positive transformants were selected on plates containing MS-medium with 1 % sucrose, 0.8% agar and 50 µg/ml kanamycin. Surviving antibiotic resistant seedlings were transferred to soil after 14 days and at the end of the lifecycle seeds were harvested.

T2 seeds were sown and grown on MS-plates containing kanamycin and harvested for GUS activity assays after 14 days. For the determination of flower-specific staining, plants were transferred to soil after 14 days and grown until flowering. Subsequently, flowers were harvested and tested for GUS activity.

Table 2.6: Length of promoter elements upstream of the ATG for each AMT gene, which were fused to the GUS gene in pBI101.3

gene	Promoter length (bp)
AMT 1.1	~ 1000
AMT 1.2	~ 1200
AMT 1.3	~ 1100
AMT 1.4	~ 800
AMT 1.5	~ 1200
AMT 2.1	~ 1100

GUS activity assay:

24-well plates containing plants and 1ml GUS-Staining Buffer (1.9.2.)were vacuum infiltrated for 30 min and then incubated at 37 ^{o}C in darkness over night. Plants were destained in 50% ethanol for 2 hours, destained in 70% ethanol for 2 hours, and finally destained and subsequently stored in 100% ethanol until the end of the experiment.

Staining of plant organs was visualized using a photographic binocular with up to 32x magnification.

2.7 Morphological Characterization of Plants

2.7.1 Characterization of Root Growth

Arabidopsis thaliana seedlings were germinated and grown in upright square petri dishes on MS-medium containing 1 % sucrose and 0.8% agar in a 16 hours light cycle and constant temperature conditions (20℃). The petri dishes were placed in bl ack boxes in order that light could not directly reach the root system. The length of the main root was measured from day 4 to day 8, once a day at the same time.

To identify possible specific responses of individual T-DNA lines or RNAi lines to different nitrogen conditions (gauntlets), the individual lines were grown on media differing in nitrogen concentration and nitrogen source (Table 2.7.1).

Table 2.7.1 Nitrogen sources and concentrations used for the gauntlet studies

I.	**NH_4Cl**	100 µM	1mM
II.	**NH_4NO_3**	100 µM	1mM
III.	**glutamine**	500 µM	1mM

2.7.2. Characterization of Shoot Growth

Seedlings of each line were germinated on *Arabidopsis* GS 90 soil and half of the plants were transferred to soil type-0, as described in 2.2.4.2. The plants grown on type-0 soil were fertilized every 2nd day with 5 ml 10 µM NH_4Cl – fertilizer.

To identify differences in developmental characteristics, the on which a plant reached a specific developmental stage, and additional growth parameters were measured, as follows:

1. day of bolting
2. day of opening of the first flower
3. inflorescence length at day 29, 32, 52
4. final inflorescence length
5. total seed weight

To avoid errors due to the positon of the plants in the green house cabin, 20 plants of each line were grown on GS 90 soil and type-0 soil, respectively, and distributed that an equal number of plants from each line was growing at the same distance to the lights and windows.

2.8. Creation of Double Mutants

The homozygous T-DNA insertion lines Sy-*AMT1.1*, Sy-*AMT1.2*, Sy-*AMT1.4* and Sy-*AMT2.1* (1.6.2.) were crossed in all combinations (Table 2.8). The crosses were performed reciprocally to eliminate possible gametophytic effects.

Table 2.8
Double mutants by reciprocal crosses of Syngenta T-DNA insertion lines (indicated by an X).

♂\♀	**Sy-*AMT* *1.1***	**Sy-*AMT* *1.2***	**Sy-*AMT* *1.4***	**Sy-*AMT* *2.1***
Sy-*AMT* *1.1*		**X**	**X**	**X**
Sy-*AMT* *1.2*	**X**		**X**	**X**
Sy-*AMT* *1.4*	**X**	**X**		**X**
Sy-*AMT* *2.1*	**X**	**X**	**X**	

F1 seeds from each cross were harvested and selfed and the resulting F2 individuals were screened by PCR to identify homozygous double mutants(Fig. 2.8.a). The PCR screen consisted of 2 reactions for each F2- plant and a control. PCR was triggered by a forward primer that annealed upstream of the T-DNA insertion and a reverse primer that annealed in the coding region of each *AMT* gene of the repective crossing combination. The T-DNA insertion between the two annealing sites prohibited PCR amplification because of the increased distance between the primers. F2-plants were selected as homozygous double mutants if both PCR gave no product with each primer pair. The qualitiy of the

PCR reactions was tested by a control PCR which was triggered by a primer pair that amplified the same region of another *AMT*-gene not belonging to the respective crossing combination. This PCR was performed under the same reaction conditions as the other. The selected plants were confirmed by two additional PCR (Fig. 2.8.b). The reverse gene-specific primer was combined with a forward primer that annealed in the T-DNA insertion. Templates with an insertion in the respective *AMT* gene gave a PCR product of about 300 bp length. Homozygous double mutants gave PCR products for both genes of the respective crossing combination.

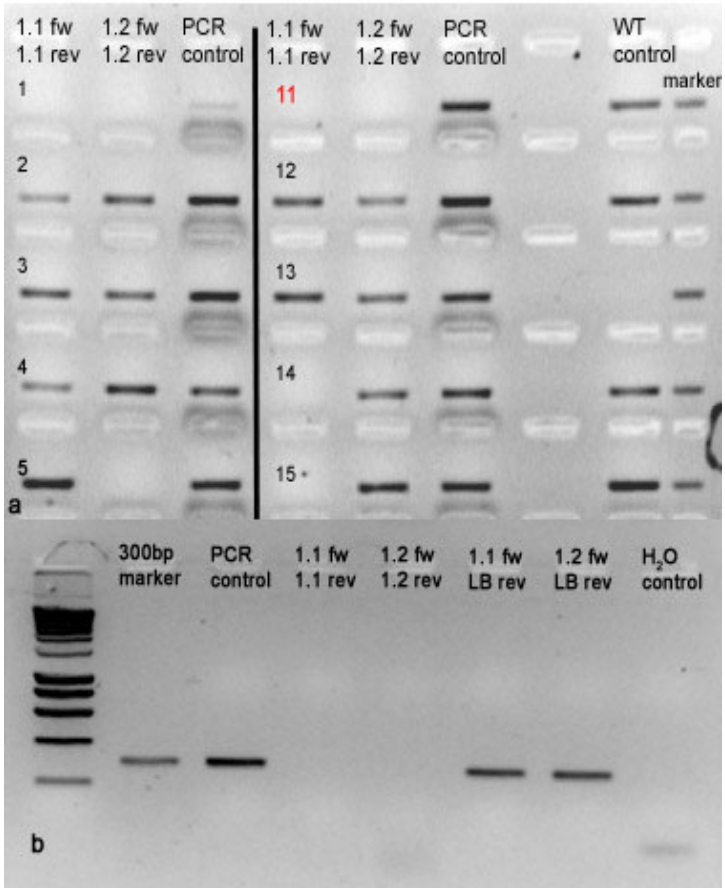

Figure 2.8.
a. PCR-screening for homozygous T-DNA double mutants. Each DNA sample of an F2-plant was submitted to three reactions The first two tested the presence of the T-DNA in each *AMT*-gene of the respective crossing combination, here *AMT1.1* and *AMT1.2* (lane 1 and 2). The quality of the PCR was tested by a third reaction on an *AMT* gene not belonging to the respective crossing combination, producing a product of the same length under the same conditions (lane 3). Included were water controls (lane 7) to test the reaction mix for possible DNA contaminations and PCR reactions with WT-templates to test the quality of each primer pair (lane 8). As a size control of the products, a 300bp marker was run. (the vertical numbers indicate the F2-plants tested; F2-11 is homozygous for a T-DNA insertion in gene *AMT1.1* and gene *AMT1.2*, depicted in red).
b. Confirmation of the T-DNA double mutant *AMT1.1* ; *AMT1.2*: Lane 1: Smart Ladder, lane 2: 300bp ladder, lane 3: PCR with primers of an additional wildtype *AMT* gene on the same DNA sample to test the quality of the reaction , lane 4 and 5: products of PCRs from the mutated genes, lane 6 and 7: products of PCRs on the LB of the T-DNA and the promoter region of the respective gene, lane 8: water control.

2.9. Segregation Analysis

For the identification of the T-DNA insertion number in Syngenta-lines and the RNAi-lines, as well as for the identification of homozygous RNAi-lines of the T3 generations, a segregation analysis was performed. Transformed plants were grown as described in 2.4.2 and sprayed with BASTA after day 16, day 18 and day 20. The resistant and non-resistant plants were counted and a segregation ratio calculated.

III. Results

1. Sequence Analysis of Ammonium Transporters in *Arabidopsis thaliana*

Sequence comparisons of the *AMT1* family were performed with the cDNA and the amino acid sequence of each *AtAMT1* gene using the 'BLAST 2 sequences' tool of NCBI (BLASTN for nucleotide alignments and blastP for amino acid alignments; www. ncbi.nlm.nih.gov.; Tatusova and Madden, 1999). The alignments of the cDNA and the amino acids showed that this family of ammonium transporters is relatively conserved (Tab. 1.1 and 1.2.). On the nucleotide level, *AtAMT1.4* has the most similarity to *AtAMT1.1* (83 % identity, Tab.1.1.). On the amino acid level, *AtAMT1.3* and *AtAMT1.5*, which are closely related to each other (85 % identity, Tab. 1.1.), share the highest homology to *AtAMT1.1* (77 %). The divergences between the other family members are similar and range between 71 % and 81 % on both the nucleotide and amino acid level. The *AtAMT2* gene was not integrated into these comparisons because the amino acid sequence is less than 25 % identical to AMT1 family proteins (Howitt and Udvardi *et al*., 2001) and *AtAMT2* is more closely related to bacterial ammonium transporters (Altschul *et al*., 1999).

Tab. 1.1. Comparison of DNA sequence identity (%) within the *AtAMT1* family.

AtAMT1.2	74 %			
AtAMT1.3	77 %	86 %		
AtAMT1.4	83 %	76 %	78 %	
AtAMT1.5	76 %	84 %	88 %	76 %
	AtAMT1.1	***AtAMT1.2***	***AtAMT1.3***	***AtAMT1.4***

Tab. 1.2. Comparison of amino acid sequence identities (%) within the *AtAMT1* family.

AtAMT1.2	71 %			
AtAMT1.3	77 %	74 %		
AtAMT1.4	72 %	81 %	75 %	
AtAMT1.5	77 %	80 %	85 %	71 %
	AtAMT1.1	***AtAMT1.2***	***AtAMT1.3***	***AtAMT1.4***

A phylogenetic analysis was performed by comparison of the cDNA sequences using the analysis software Lasergene v.6 (DNA Star™ Inc., Madison, USA) and the clustal W algorithm. The analysis reflects the close relationship of *AtAMT1.3* and *AtAMT1.5*, which are placed on the same branch and diverged relatively recently from *AtAMT1.1* (Fig. 1.). Placed opposite to these genes are *AtAMT1.2* and *AtAMT1.4*, which both branched independently from the putative ammonium transporter ancestor. AtAMT 2.1 has only a weak homology to the members of the *AtAMT1* family and is placed at a long distance from these genes. However, the phylogenetic analysis points to a divergence from a common ancestor with *AtAMT1.4*.

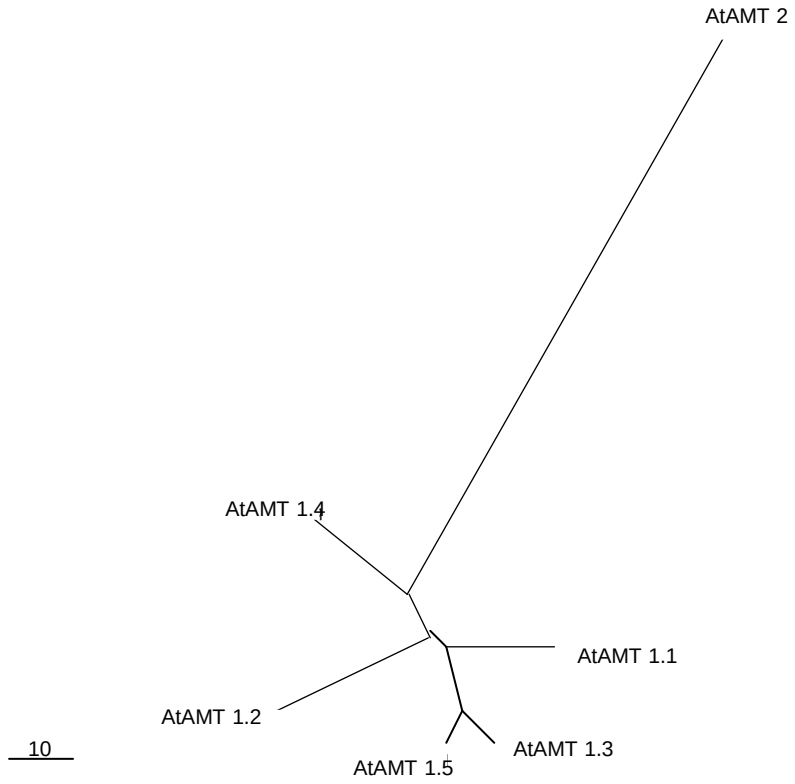

Fig. 1. Phylogenetic unrooted guide tree of ammonium transporters in *Arabidopsis*. The length of the branches indicate the phylogenetic distances to the potential common ancestor. Genes on one branch are more closely related and phylogenetically younger than genes on different branches, given the prerequisite that the genes are under equal selection pressure and mutations are chronologically constant (The tree was performed using the software DNA Star™ and visualised using the software TreeView; www.treeview.net).

2. Quantification of *AtAMT* Transcript Levels in *Arabidopsis thaliana*

2.1 *AtAMT* Expression Patterns on the Whole Plant Level

Quantitative real-time PCR (qRT-PCR) was used to measure the transcript levels of all six *AtAMT* genes on the whole plant level. *A. thaliana* var. Col-0 was grown for six weeks in hydroponic medium and exposed to different nitrogen conditions as described in Material and Methods. Transcript levels for all six *AtAMT* genes were measured for both, nitrogen-replete and nitrogen-deprived plants. Although the transcript levels of *AtAMT* genes varied over three orders of magnitude, transcripts of all genes were detected (Fig. 2.1.1).

The following order of relative transcript abundance was found in nitrogen-supplied plants:

AtAMT1.1 > AtAMT1.3 > AtAMT1.2 > AtAMT2.1 > AtAMT1.4 > AtAMT1.5

AtAMT1.1 was the highest expressed ammonium tranporter gene and in nitrogen supplied conditons the transcript level of this gene was 60 % of that for the household gene *UBQ-10*. However, in respect

to the other *AMT* genes *AtAMT1.1* transcript levels were four-times and six-times higher than transcript levels of *AtAMT1.3* and *AtAMT1.2*, respectively. The other two members of the *AtAMT1* gene family, *AtAMT1.4* and *AtAMT1.5* were lower expressed on whole plant level, which was 40- and 80-fold less, respectively. The *AtAMT2* gene family member *AtAMT2.1* was expressed at an intermediate level similar to *AtAMT1.2*, which was five-fold less than transcript levels of *AtAMT1.1* (Tab. 2.1.1).

The effects of changes in nitrogen nutrition on *AtAMT* gene expression was also investigated by qRT-PCR. After 24 hours nitrogen deprivation, *AtAMT1.1*, *AtAMT1.3,* and *AtAMT1.5* showed a positive response, which led to a considerable increase in total transcript levels. Transcript levels of *AtAMT1.1.* and *AtAMT1.3* were about two fold increased, while *AtAMT1.5* was over 20-fold increased in response to nitrogen deprivation of plants (Fig. 2.1.1). Thus, *AtAMT1.5* showed the strongest response to nitrogen starvation of all *AMT* genes. However, in order of absolute transcript levels it was only third. *AtAMT1.2*, *AtAMT1.4,* and *AtAMT2.1* did not show an increase in transcript levels (Fig.2.1.1.).
The strong upregulation of *AtAMT1.5* expression in response to nitrogen deprivation led to a changed order of relative transcript abundance under these conditions:
AtAMT1.1 > AtAMT1.3 > AtAMT1.5> AtAMT1.2 > AtAMT2.1 > AtAMT1.4

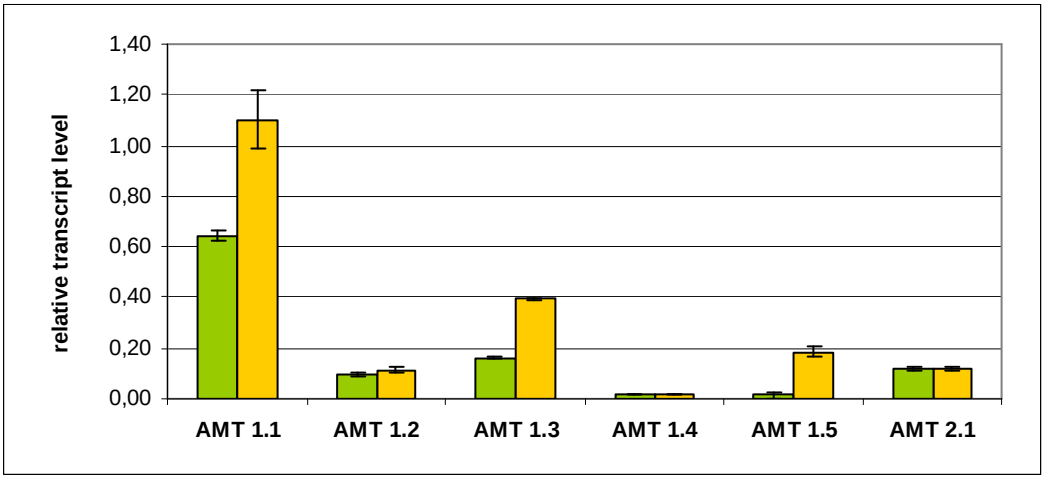

Fig. 2.1.1 Transcript levels of *AtAMT* genes relative to the household gene *UBQ-1*0 in WT plants grown in a hydroponic system under full nutrient (green bars) and nitrogen depleted (yellow bars) conditions (error bars indicate the standard errors of three replicates).

Tab. 2.1.1 Expression of *AtAMT* genes relative to that of *AtAMT1.1* in *A. thaliana* grown under nitrogen replete and nitrogen deprived conditions.

Nitrogen condition	gene	Relative transcript levels	N-deprived / N-replete	expression relative to *AtAMT1.1* (%)
N-replete	***AMT 1.1***	0.64	1.71	100,0
	AMT 1.2	0.10	1.15	15,1
	AMT 1.3	0.16	2.44	24,8
	AMT 1.4	0.02	0.78	2,3
	AMT 1.5	0.01	13.57	1,2
	AMT 2.1	0.12	0.97	18,6
N-deprived	***AMT 1.1***	1.10		100,0
	AMT 1.2	0.11		9,7
	AMT 1.3	0.39		34,2
	AMT 1.4	0.01		1,0
	AMT 1.5	0.19		15,5
	AMT 2.1	0.12		10,2

2.2 *AtAMT* Expression Patterns in Roots, Shoots, and Flowers

To specifiy the expression patterns of the *AtAMT* genes more in detail, qRT-PCR was used to measure the transcript levels in roots, leaves, and flowers seperately. In roots, all *AtAMT* genes except *AtAMT1.4* and *AtAMT1.5* were expressed under nitrogen replete conditions (Fig. 2.2.1). *AtAMT1.1* and *AtAMT1.3* showed the highest transcript levels in roots (Tab. 2.2.1). *AtAMT1.3* was expressed in a root-specific manner and showed considerably higher transcript levels in roots than in whole plants. *AtAMT1.2* and *AtAMT2.1* was expressed five-fold and eight-fold less than *AtAMT1.1* in roots. Responses to changes in N-nutrition were strong in roots. *AtAMT1.1* was four-fold induced by N deprivation and *AtAMT1.3* was induced three-fold (Fig. 2.2.1). Both represent the highest expressed *AMT*s in roots under N-deprivation. *AtAMT1.5* responded very strongly to N-deprivation with transcript levels increasing 40-fold. Thus, it became the third highest expressed *AtAMT* in roots under nitrogen deprived conditions (Tab. 2.2.1).

AtAMT2.1 and *AtAMT1.2* expression increased twofold in response to N-deprivation. *AtAMT1.4* expression remained at levels close to the detection limit.

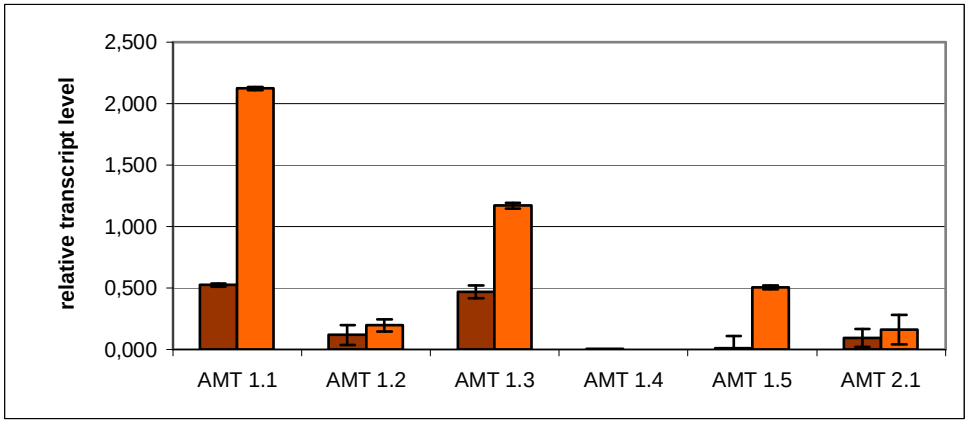

Fig. 2.2.1 *AtAMT* transcript levels relative to the household gene *UBQ-10* in roots under full nutrient and nitrogen deprived conditions (error bars indicate the standard error of three replicates).

In leaves, only three *AtAMT* genes were expressed (Fig. 2.2.2). *AtAMT1.1* and *AtAMT1.2* were expressed under nitrogen-replete as well as deprived conditions. *AtAMT1.1* showed the highest transcript levels, although transcript levels for this gene were slightly lower in leaves than in roots under N-replete conditions. Transcript levels of *AtAMT1.1* were very similar in leaves and roots of N-deprived plants. *AtAMT1.1* transcript levels were approximately ten-fold higher than those of *AtAMT1.2* in leaves under all conditions (Tab. 2.2.2).

AtAMT1.2 transcript levels were three-fold lower in leaves than in roots under N supplied conditions but only slightly lower in N deprived conditions.

AtAMT2.1 was also expressed in leaves. However, it was three times less expressed there than in roots under N replete conditions and nearly two times less than under N deprived conditions. Compared to *AtAMT1.1* leaf expression, *AtAMT2.1* transcript levels were 16 times and 22 times lower in N-replete and N-deprived conditions, respectively (Tab. 2.2.1).

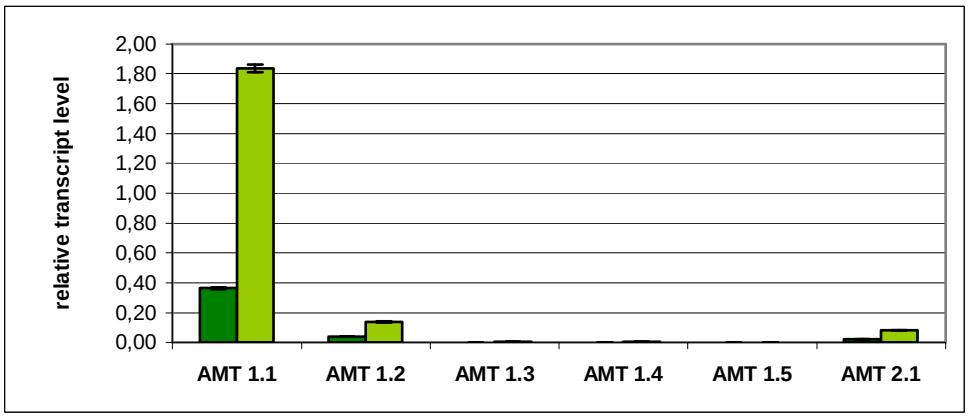

Fig. 2.2.2 *AtAMT* transcript levels relative to the household gene *UBQ-10* in leaves under full nutrient and nitrogen deprived conditions (error bars indicate the standard error of three replicates).

In flowers four *AtAMT* genes showed stable expression in the face of changes in N-supply (Fig. 2.2.3). These were *AtAMT1.1* with the highest expression levels, followed by *AtAMT1.2* and *AtAMT2.1* with five-fold lower levels and *AtAMT1.4* with transcript transcript levels nearly 20-fold lower than *AtAMT1.1* (Tab. 2.2.1).

AtAMT1.1 transcript levels were slightly higher in flowers than in either roots or leaves (Tab. 2.2.2). *AtAMT1.4* expression was higher in flowers than in any other organ. Relatively low transcript levels were detected for *AtAMT1.5* in flowers, although levels were simnilar to those in roots under full nutrient conditions.

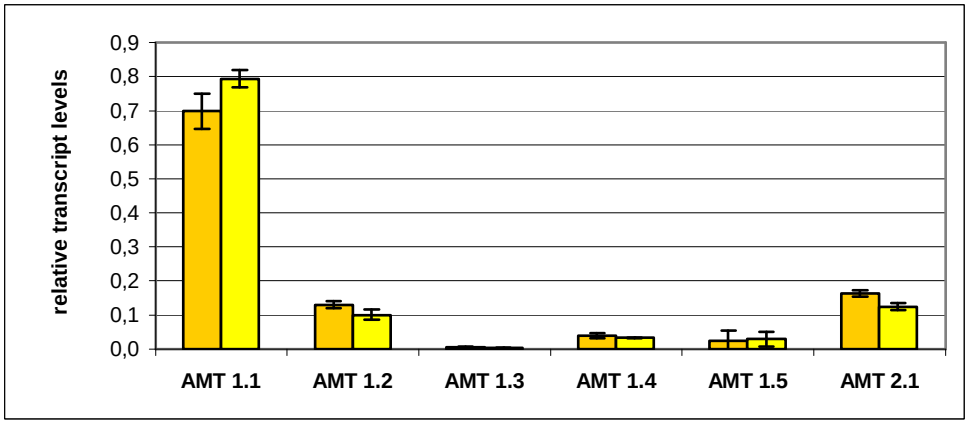

Fig. 2.2.3 *AtAMT* transcript levels relative to the housekeeping gene *UBQ-10* in flowers under full nutrient (dark bars) and nitrogen deprived conditions (light bars; error bars indicate the standart error of three replicates).

Tab. 2.2.1 Relative transcript levels (rel. tr. Level) of *AtAMT* genes for roots, leaves, and flowers from plants grown under nitrogen replete and deprived conditions, and the gene specific response to nitrogen deprivation in respect ot transcript levels (ratio –N / + N).

condition	gene	roots		leaves		flowers	
		rel. tr. level	-N / +N	rel. tr. level	-N / +N	rel. tr. level	-N / +N
N-replete	***AMT 1.1***	0.52	4.06	0.36	5.06	0.70	1.14
	AMT 1.2	0.12	1.67	0.04	3.55	0.13	0.77
	AMT 1.3	0.47	2.50	not determ.		not determ.	
	AMT 1.4	not determ.		not determ.		0.04	0.85
	AMT 1.5	0.01	43.58	not determ.		0.03	1.16
	AMT 2.1	0.09	1.73	0.02	3.75	0.16	0.76
N-deprived	***AMT 1.1***	2.12		1.84		0.79	
	AMT 1.2	0.19		0.14		0.10	
	AMT 1.3	1.17		not determ.		not determ.	
	AMT 1.4	not determ.		not determ.		0.03	
	AMT 1.5	0.50		not determ.		0.03	
	AMT 2.1	0.16		0.08		0.12	

3. Spatial Expression Patterns of *AtAMT* Genes in *Arabidopsis thaliana*

To obtain more information about tissue expression domains of the different *AtAMT* genes, promoter-GUS fusions of each gene (designated *pAMT-GUS*) were made and transformed into *A. thaliana var. Col-0*. Lines of three independently transformed plants were created for each *pAMT-GUS* construct. The results described below represent the consistent staining patterns observed in these lines. All lines were grown under N-replete conditions and prior two the analysis the plants were N-deprived for 24 hours (see II.2.2.6.).

3.1. *pAMT1.1-GUS* expression

Expression of *pAMT1.1-GUS* in *Arabidopsis* led to strong GUS staining in roots, leaves, and flowers , although staining showed distinct spatial and developmental patterns.

In all transformed plants, staining was strong in the primary as well as in the lateral roots but GUS staining was restricted to cortical cells only and not observed in the pericycle including the vascular tissue, the root hairs, or the root tip (Fig. 3.1.1). No staining was visible in emerging lateral roots.

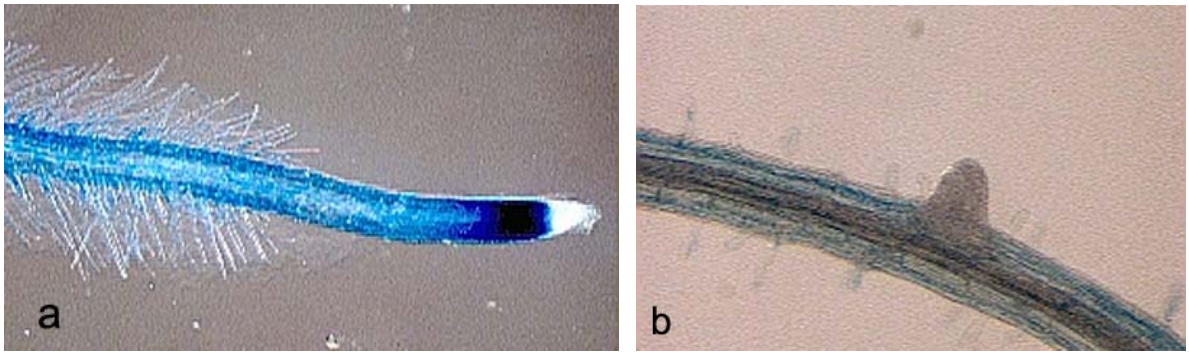

Fig. 3.1.1. *pAMT1.1-GUS* expression in roots. GUS staining was strong in cortical tissue of primary and lateral roots. No GUS staining was detectable in the pericycle, the root tips, or newly emerging lateral roots (a and b).

GUS staining was very strong in developing and fully matured leaves. It was detected in cells throughout the whole leaf with highest activity in vessels (Fig. 3.1.2.).

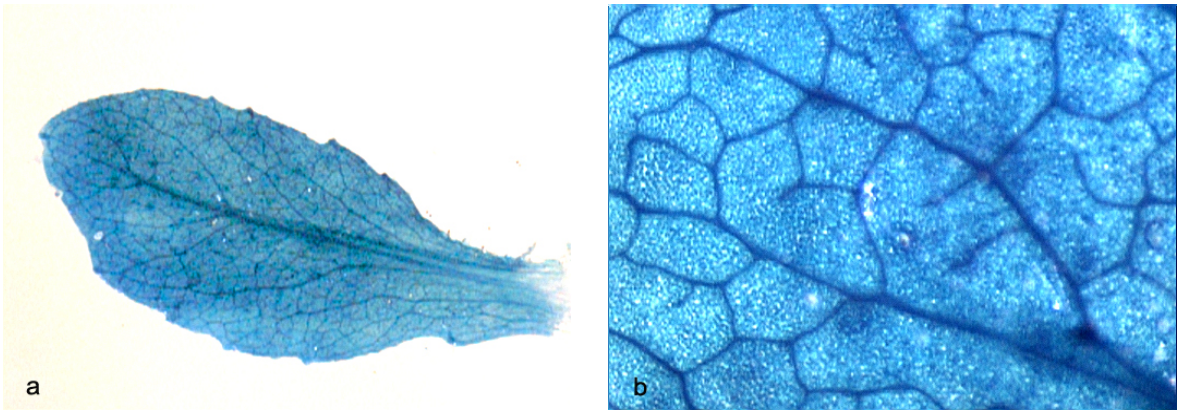

Fig. 3.1.2. *pAMT1.1-GUS* expression in leaves. GUS staining was strong in all parts of the leaf (a). Stongest expression was found in leaf veins (b).

In the inflorescences, *pAMT1.1-GUS* showed a very distinct expression pattern. It was mainly expressed in petals and the stems of siliques (Fig. 3.1.3 a). Staining in the petals became faint during flower development as the flower opened and stamens grew. In petals, the strongest GUS-staining was visible in closed buds (Fig. 3.1.3 b). Parallel to the decrease in expression in petals, *AMT1.1* began to be expressed in the stems of the fertilised flowers. The longer the siliques grew, i.e. the older and more mature the siliques became, the stronger was the GUS staining (Fig. 3.1.3 a and c). As in leaves, *AMT1.1* was expressed throughout the whole petals and the stem of the growing siliques with a stronger expression in the vascular tissue (Fig. 3.1.3 d). In ripening siliques, GUS staining was hardly visible except for the veins.

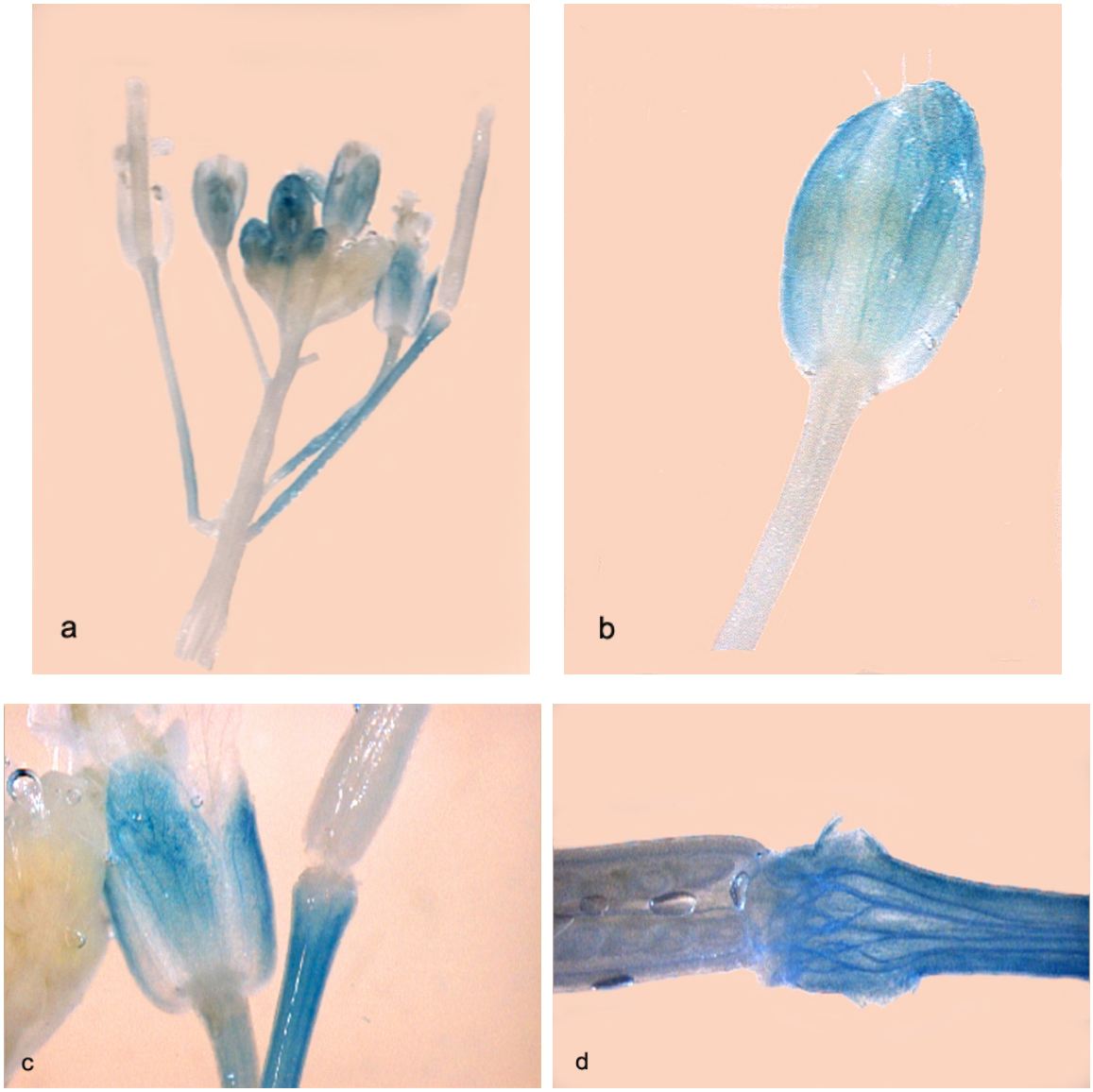

Fig. 3.1.3. *pAMT1.1-GUS* expression in flowers. *AMT1.1* was mainly expressed in petals and stems of ripening siliques (a). In petals, *AMT1.1* expression was strongest in closed buds (b) When flowers were fertilised and opened, *AMT1.1* expression decreased in petals, whereas it became expressed in stems of siliques (c). In stems of ripening siliques, *GUS* was expressed in all cells with a stronger expression in the veins (d).

3.2. *pAMT1.2-GUS* expression

In roots of *pAMT1.2-GUS* plants, GUS staining was very strong in the central cylinder adjacent to the root tip. No staining was visible in the root tip or in root hairs (Fig. 3.2.1.). GUS-staining was less intense in older parts of the root hair zone where it was entirely limited to the central cylinder.

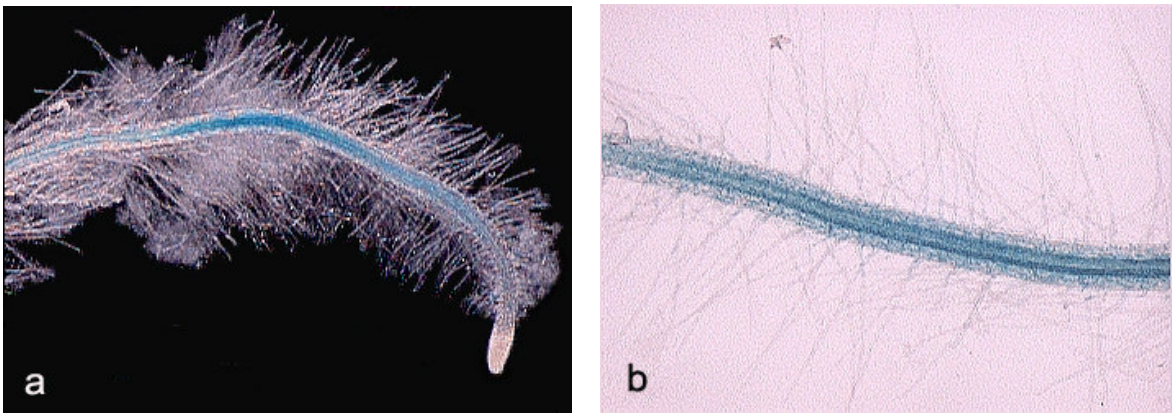

Fig. 3.2.1. *pAMT1.2*-GUS expression in roots. Expression was very strong in the central cylinder. In the root tip and in root hairs no expression was detected (a). In the root hair zone, weak expression was visible in the cortex but entirely lacked in root hairs (b).

In leaves, *pAMT1.2-GUS* driven GUS staining was found in all cells. However, staining was stronger in leaf veins than in parenchymatic tissue (Fig. 3.2.2.). Nevertheless, the staining was present throughout the leaf blade in young as well as in fully grown leaves.

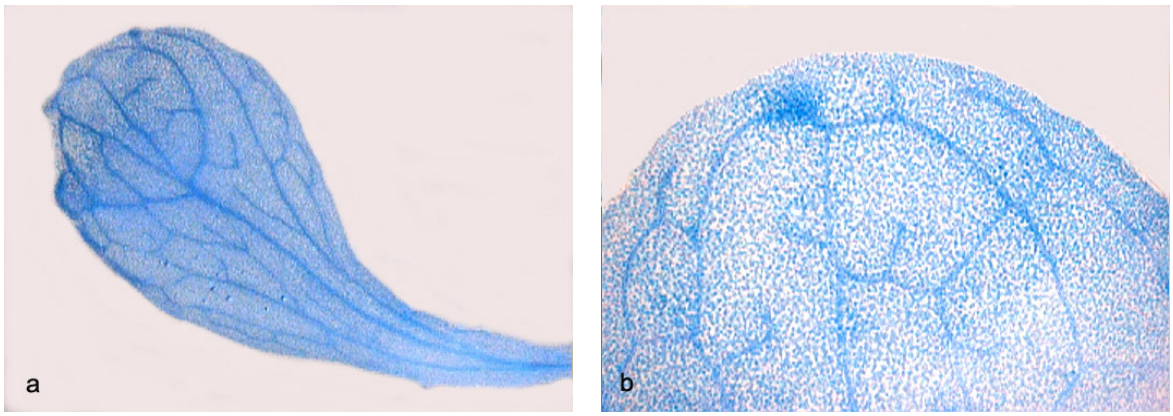

Fig. 3.2.2. *pAMT1.2*-GUS expression in leaves. The *AMT1.2* promoter was active in all cells of the leaf (a). GUS-staining was stronger in leaf veins than in parenchymal cells (b).

In flowers, expression of the *pAMT1.2-GUS* construct was not detected in any of the transformed plants.

3.3. *pAMT1.3-GUS* expression

The *pAMT1.3-GUS* construct showed a root expression pattern that was different to *AMT1.1* and *AMT1.2*. Unlike the latter, *AMT1.3* was only expressed in lateral roots and there only in the elongation zone. In this part, it was expressed in the central cylinder as well as the cortex and additionally in root hairs (Fig. 3.3.1 a and b), whereas *AMT1.1* and *AMT1.2* were solely expressed in the cortex and the central cylinder, respectively, and not in the root hairs. No GUS-staining was observed in other root parts.

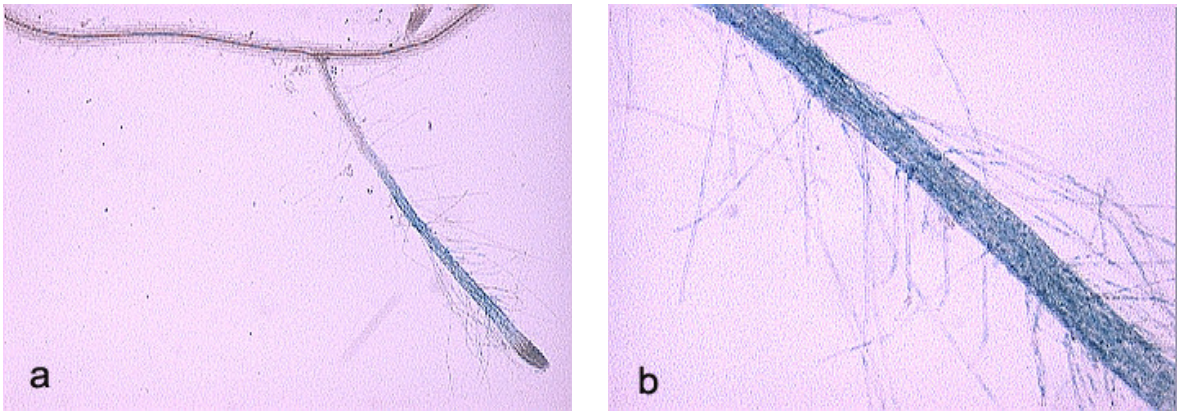

Fig. 3.3.1 *pAMT1.3* GUS expression in roots. GUS-staining was confined to the root hair zone and was not found in the main roots (a). In the root hair zone, staining was strong in the cortex, the central zylinder, and the root hairs (b).

In leaves, *pAMT1.3*-GUS staining was less distinct than in roots. It was expressed at low levels in the leaf blade. Here, the veins exhibited greater GUS-activity than parenchyma cells. However, no staining was detected in the leaf margins (Fig. 3.3.2 a and b).

No staining was detectable in any parts of the flowers in any of the investigated lines.

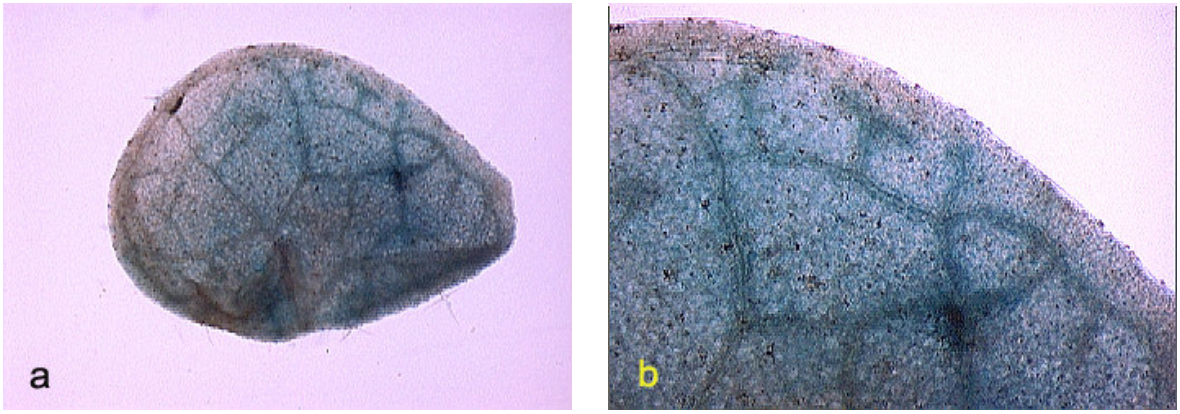

Fig. 3.3.2. *pAMT1.3*-GUS expression in leaves. GUS-staining was present in the parenchyma cells at low levels and at higher levels in the leaf veins (a). No staining was visible in the leaf margins (b).

3.4. *pAMT1.4-GUS* expression

In roots no GUS-staining was detected in any of the *pAMT1.4-GUS* plants investigated.

In leaves, faint but distinct staining was seen in all veins (Fig. 3.4.1.), but no other leaf cells were GUS-stained. This pattern was found in young growing leaves as well as in fully-grown leaves.

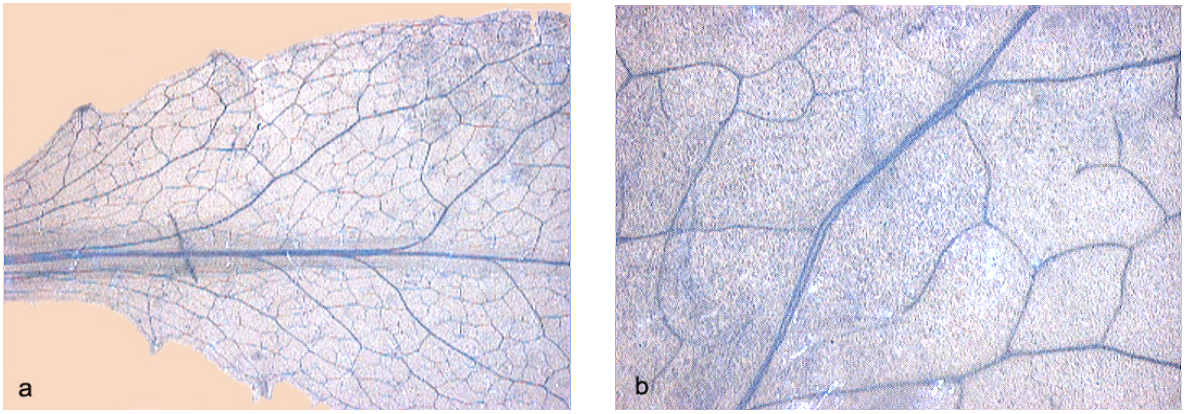

Fig. 3.4.1. *pAMT1.4*-GUS expression in leaves. Faint staining was restricted to leaf veins. No staining was detectable in parenchyma or meristematic cells.

A very strong and specific GUS-staining was observed in flowers. Here, only the pollen grains and no other flower part was stained at any stage of development (Fig. 3.4.2.). The staining of the pollen grains was much more intense than the staining of the leaf veins.

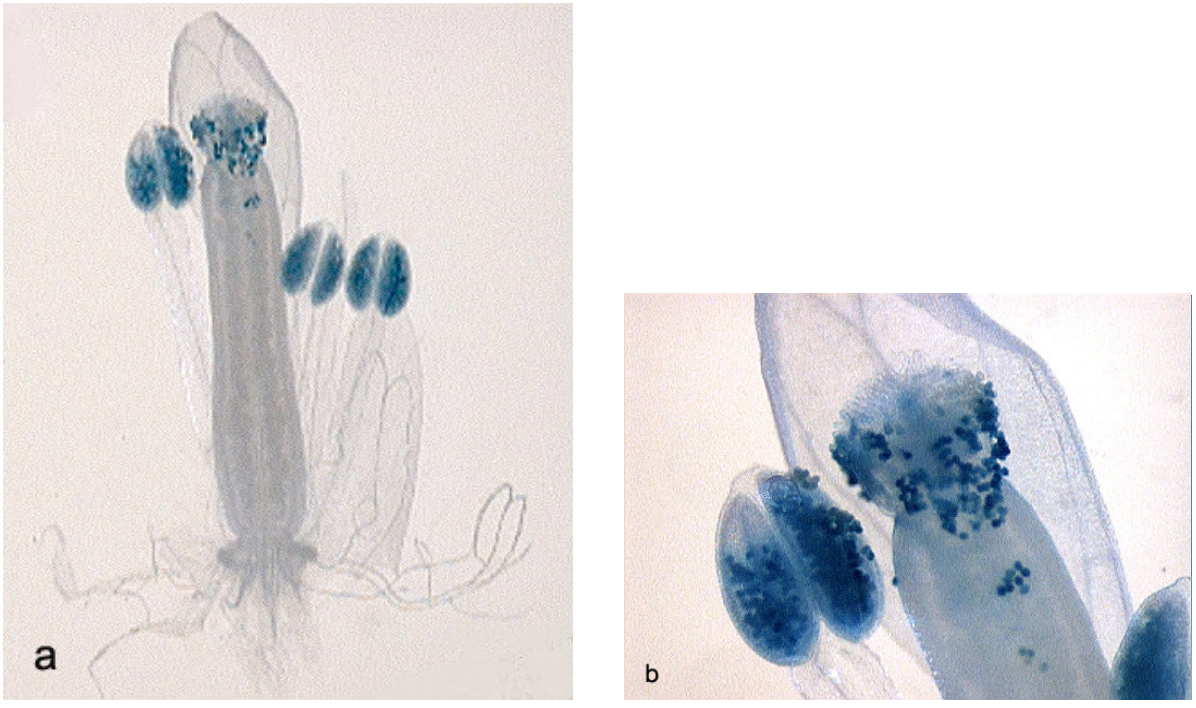

Fig. 3.4.2. *pAMT1.4*-GUS expression in flowers. Staining was restricted to pollen where it was very strong. No staining was detectable in other parts of the flower at any developmental stage.

3.5. *pAMT1.5-GUS* expression

In nitrogen deprived roots, expression of *pAMT1.5::GUS* was ubiquitous and intense. Staining was found in all parts of the root, i.e. the rizodermis, the cortex and the root hairs (Fig. 3.5.1. a). However, no staining of the root tip was observed (Fig.3.5.1. b).

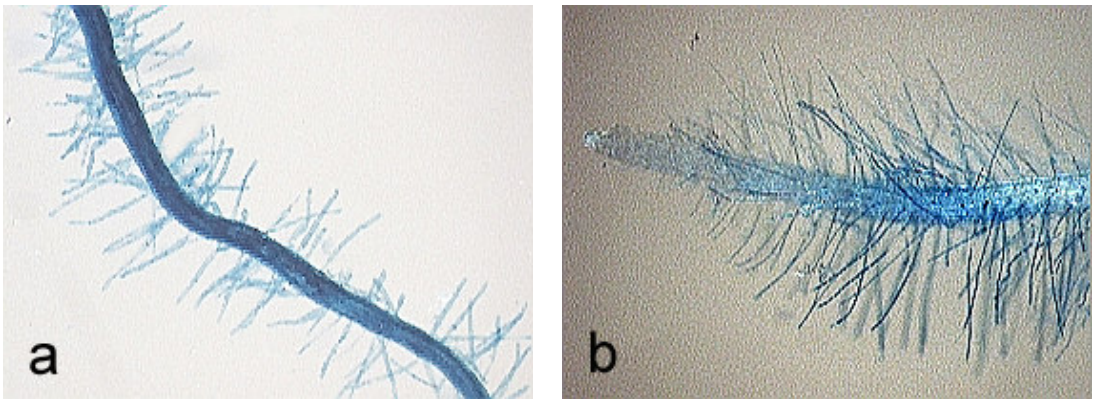

Fig. 3.5.1 *pAMT1.5 -GUS* expression in roots. GUS staining was ubiquitous in all parts of the root including root hairs (a). No staining was found in root tips (b).

In leaves and flowers, no staining was detected in *pAMT1.5-GUS* plants. However, intense staining occurred in the leaf blades of cotyledons (Fig. 3.5.2. a). Here, both parenchyma cells and veins were stained, with a slightly higher intensity in the latter. The stained part of the cotyledons was sharply separated from the unstained cotyledon stems. In some cotyledons, additional staining was visible in the leaf ground of the lower leaf. In these cases the stained leaf ground was again sharply separated from the unstained cotyledon stem (Fig. 3.5.2.b).

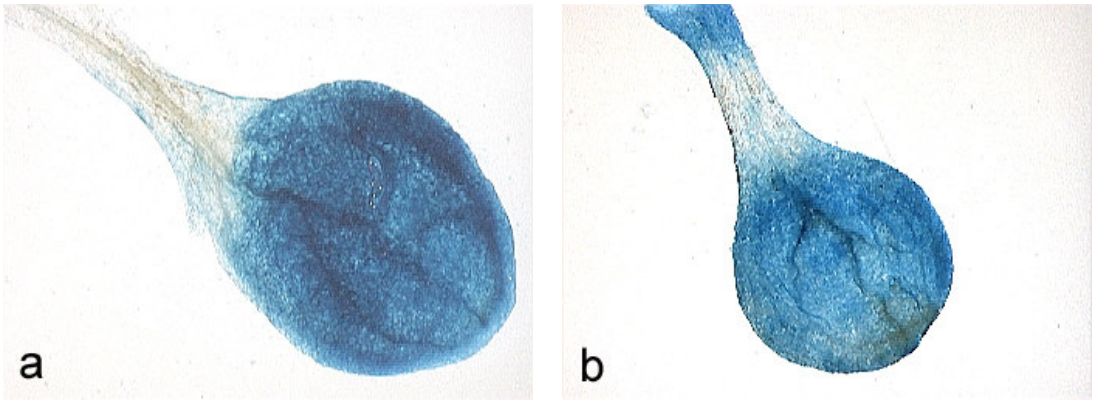

Fig. 3.5.2. *pAMT1.5* -GUS expression in cotyledons. The cotyledon blade expressed strong staining, which was distinct from the unstained cotyledon stem (a). When staining occurred in the cotlyedon ground, it was again distinct from the unstained stem (b).

3.6. *pAMT2.1-GUS* expression

In roots, *pAMT2.1-GUS* was exclusively expressed in lateral roots and not in primary roots (Fig. 3.6.1. a). GUS-staining was detected at a very early stage of lateral root development and was confined to the elongation zone. In this zone, GUS-staining was present in all parts of the root, i.e. cortex, central zylinder, and root hairs (Fig. 3.6.1 b). The root tips remained unstained, as did older sections of lateral roots.

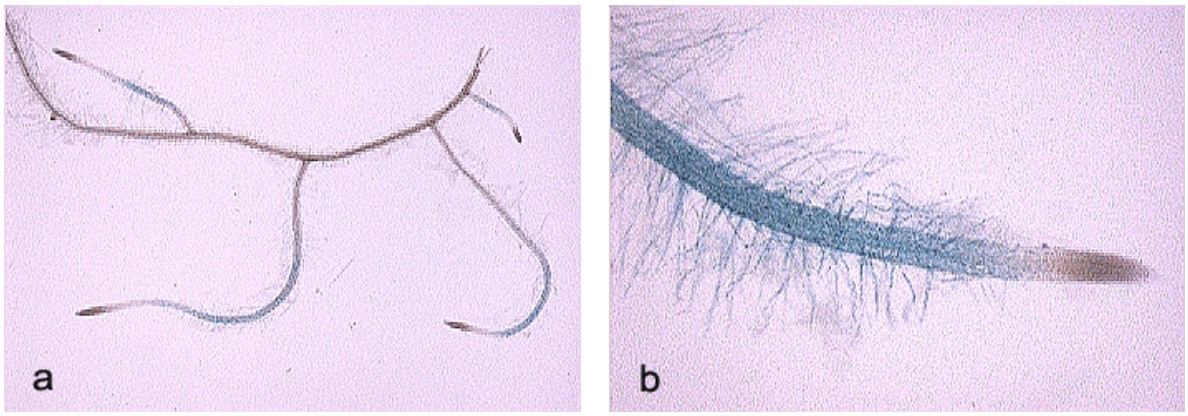

Fig. 3.6.1. *pAMT2.1-* GUS expression in roots. GUS-staining was confined to the elongation zone of lateral roots and not detectable in primary roots (a). In lateral roots, staining was present in the cortex and in the pericycle as well as in root hairs (b).

In leaves, *AMT2.1* driven GUS-staining was expressed in a development specific pattern in growing leaves. Only meristems at the leaf margins and the leaf veins were stained (Fig. 3.6.2. a). The staining was confined to the area of meristematic activity and to leaf veins (Fig. 3.6.2. b). Occasionally, the mid-rib also displayed GUS activity.

No staining was detected in other parts of the leaves at any developmental stage.

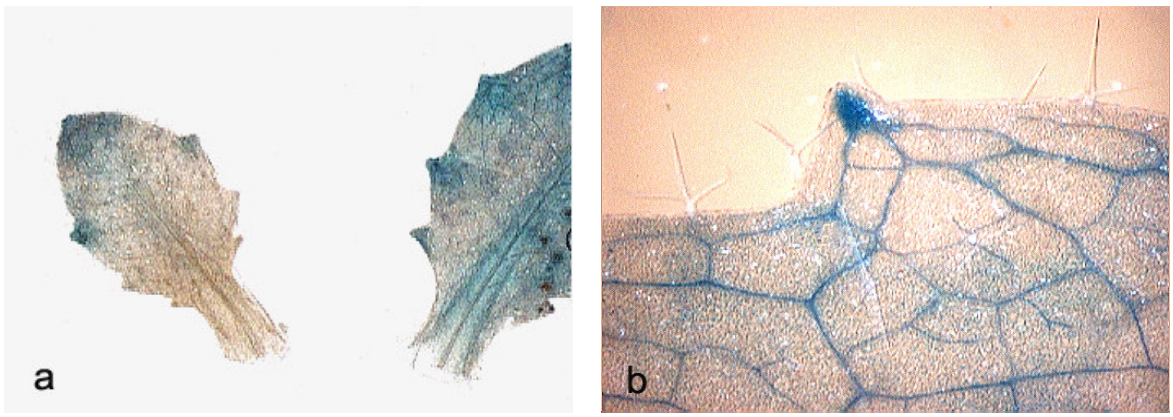

Fig. 3.6.2. *pAMT2.1*-GUS expression in leaves. GUS staining was confined to meristems at the leaf margin and to leaf veins.

In flowers, no GUS staining was observed in any of the investigated *pAMT2.1-GUS* lines, at any stage of development.

III.4. Characterization of *AtAMT* -T-DNA Insertion Lines

T-DNA insertional mutagenesis is a key resource for studying the gene functions of *Arabidopsis* and over than half of the estimated total number of genes in *Arabidopsis* are represented by T-DNA insertion lines in the various *Arabidopsis* stock centers (Winkler *et al*., 1998). Therefore, all accessible knock-out databases were searched for insertion lines of the *AtAMT*-genes. It was aimed to obtain a T-DNA insertion line for each *AMT*-gene, representing a complete loss of function mutation. Four different *AMT* T-DNA insertion lines were identified at the Syngenta®-T-DNA library and ordered. These four lines carried a T-DNA insertion in either At*AMT1.1, AtAMT1.2, AtAMT1.4*, or At*AMT2.1*. The lines were analysed on the genetic, physiological, developmental, and biochemical levels to identify any defects in the mutants due to the insertion of T-DNA into a specific *AMT* gene.

4. 1. Insertion Sites of T-DNA in *AtAMT* Genes

The insertion site of T-DNA in each mutant was identified initially by the sequence information provided by Syngenta®. Figure 4.1.1. gives the insertion sites of the T-DNA into the genes for each line which were named *SyAMT1.1*, *SyAMT1.2*, *SyAMT1.4* and *SyAMT2.1*. Furthermore, the distances of the T-DNA to the start codon of the translated region (ATG) and the length of the untranslated regions (UTR) are given.

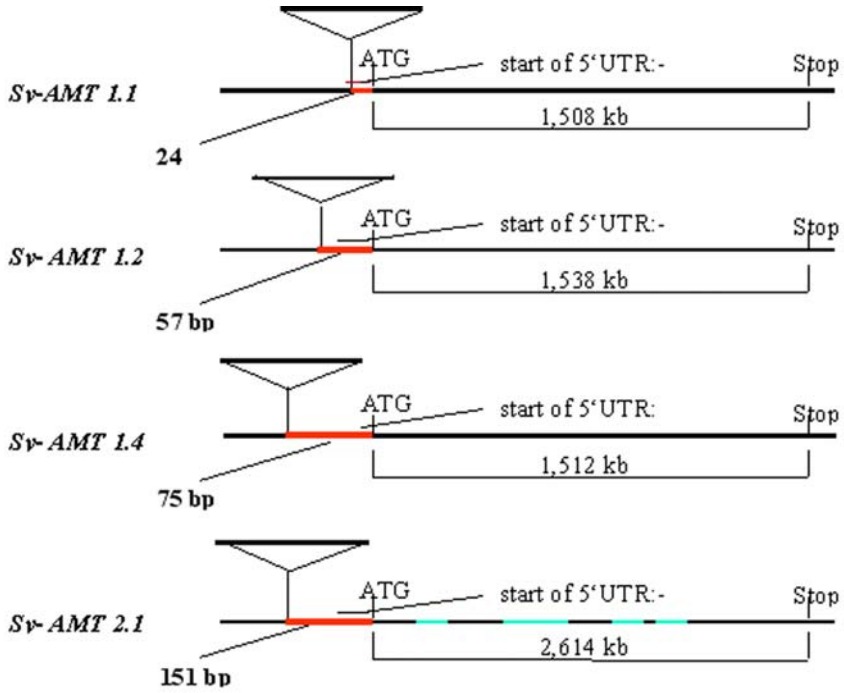

Fig. 4.1.1. Insertion Sites of T-DNA in *AMT1.1, AMT1.2, AMT1.4* and *AMT2*.1. For each T-DNA insertion line, named *SyAMT1.1, SyAMT1.2, SyAMT1.4* and *SyAMT2.1*, the distance from the T-DNA to the start codon (ATG, red) and the length of the untranslated region upstream of the ATG is given in basepairs (bp). *AMT2.1* carries 4 introns in the coding region, depicted in blue. Stop indicates the end of the translated region.

Figure 4.1.1. shows that all T-DNAs are inserted upstream of the start codon. In *SyAMT1.1* the T-DNA inserted into a position relatively close to the ATG within the 5'-UTR (24 bp). In *SyAMT1.2* the T-DNA inserted at the beginning of the 57 bp long UTR, while *SyAMT1.4* and *SyAMT2.1* carried the T-DNA 75 bp and 151 bp upstream of the UTR, respectively.

Although the coding region was not directly hit by these insertions it was assumed that the insertion of the T-DNA into the 5'-UTR or promoter would lead to a reduction of transcript if not to a complete loss of function of the genes.

III.4.2. Developmental and Morphological Characterization of the T-DNA Lines

A phenotype of mutant plants obtained by T-DNA insertional mutagenesis is, if observable at all (Bouche and Bouchez, 2001), often rather variable. To phenotypically characterise such mutants, it is often necessary to closely investigate developmental stages in detail and by means of statistical approaches. Ammonia plays an essential role in all growth and developmental processes. An impairment of the ability to synthesise specific ammonium transporters could lead to a reduction of ammonia uptake from the soil or retention in root or shoot cells. This could lead to retardation in growth and/or changes in the timing of developmental events. These effects could be apparent under normal nutritional conditions or might be exposed under artificial shortages of ammonia. To determine possible impairments in developmental and morphological traits, the *AMT* T-DNA lines (Fig. 4.2.) were screened for differences in vegetative and

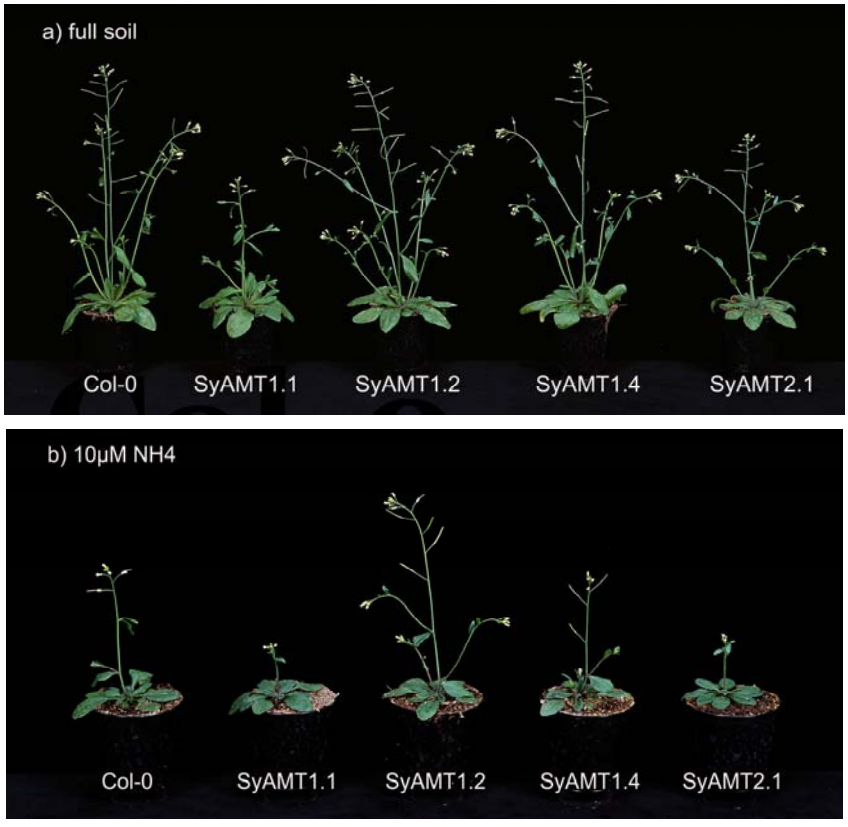

Fig. 4.2. T_3-phenotypes of the SyAMT-lines and WT plants grown on soil (a) and o-soil containing 10 µM NH_4Cl (b), 29 days after germination. Note that moderate variation in phenotype occurred within individual lines (see text).

reproductive growth. Vegetative development was analysed with respect to root growth. The reproductive period was analysed in respect to the parameters infloresence length at different time points, bolting and flowering time, and total seed mass.

4.2.1. Root growth of *AMT* T-DNA Lines Under Different Nutritional Conditions

Seeds of homozygous T-DNA lines were grown on vertical sterile culture plates at constant light conditions for 8 days (see Methods). Each line and the corresponding WT was grown on media containing low and high concentrations of ammonium, nitrate (both 100 µM and 1mM) and glutamine (500 µM, 1 mM). At day 3, 4, 6, and 8 the root lengths were measured under a binocula microscope (Fig. 4.2.1.1.) and the mean values of the root length were calculated. Figure 4.2.2. shows the root development of seedlings grown on plates containing 100µM (a) and 1mM (b) ammonium. Root growth was approximately linear during the first week. At the last measurement at day 8 the root growth was slower, possibly due to the physiological stress the plants experienced on the sterile media in the artificial environment. Root growth was not significantly different between T-DNA lines and the WT at any concentration and time point. The toxicological effect of high ammonium concentrations became visible at 1 mM. At this concentration, root growth was slower than at 100 µM (e.g. 85 % shorter at day 6 for the WT). WT and T-DNA lines were equally susceptible to the growth inhibiting effect of the 1 mM ammonium concentration (Fig. 4.2.1.2.).

Fig. 4.2.1.1. Four days old seedling, grown on 100 µM ammonium on vertical plates, at constant lines for root growth assay (bar= 2 cm.)

Plants that were grown on plates containing nitrate as the sole nitrogen source exhibited linear root growth during the first 6 days. Plants grown on 100 µM nitrate grew slower than plants with a 1 mM nitrate supply. Root growth of WT plants was not significantly different to the growth of the *SyAMT T*-DNA lines (Fig. 4.2.1.3.).

Plants grown on plates containing glutamine as the sole source of nitrogen showed a faster root growth on 500 µM glutamine than on 100 µM of ammonium or nitrate. Roots grew faster on 1 mM glutamine than on 1 mM ammonium, but root growth on 1 mM glutamine was not siginificantly different to that on 1 mM nitrate. To summarise, no significant differences in root growth were observed between the WT and the T-DNA lines (Fig. 4.2.1.4.).

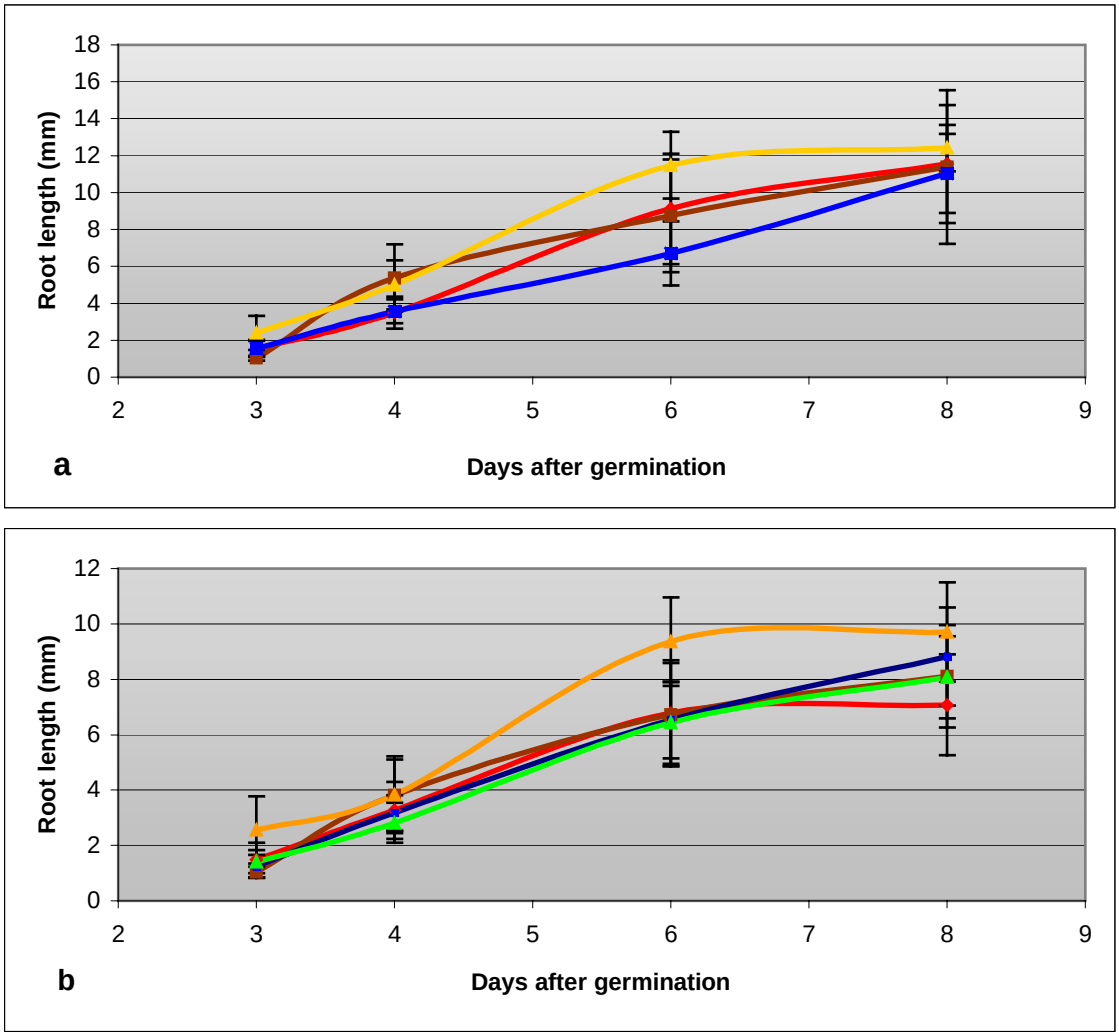

Fig. 4.2.1.2. Root growth of T-DNA lines and the WT at 100 µM NH_4 (a) and 1 mM NH_4Cl (b) during 8 days after germination (the WT is depicted in red, *SyAMT1.1* brown, *SyAMT1.2* yellow, *SyAMT1.4* blue, and *SyAMT2.1* green). Data points are averages of 20-30 separate plants. Error bars represent the standard error.

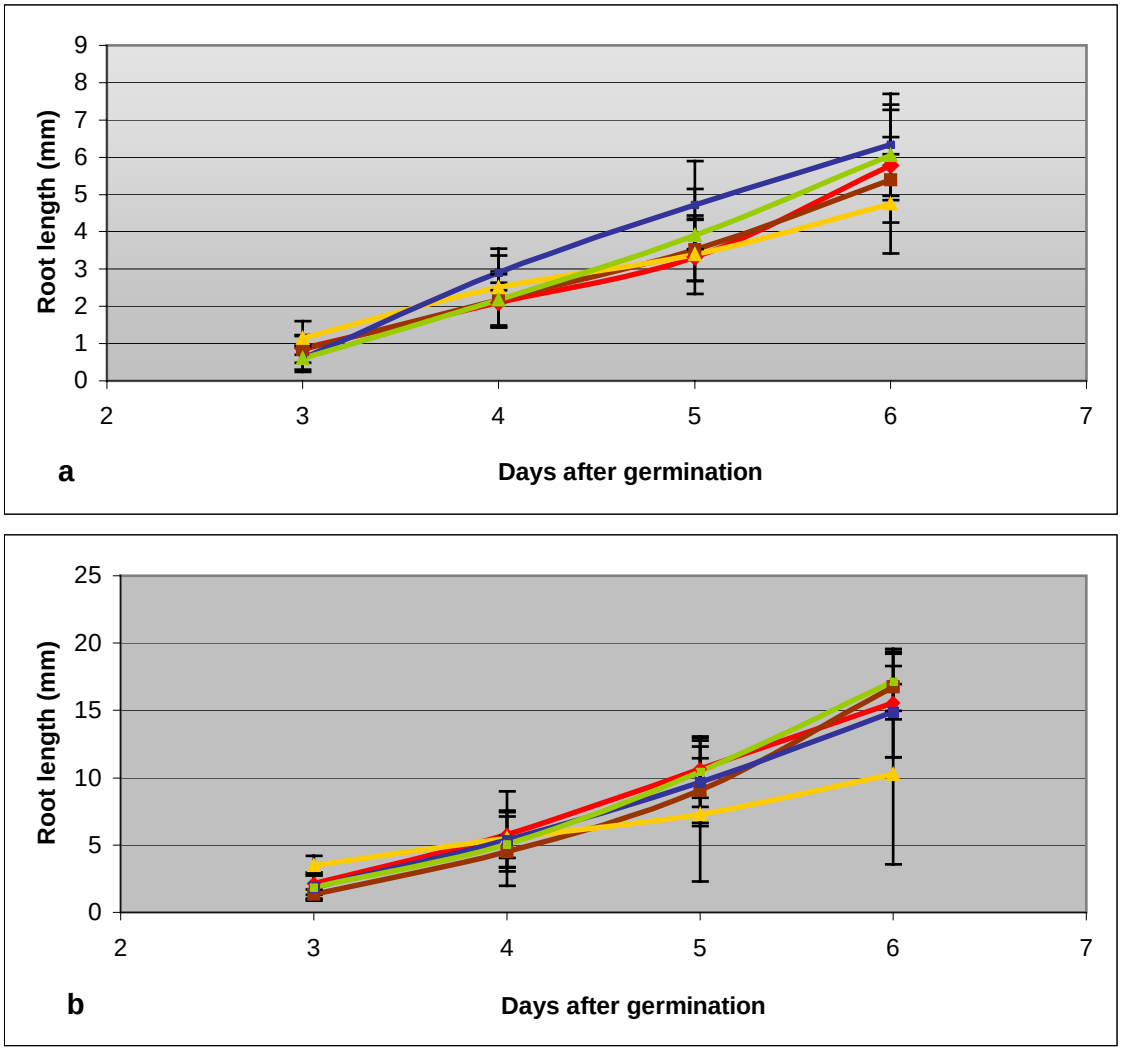

Fig. 4.2.1.3 Root growth of T-DNA lines and the corresponding WT at 100 µM NH_4NO_3 (a) and 1 mM NH_4NO_3 (b) during 6 days after germination (the WT is depicted red, *SyAMT1.1* brown, *SyAMT1.2* yellow, *SyAMT1.4* blue, and *SyAMT2.1* green). Data points are averages of 20-30 plants. Error bars represent the standard error.

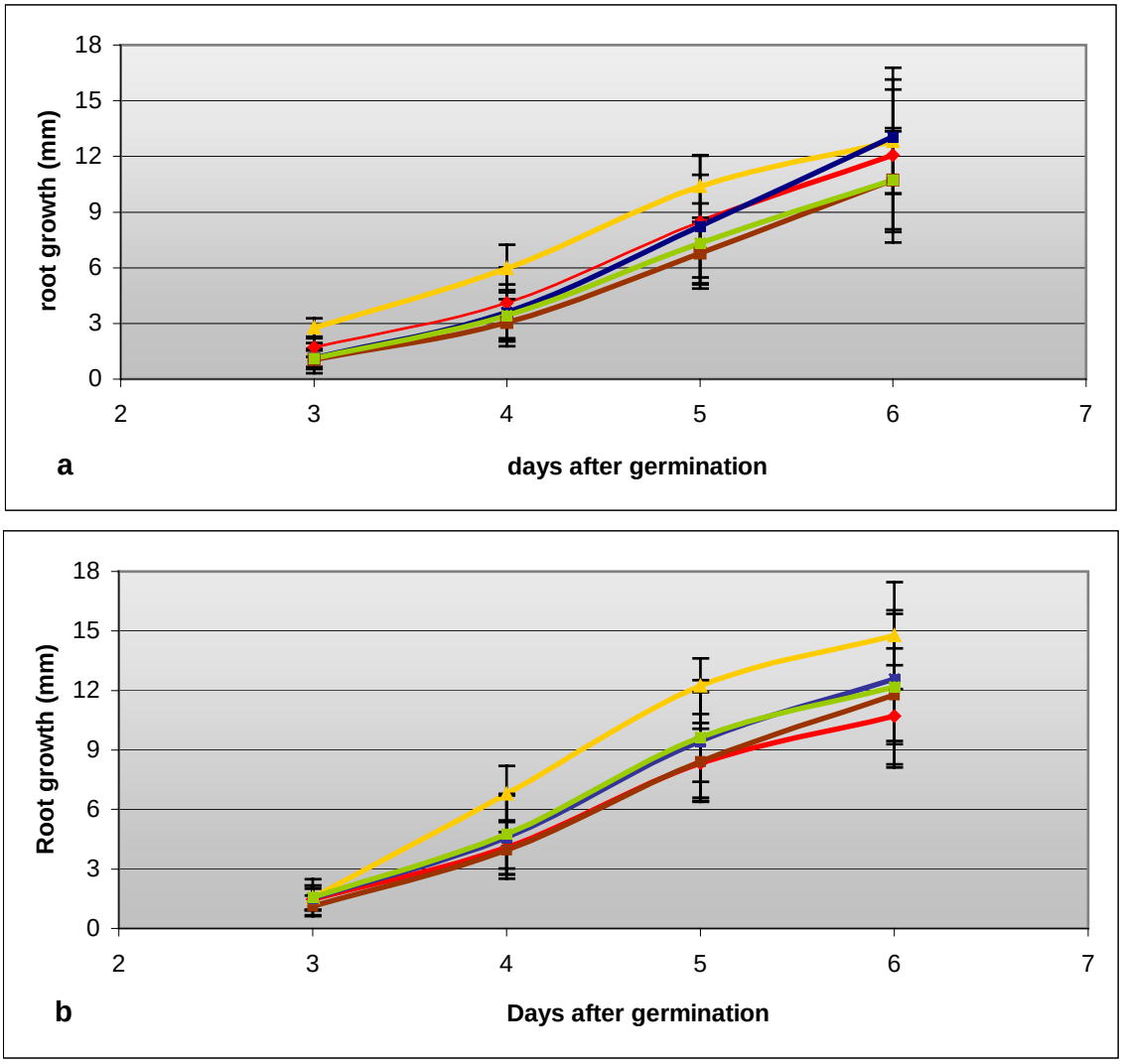

Fig. 4.2.1.4. Root growth of T-DNA lines and the corresponding WT at 500 µM glutamine (a) and 1 mM glutamine (b) during 8 days after germination (the WT is depicted red, *SyAMT1.1* brown, *SyAMT1.2* yellow, *SyAMT1.4* blue, and *SyAMT2.1* green). Data points are averages of 20-30 plants. Error bars represent the standard error.

4.2.2. Infloresence Development of *AtAMT*-T-DNA Lines

The infloresences are plant organs with rapid growth, which together with subsequent flower development and seed production increases the demand for nitrogen. For that reason the inflorescence development of the T-DNA lines were analysed in detail and compared to the WT (Fig. 4.2.2.1.). 20 plants of each line were grown on soil and on low nutrient soil plus10 µM NH_4Cl as nitrogen source. This concentration was maintained by fertilizer application every second day (2.4.2). Plants were grown in seperate trays at different locations in the greenhouse to avoid growth differences due to small environmental variations in the green house.

On full soil, the inflorescence length of all lines was similary to the wild-type at all time points. No significant differences were observed (Fig. 4.2.2.1.a). On soil, containg 10 µM NH_4Cl, the *SyAMT1.1* and *SyAMT1.2* lines showed on average shorter stems relative to the WT. However, these differences were not significant and the relative differences in mean stem length decreased in the course of the development

(Fig. 4.2.2.1.b). At the end of the flowering period all lines had the same infloresence length on average, with differences in mean length falling within the standard deviation. Among the *SyAMT1.1* line, a few plants grew relatively small infloresences, which led to a comparably high standard deviation at 10 µM NH_4Cl.

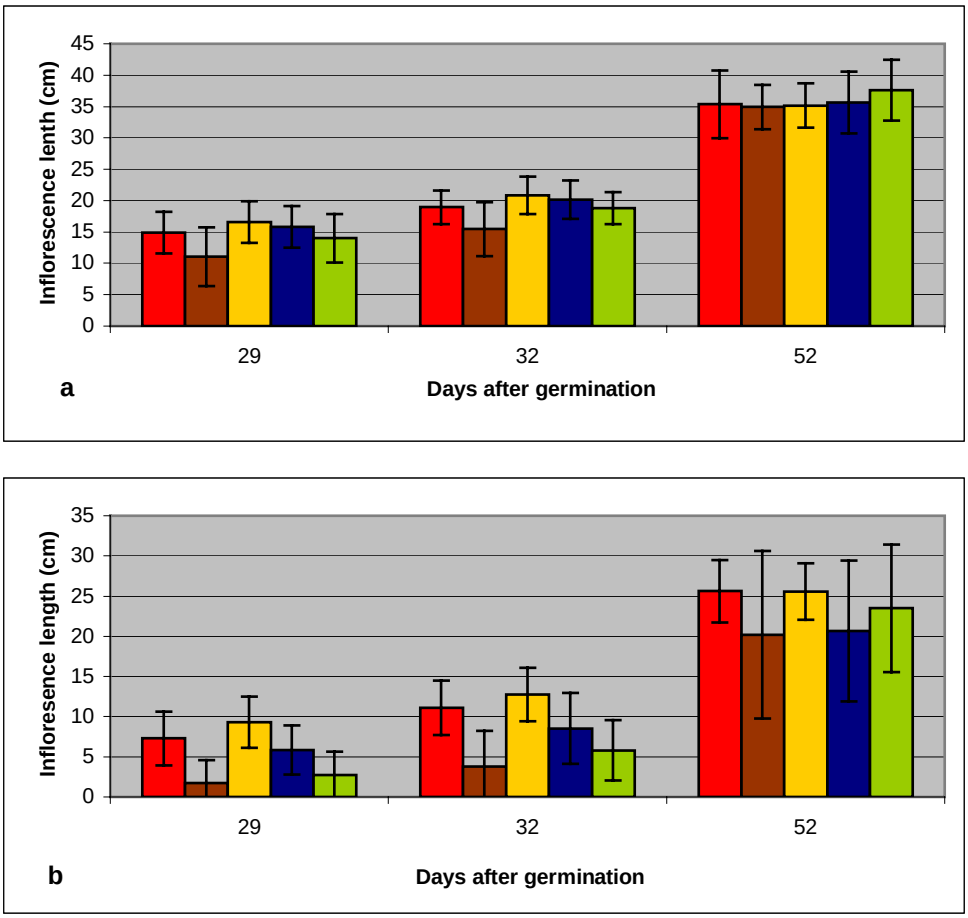

Fig. 4.2.2.1 Infloresence length of T-DNA lines and the WT grown on full soil (a) and 10 µM NH_4 containing soil (b). The measurements were taken 29, 32, and 52 days after germination (WT-red, *SyAMT1.1*-brown, *Sy-AMT1.2* yellow, *Sy- AMT1.4,* blue and *SyAMT2.1*-green). Data points are averages of measurements of 20-30 plants. Error bars represent the standard error.

Apart from measurements of the infloresence length at different time points, infloresence development was monitored with respect to three distinct stages: Bolting, which is the first appeareance of the buds, flower opening, and the total seed weight at the end of flowering.

At the time when about half of the soil grown WT showed buds, the percentage of bolting plants of each line was determined. At the day when almost all WT plants had opened flowers, the percentage of plants with opened flowers from every line was determined. Finally, at the end of flowering, when no further flowers were produced, seeds of individual plants were collected and the total seed mass for each plant was determined (Tab. 4.2.2.1.).

Seventeen days after germination, the number of plants with emerged buds was determined. At this time 65 % of the WT plants grown on normal soil were bolting (Tab. 4.2.2.1.). Among the T-DNA lines, *SyAMT1.2* was more advanced in inflorescence growth with 80 % bolting at this point. However, the growth was not

significantly faster and the differences in means became less apparent at the late stages of the flowering period. *SyAMT1.4* had the same percentage of bolting plants as the WT at seventeen days after germination but *SyAMT1.1* and *SyAMT1.2* were much less advanced with only 45 % and 10 %, respectively. This pattern was repeated at 10 µM NH_4Cl but at this concentration *SyAMT1.1* was as strongly retarded as *Sy-AMT2.1* with only 2.5 % bolting. At this concentration 25 % of WT-plants had emerged buds after 17 days.

Twenty six days after germination, the number of plants with opened flowers was counted. At this time 95 % of the WT, 95 % of *SyAMT1.2* and 90 % of *SyAMT1.4* had opened flowers. *SyAMT1.1* and *SyAMT2.1* were less advanced in flower development. Although most of the plants had emerged buds at that time point, only 55 % and 50 % had opened flowers, respectively. This pattern was repeated on 10 µM NH_4 but the retardation of flowering time was much stronger for *SyAMT1.1* and *SyAMT2.1* (Tab. 4.2.2.1.).

At the end of the vegetative period the seed weight of each plant was measured and the average seed weight for a plant for each line was determined. For plants grown on normal soil, there was no significant difference between the WT and *SyAMT1.1* and *SyAMT1.2* although average seed weight for *Sy-AMT1.1* and *Sy-AMT2.1* was less than that of the WT. The pattern changed for plants grown on 10 µM NH_4Cl. At this concentration the total seed weight of all T-DNA lines was smaller than the seed weight of the WT, but again these differences were not significant (Tab. 4.2.2.1.).

Tab. 4.2.2.1. Developmental parameters, growth conditions, and growth patterns of the T-DNA insertion lines and the wildtype control.

Parameters	Growth Condition	Col-o	*Sy-AMT1.1*	*Sy-AMT1.2*	*Sy-AMT1.4*	*Sy-AMT2.1*
Bolting plants (%)*	Full soil	65	45	80	65	10
	10µM NH_4	35	2,5	30	22,5	2,5
Flowering plants (%)*	Full soil	95	55	95	90	50
	10µM NH_4	60	15	65	45	10
Average Plant Seed Weight (mg)	Full soil	172 (± 88)	131 (± 50)	172 (± 45)	172 (± 54)	156 (± 43)
	10µM NH_4	50 (± 12)	45 (± 12)	41 (± 14)	39 (± 20)	31 (±10)

*of a total of 40 plants

4.3. Quantification of *AMT* Transcript Levels in *AtAMT*-T-DNA Lines

Homozygous single insert T-DNA lines were selected by PCR and propagated. Samples of the obtained seeds and control *Col-o* seeds were sown on full nutrient soil and grown for 21 days in green house conditions. Leaves were harvested, the RNA extracted and reverse-transcribed into cDNA (see Methods 2.3.2.). The cDNA levels of the *AMT* genes that carried the T-DNA insertion were analysed by quantitative real time PCR (qRT-PCR) and compared to WT gene expression levels under the same conditions (Fig. 4.3.1). WT expression levels were similar to leaf specific expression detected in earlier qRT-PCR experiments (2.1.).

AtAMT1.1, which is generally expressed at high levels in leaves was also expressed at relatively high levels in the *SyAMT1.1* line. However, the expression was reduced to 73 % of the WT level (Table 4.3.1). At*AMT1.2* which is constitutively expressed in leaves in the WT was also expressed in the SyAMT1.2 line but was reduced to 89 % of the WT level. At*AMT1.4* is generally expressed at low levels in the vegetative tissues of WT plants (see 1.1.2 and 2.4) and was detected at low levels in WT-leaves. However, it was also detected at comparable levels in the *SyAMT1.4* line at 88 % of WT expression level. At*AMT2.1* which is expressed at low levels in WT leaves under full nutrient conditions showed no reduction in transcript levels in the *SyAMT2.1* line relative to the WT.

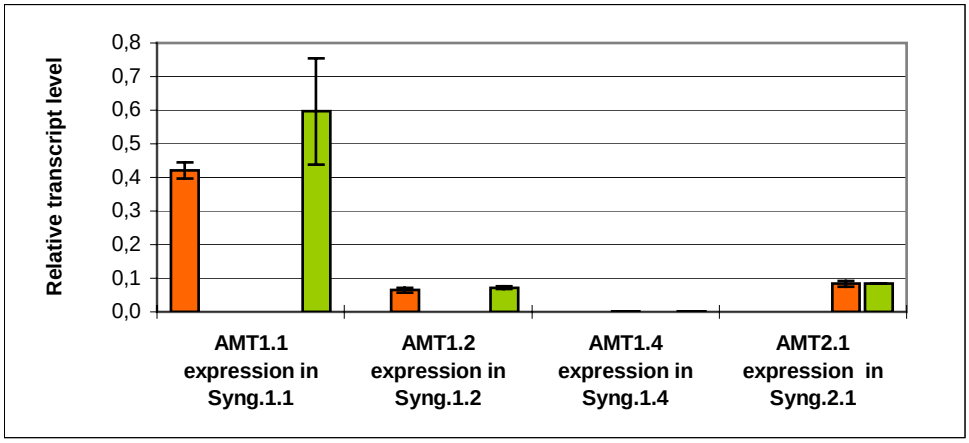

Fig. 4.3.1 At*AMT* transcript levels in T-DNA insertion lines relative to *UBQ-10*. *SyAMT* transcript levels are depicted in red and WT (var. *Col-0*) transcript levels are depicted in green. (*AMT1.4* transcript levels are very low for both, *SyAMT1.4* and the WT, and not shown on this picture; see text for details).

4.4. ^{14}C-Methylammonia Uptake Kinetics of *AtAMT* T-DNA Lines

The ammonia uptake kinetics of the T-DNA-insertion lines were analysed and compared to the WT, using the radioactive analogue ^{14}C-methylammonium (^{14}C-MA) as substrate. Based on the relatively high expression of the transporters AMT1.1 and AMT1.2 in vegetative tissues (1.2.) and their high affinity and high V_{max} for MA transport (Wood, personal communication), it was expected that these would contribute most to MA uptake in vegetative wildtype plants. Therefore, ^{14}C-MA uptake was measured for T-DNA lines SyAMT1.1 and SyAMT1.2.

Plants were grown in a liquid culture system for seven days and subsequently deprived of nitrogen for 24 hours, as described in Material and Methods. Plants were then harvested and washed in N-free medium to eliminate all traces of ammonium. Subsequently, 16 pools of 5 to 10 seedlings of the WT, SyAMT1.1 and SyAMT1.2, were incubated in 10 µM or 100 µM for 10 minutes or in 1 mM for 15 minutes. After these times, plants were washed three times and the ^{14}C -MA in plants was determined by liquid scintillation.

There were no significant differences between ^{14}C -MA uptake by wildtype and mutant plants (Fig. 4.4.1. and 4.4.2.).

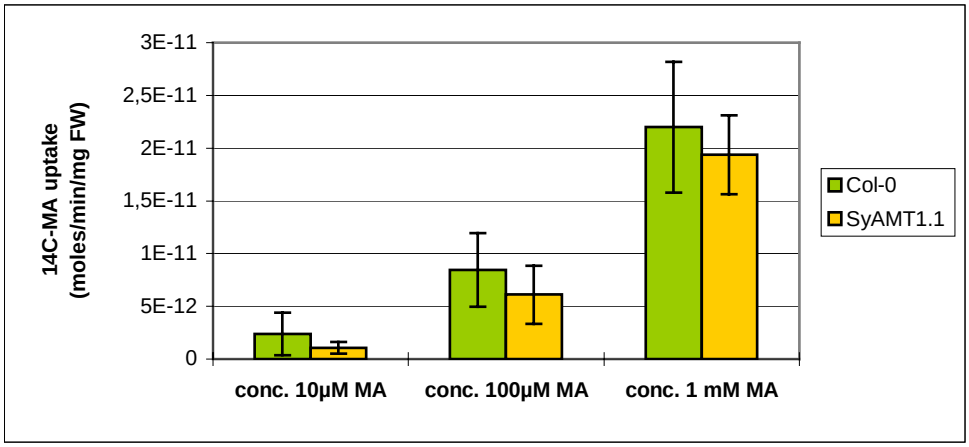

Fig 4.4.1. ^{14}C-MA uptake of *Col-0* and SyAMT1.1 at 10 µM, 100 µM and 1 mM MA (each bar represents the mean of 16 plants, error bars represent standard errors).

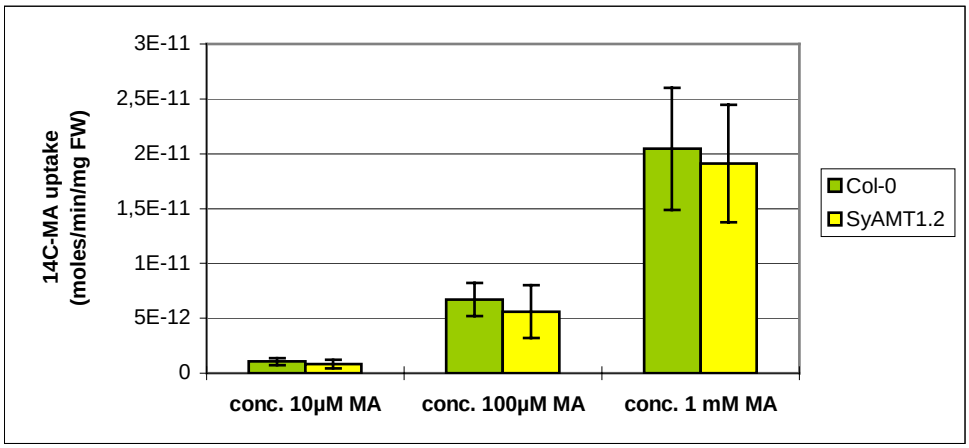

Fig. 4.4.2. ^{14}C-MA uptake of *Col-0* and SyAMT1.2 at 10 µM, 100 µM and 1 mM MA (each bar represents the mean of 16 plants, error bars represent standard errors).

4. 5. Creation of Double Mutants of the T-DNA Lines

Due to the relatively long time that is required to create and isolate homozygous double mutant lines, reciprocal crossing was begun immediately after homozygous T-DNA single insert lines were isolated. Crossings were performed in all possible combinations to obtain a complete set of *AMT* double knock out lines (Table 4.5.1) and to provide a basis for later crossing to produce quadruplet *AMT* knockout lines. The crossings were performed reciprocally to eliminate possible gametophytic effects.

Table 4.5.1: Combinations of double mutants by crossing the Syngenta T-DNA insertion lines reciprocally (indicated by an X).

♂\♀	*Sy-AMT 1.1*	*Sy-AMT 1.2*	*Sy-AMT 1.4*	*Sy-AMT 2.1*
Sy-AMT 1.1		X	X	X
Sy-AMT 1.2	X		X	X
Sy-AMT 1.4	X	X		X
Sy-AMT 2.1	X	X	X	

F1 seeds from each cross were harvested and selfed and the resulting F2 individuals were screened by PCR to identify homozygous double mutants (II.2.8.) The identified homozygous double mutants were grown until flowering. The phenotypes of these F2-plants were not different to the WT at any stages of development (e.g. leaf size and shape, infloresences, flowering). Since the T-DNA effects on *AMT* gene transcript levels were considered too weak to make further experiments with the selected double mutants worthwhile, no experiments were performed with them.

III. 5. Characterization of *AMT1.1*RNAi lines in *Arabidopsis thaliana*

The principle of RNA-induced gene silencing (RNAi) involves the expression of double-stranded RNA, (dsRNA) which triggers a sequence-specific RNA degradation mechanism that effectively silences the targeted gene (Waterhouse *et al*., 2001). Initiation of silencing occurs upon recognition of the dsRNA by an enzyme complex called Dicer (Fig. 5.1.) that processes double-stranded RNA into about 21–25 nucleotide RNAs, known as small interfering RNAs (siRNAs). These siRNA molecules become incorporated into a nuclease-containing enzyme complex called RISC (RNAi silencing complex, Fig. 5.1.) and guide the complex to the homologous RNA substrate. There, the RISC complex degrades the mRNA that is complementary to the siRNA, associated with this complex (McManus&Sharp, 2002). By the use of transgenes that express a self-complementary hairpin RNA (hpRNA) the targeted gene is silenced consistently. The hpRNA structure mimics dsRNA and provides the specifity of the RNAi (Hannon, 2002). Since the siRNAs are only of 21-25 bp in length, complete homology between the introduced gene and the target gene is not a requirement for the successful initiation of RNA silencing (Voinnet *et al*., 1998). The homology required to initiate RNA silencing can be as short as 21 identical nucleotides. However, in this case silencing is less extensive and more transient than with larger inserts (Thomas *et al*., 2001). In an attempt to target a whole gene family, it is essential that all members share sufficient homology. Thus, prior to the construction of the At*AMT1.1*-hpRNA construct, the cDNAs of *AtAMT1* and *AtAMT2* were checked for extent of identities (Fig. 5.2.). The alignment of the cDNAs of the *AtAMT* genes was performed with the Multiple

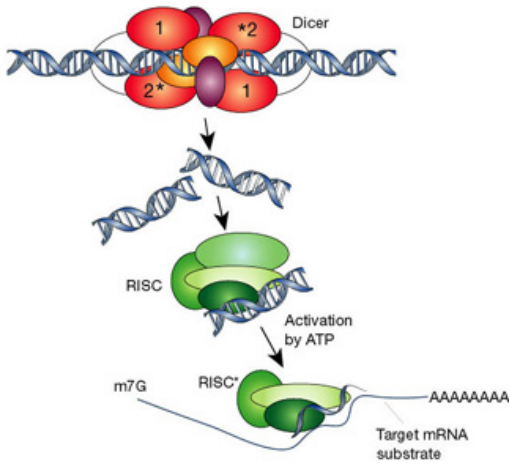

Fig. 5.1. The Mechanism of RNA interference. RNAi is initiated by the Dicer enzyme which processes dsRNA into ~ 22 nucleotide siRNA. The siRNAs are incorporatedinto the RISC and guide that complex to homologous RNA substrates which become degraded (picture taken from Hannon, 2002, slightly modified.)

A

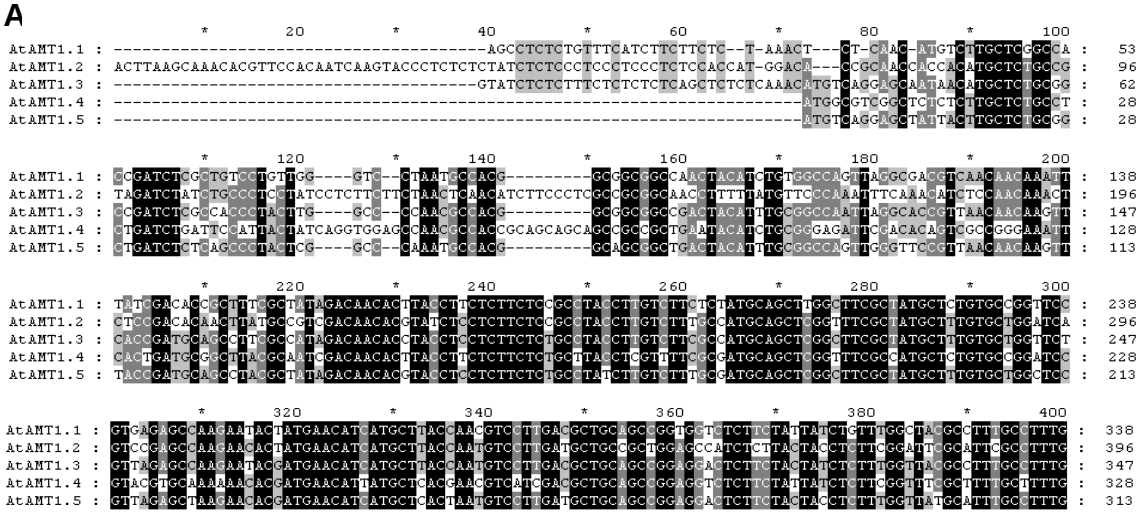

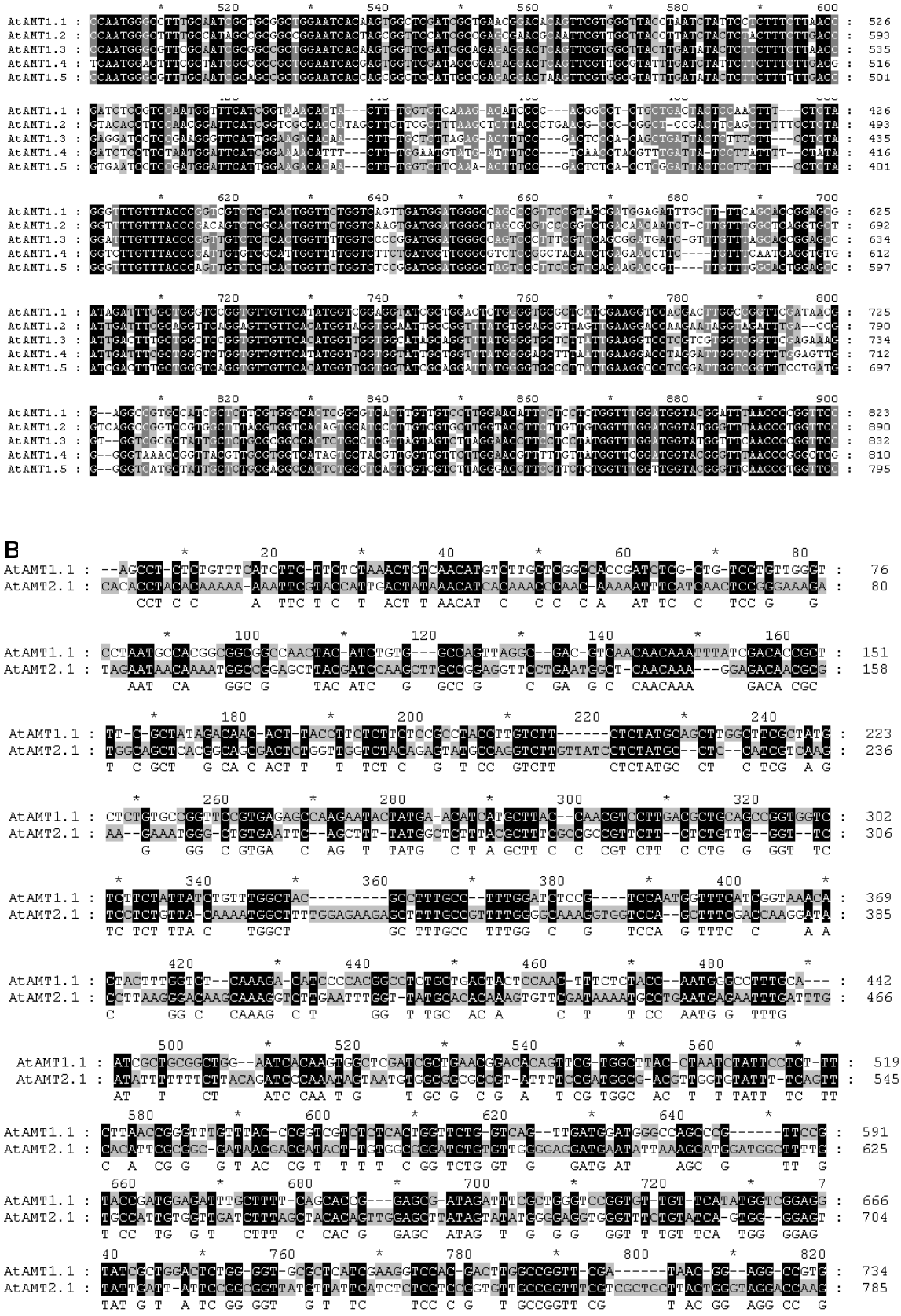

Fig. 5.2. Alignment of the nucleotides 1-800 (5'-end) of the cDNAs of the *AtAMT1* gene family (A) and the cDNA of *AtAMT2* (B). In the *AtAMT2,1* sequence, short stretches of identical nucleotides are interrupted by short non-identicl stretches. (Black Shadings indicate identical nucleotides.)

Sequence Alignment Editor & Shading utility 2.6.002 (www.psc.edu/biomed/genedoc) and is given for the first 800 bp. Among the *AtAMT1* gene family all genes except for *AtAMT1.5* share several 21-25 bp long stretches which are identical to *AtAMT1.1* within the first 800 bp. *AtAMT1.5* does not share continous 21-25 bp long identical stretches, but a few up to 19 bp ling identical stretches which are interrupted by single nucleotide substitutions (Fig. 5.2.A). RNAi induced gene silencing of the *AtAMT1* gene family by a 800 bp long *AtAMT1.1*-hp construct was considered promising. *AtAMT2.1* is much less related to *AtAMT1.1* and shares only short identical sequences up to eight base pairs in length (Fig. 5.2.B). Although these sequences were frequent, it was uncertain if these identities were sufficient to serve as recognition sites for the siRNAs.

5. 1. Creation of single insert *AtAMT1.1RNAi* Lines

After the construction of the GATEWAY™ *AMT1.1*-hpRNA destination vector (see Methods 2.2.1.1) it was transformed into wildtype *A. thaliana*. The seeds of the T_0-generation were harvested and the T_1-generation was selected by BASTA-resistance (Fig. 5.1.1).

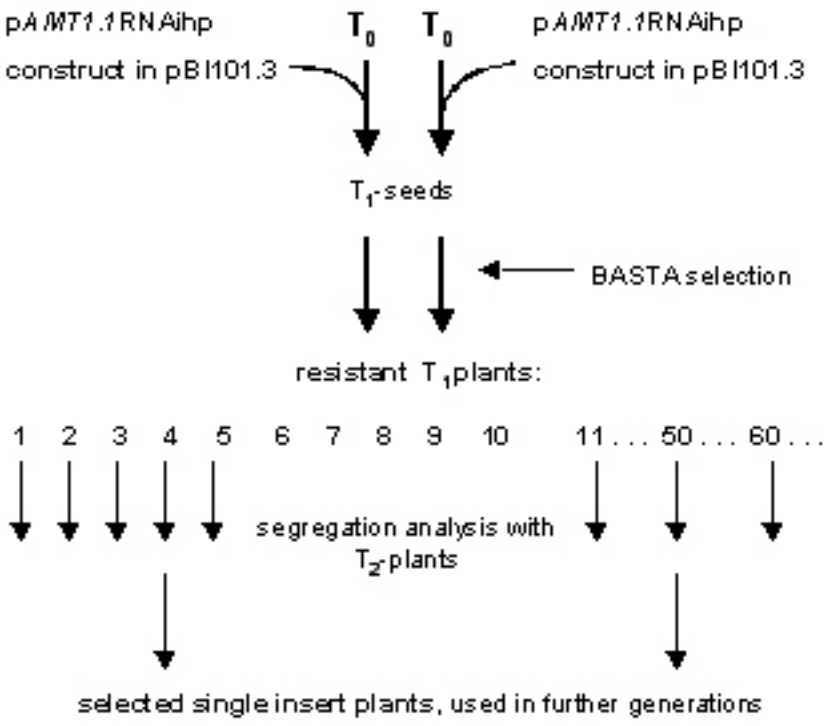

Fig. 5.1.1 Creation of *AtAMT1.1*RNAi lines and isolation of single insert lines in the T_2 generation. T_1-seedlings were selected by BASTA for a functional insertion. BASTA resistant T_1-plants were selected and the descendants of these plants were submitted to segregation analysis in the T_2-generation. Plants with one functional insertion were selected for further analysis.

The phenotype of the T_1-generation was very heterogenous (Figure 5.1.2). Many BASTA resistant plants had wildtype appearance but a lot of plants had a phenotype different to the WT. These could be roughly clustered into 4 different phenotypes but many intermediates existed between the respective categories and wildtype plants. In the still segregating populations some of the phenotypes and intermediates were possibly due to stochastic epigenetic effects caused by the insertion events and not by the RNAi activity. The first category was a set of plants which was very small in size and relatively late flowering (see Figure 5.1.2. - dwarfed). The leaves remained small throughout the life cycle and less leaves were produced compared to any other group or the WT. The shape of the leaves was similar to the wildtype leaves. The second category contained plants which had a densely filled rosette. Compared to the WT, the rosettes remained small in diameter and except for the oldest leaves the leaves remained smaller than the wildtype leaves throughout the life cycle. When rosette growth of the WT had stopped after flowering, new rosette leaves were continously produced by category two plants during flowering. This gave plants of this category a bushy phenotype due to the many densely packed and small leaves (Fig. 5.1.2 – bushy). The late leaves remained small in size and senescence was delayed. The shape was not different to wildtype leaves. The infloresence of these plants remained relatively short.

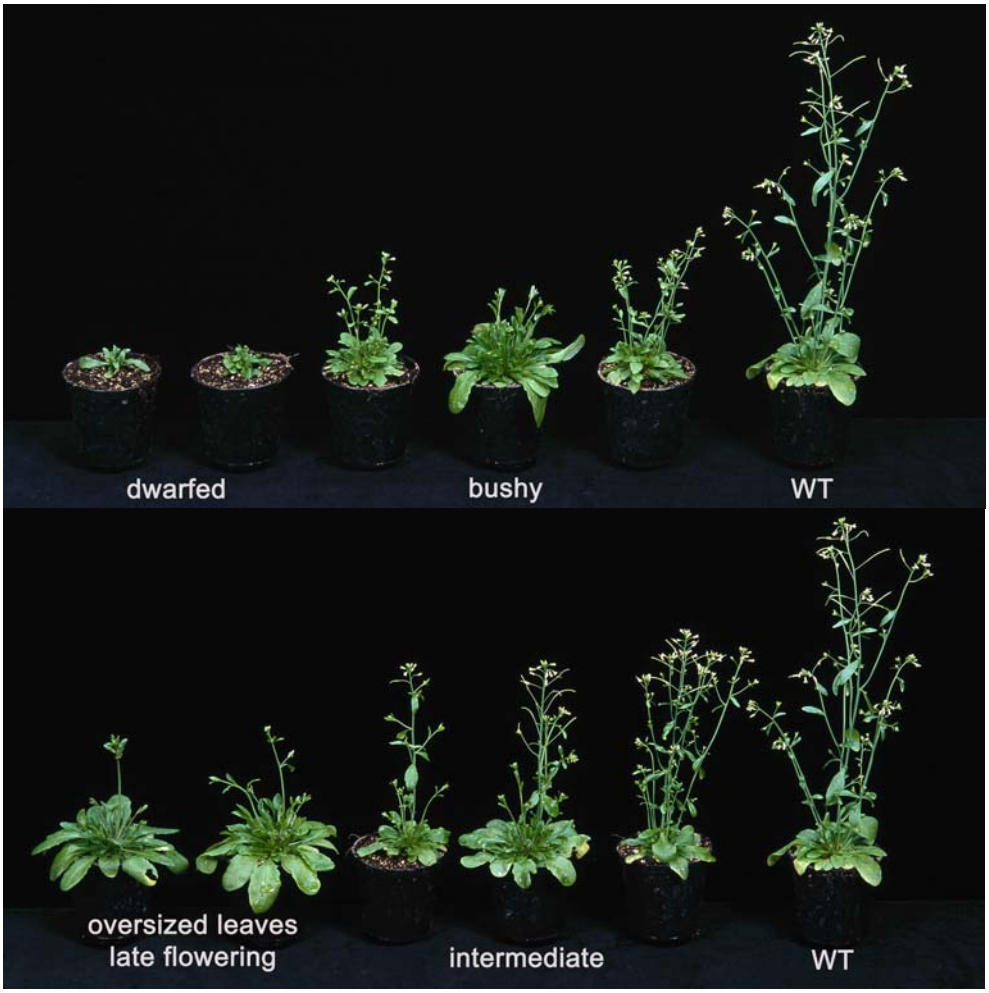

Fig. 5.1.2 Phenotypes of the *AMT1.1*RNAi T_1- generation. Many BASTA resitant plants of the T_1-generation were WT-like but some differed from the WT. These plants were grouped in 4 categories: dwarfed, bushy, oversized leaves/late flowering and intermediate. For comparison a WT plant was put on the right of 2 groups. In the wildtype control group, little variation was observed.

The third category consisted of plants which had relatively large rosette leaves compared to the WT. Although the shape of the leaves was not different to the WT they grew larger. This was also the case for leaves which emerged late in the vegetative period. This resulted in rosettes which were larger in diameter and in height than the wildtype rosettes (Fig. 5.1.2.). Additionally, the infloresences emerged later in development but eventually reached the same size as the wildtype rosettes. Senescence was delayed in these plants.

The phenotypes of the fourth category was similar to the WT but plants of this group remained smaller. In general, this was true for rosettes as well as for inflorescences (Fig. 5.1.2). Some rosette leaves continued to emerge during the flowering period which made these rosettes appear bushy but this was not the case for all plants. These late emerged leaves remained small. The shape of the leaves were wildtype like. Senesence began at a similar time as in the wildtype control groups.

To test the functionality of the *AtAMT1.1*-hpRNA construct in different transgenic lines, one T_1-plant with a wildtype like phenotype and 3 plants of the dwarfed category were chosen (the later generations of these plants were named line 1 to line 4) and the descendants of these T_1-plants were submitted to ^{14}C-MA uptake experiments (5.2.1.1). To analyse the number of insertions of the *AMT1.1*-hpRNA construct in T_1-plants and to isolate single insert lines (to simplify selection of homozygous lines and to avoid segregation of the RNAi construct in later generations), the segregation ratio of each line in the T_2-generation was determined (2.9). Tab. 5.1.1. gives the segregation ratio and the inferred number of insertions of the hpRNA construct for the T_2-generation of lines 1 to 4 and a number of other lines. Additionally, the phenotypes of the T_1 and T_2 generations are given. Line 1 and line 2 probably had two insertions and line 3 had three insertions. However, line 4 probably had only one insertion.

Based on T_2 segregation ratios, only four lines appeared to have a single insertion. In addition to line 4, these were lines 50, 84, and 94 (Tab. 5.1.1).

Tab. 5.1.1 Phenotypes of T_1- and T_2-generations, segregation ratios, and inferred number of insertions for various *AtAMT*RNAi lines.

	Line 1	Line 2	Line 3	Line 4	Line 50	Line 84	Line 94	Line 81	Line 109
Phenotype in T1	WT-like	dwarfed	dwarfed	dwarfed	WT-like	Intermediate	WT-like	WT-like	WT-like
Segregation ratio	1:6	1:7	1:25	1:3	1:3	1:3	1:3	1:16	1:16
Number of insertions	2	2	3	1	1	1	1	2	2
Phenotypes of T2	WT-like	many plants WT-like some small	WT-like	many plants small, some WT-like	many plants oversized, some WT like	many plants WT-like, some oversized or intermediate	many plants WT-like, some small	WT-like	WT-like

5.2. Quantification of *AtAMT* Transcript Levels in *AtAMT1.1*RNAi T_2-Plants

To test the functionality of the *AMT1.1*-hpRNA construct in the transformed plants, T_2-seeds of plants of the WT-like category (line 1) and two plants of the dwarf category (line 2 and 4) were sown on soil. The seedlings were BASTA selected and leaves of the resistant T_2-plants were harvested. Transcript levels of the leaf expressed *AMT* genes *AtAMT1.1, AtAMT1.2* and *AtAMT2.1* were measured by qRT-PCR using gene specific primers (II.2.3.).

AtAMT1.1 transcipt levels were reduced substantially. RNAi-line 4 had the strongest reduction with 22 % of WT levels (Table 5.2.), followed by RNAi lines 2 and 1 with 40 % and 45 % of WT levels for this gene, respectively. AMT1.2 transcripts were less efficiently reduced and the reduction ranged from 34 % of WT levels for line 4 and 51 % of WT levels for line 1, to 70 % of WT levels for line 2. Transcript levels of the distantly related *AtAMT2* gene were reduced to about 61 % of WT-levels, except in line 4 plants, where no reduction was observed (Table 5.2.).

Table 5.2. *AtAMT* transcript levels in T_2 *AtAMT1.1*RNAi lines relative to the WT (%).

cDNA-template	*Col-0*	RNAi line1	RNAi line2	RNAi line 4
AtAMT1.1	100	45 %	40 %	23 %
AtAMT1.2	100	51 %	70 %	34 %
AtAMT2.1	100	65 %	61 %	106 %

5.3. ^{14}C-Methylammonium Uptake Kinetics of *AtAMT1.1*RNAi Lines

5.3.1. ^{14}C-MA Uptake in *AtAMT1.1*RNAi T_2-Plants

To test the efficiency of the *AtAMT1.1* RNAi construct in reducing ammonium uptake, ^{14}C-methylammonium (^{14}C-MA) uptake studies were performed. T_2-seeds of plants of the WT-like category (line 1) and three plants of the dwarf category (line 2, 3, and 4) were grown in sterile liquid culture medium for seven days, BASTA selected, and deprived of nitrogen for 24 hours. Plants were than harvested and washed in N-free medium to eliminate all traces of ammonium. Subsequently, 5 to 8 seedlings were pooled to achieve a similar weight and the T_2-seedlings were submitted to ^{14}C-MA uptake experiments. The pooled plants were taken out after 10 and 20 minutes and the plants were immediately washed 3 times to eliminate all traces of ^{14}C-MA, attached to the plant surface. Then, plants were homogenized and the ^{14}C-scintillation counted.

T_2-RNAi lines took up significantly less ^{14}C-MA than WT plants at both 10 and 20 minutes after ^{14}C-MA addition. Uptake rates were between 15 % and 26 % of the WT on a fresh weight basis after 10 minutes and between 20 % and 50 % after 20 min. In the first 10 minutes the reduction of uptake was the same for all RNAi lines within the range of biological variation, regardless of the phenotype of the T_1-plants (Figure 5.3.1.1.). After 20 minutes this homogeneity disappeared due to differences in the uptake rate of the different lines. In line 1 and 3 the uptake was linear throughout the experiment but in

line 2 and 4 it was 2 times higher in the last 10 minutes (Figure 5.3.1.1.). After 20 minutes line 2 and Line 4 had taken up 41 % and 50 % less ^{14}C-MA than the WT, and line 1 and line 3 had taken up 21 % and 25 % less than the WT, respectively.

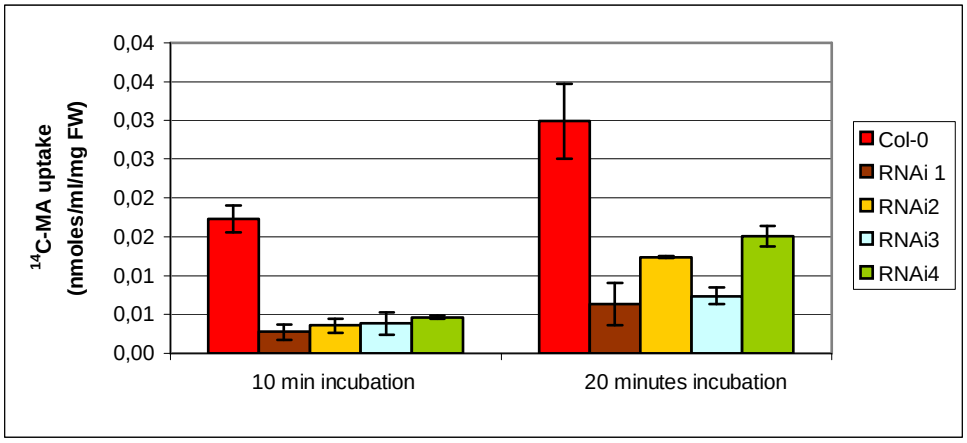

Fig. 5.3.1.1. ^{14}C-MA uptake at 50 µM ^{14}C-MA after 10 and 20 min of incubation for four T_2-RNAi lines and the WT (bars indicate standard error of four biological replicates).

A lower uptake rate must not necessarily be caused by a reduction of *AtAMT* transcript levels but could have resulted from poor growth of the RNAi lines caused by pleiotropic effects due to the the insertion of the transgenic construct. However, if the ammonium uptake rate of the WT is higher than the uptake rate of the RNAi lines, the WT should take up a finite amount of ammonium faster and subsequently become deprived of N earlier due to its subsequent metabolic consumption. The earlier N deprivation should lead to ealier senescence of the WT. To analyse this putative effect, 40 pools of the WT and each RNAi line were grown in 1 mM liquid sterile culture medium for 14 days and the phenotypes were analysed.In all WT pools, the seedlings were senescenting earlier than in the RNAi pools (Fig. 5.3.1.2.). This indicated an earlier N deprivation of the WT plants which is likely due to faster ammonium uptake and subsequent metabolic consumption.

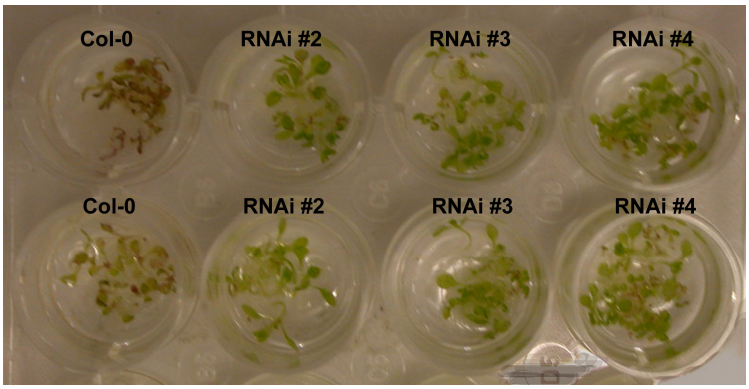

Fig. 5.3.1.2. T2-RNAi lines and the WT after 10 days growth in 1 ml sterile liquid culture medium, containing 1 mM NH_4^+ as the only nitrogen source. WT seedlings are senescent at this time whereas RNAi seedlings continue to grow.

5.3.2. ^{14}C-MA and ^{15}N-ammonium Uptake of Selected Single Insert Lines in the T_3-Generation

The above experiments were repeated for selected single insert lines in the T_3-generation. Additionally, line 2 which had two inserts was included in the analysis. Although the absolute rate of ^{14}C-MA uptake by wildtype plants in this set of experiments was lower than observed previously (Fig. 5.3.2.1.), the rate of MA uptake by plants of line 2 and 4 were once again significantly lower than the WT at both 10 and 20 min time points (Fig. 5.3.2.1.). Likewise, ^{14}C-MA uptake by lines 50, 84 and 94 were lower than that of the WT.

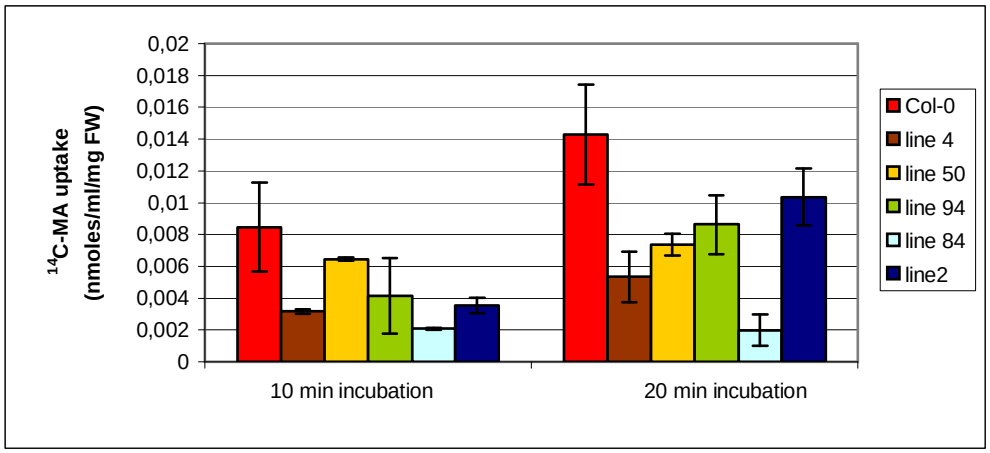

Fig. 5.3.2.1. ^{14}C-MA uptake at 50 µM MA after 10 and 20 min for five T_3-RNAi lines and the WT (bars represent standard errors of four biological replicates).

To verify the results obtained in the ^{14}C-MA uptake experiments by an alternative method, the RNAi lines 1, 2, 3 and 4 of the T_3-generation were submitted to a ^{15}N-ammonium (^{15}N-NH_4^+) uptake experiment. After uptake from the external medium into the plant, the ^{15}N- NH_4^+ gets incorporated into glutamine and ^{15}N-glutamine is detectable by mass spectrometry. Thus, the ^{15}N-glutamine concentration served as a parameter for ^{15}N-NH_4 uptake. For the quantification of the ^{15}N-glutamine concentration an LCQ DECA mass spectrometer was used that enables automated exact mass measurements of fragment ions. The high quality data delivered by the LCQ DECA mass spectrometer provides vey good specificity for the identifcation of small molecules such as glutamine. The plants were grown and treated as described in 4.4., except that four pools of each line (each consisting of 5-8 seedlings), were incubated in ^{15}N-NH_4Cl instead of ^{14}C-MA. After 20 minutes of ^{15}N-NH_4 incubation, plants were blotted dry, transferred into 2 ml tubes, and immediately frozen in liquid nitrogen. Metabolites were extracted from plant material as described in II.2.5.3. and analysed by mass spectrometry on a LC/MS system.

^{15}N-glutamine concentrations were highest for wildtype plants and significantly lower for the RNAi plants, in a way that mirrored the ^{14}C-MA uptake results (Fig. 5.3.2.2.). RNAi line 4 had the lowest level of ^{15}N-glutamine, with 47 % of the WT level. Line 2 contained 78 % as much ^{15}N-glutamine as the WT after 20 minutes, while line 3 had 60 % of the ^{15}N-glutamine WT content.

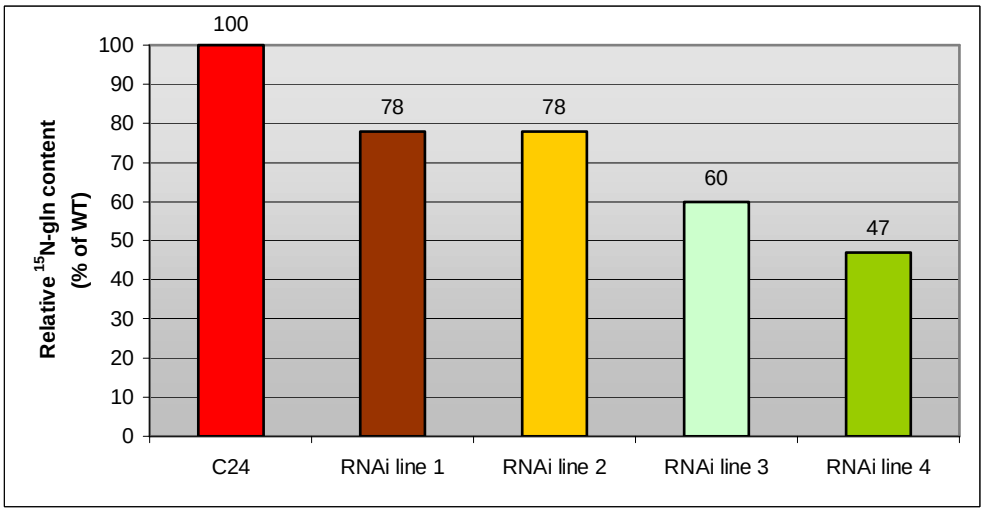

Fig. 5.3.2.2. Relative incorporation of ^{15}N-ammonium into glutamine after 20 min uptake for four T_3-RNAi lines compared to the WT.

5.3.3. ^{14}C-MA Uptake of Selected Single Insert Lines in the T_4-Generation

The ^{14}C-MA uptake experiments were repeated with the T_4-generation of the single insert lines 4, 50 and 84. Compared to the uptake rates obtained with the previous generations, the differences to the WT were less pronounced in the T_4 for all RNAi lines tested. Compared to the WT, the decrease in MA uptake after 10 min ranged from 10 % to 50 % for lines 50 through to 84, respectively, which reflected the order of transport inhibition exhibited in the T_2 generation (Fig. 5.3.1.). After 20 min, the decrease in uptake ranged from 30 % to 40 % which was a smaller reduction than in previous generations (Fig. 5.3.1., Fig. 5.3.2.).

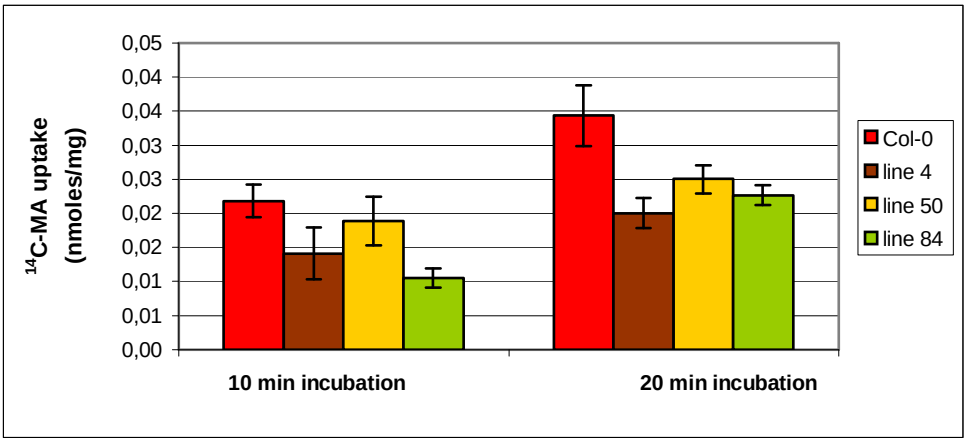

Fig. 5.3.3. ^{14}C-MA uptake (moles/ml/mg freshweight) at 50 µM MA after 10 and 20 min for three T_4-RNAi lines and the WT (bars indicate standard errors of three replicates.)

5.3.4. Time Courses of ^{14}C-MA Depletion at Various Concentrations

To specify the differences in ^{14}C-MA uptake kinetics between the RNAi lines and the WT in more detail, ^{14}C-MA was used at various concentrations in the range from 10 µM to 2 mM. Three pools of 5-8 seedlings of each RNAi line and the WT were incubated in 1ml of nitrogen free medium containing ^{14}C-MA, for 2 hours. 10 µl of the incubation medium were sampled after 5, 10, 20, 40, 60 and 120 minutes and ^{14}C-MA remaining in the medium determined.

During the two hours incubation time, evaporation occurred in the 1ml incubation medium, which lead to an increase of ^{14}C-MA concentration in the medium in the absence of plants. To correct ^{14}C-MA uptake data, the evaporation rate (cpm/min) was determined (2.5.1.).

The ^{14}C-MA uptake rates of the *AtAMT1.1*RNAi lines were lower than those of the WT over all ^{14}C-MA concentrations tested (Fig. 5.3.4.1-5.). Depletion of ^{14}C-MA was more or less linear for each line over the first half of the experiment, although depletion was typically faster during the first 5 minutes than after this time. In general, the rate of ^{14}C-MA depletion declined for all RNAi lines in the following order: WT > 84 ≈ 50 >4. Whereas line 4 was most impaired in uptake in all experiments, line 50 and 84 were similar and intermediate between line 4 and the WT (Fig. 5.3.4.1-5).

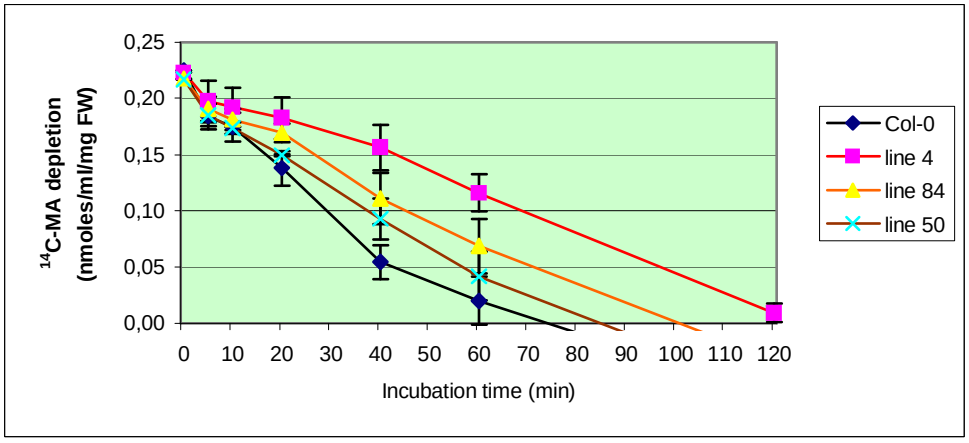

Fig. 5.3.4.1. Time course of ^{14}C-MA depletion from a 10 µM ^{14}C-MA solution for 3 *AMT1.1RNAi*-lines (mean values of three replicates) and *Col-0* (bars indicate standard errors).

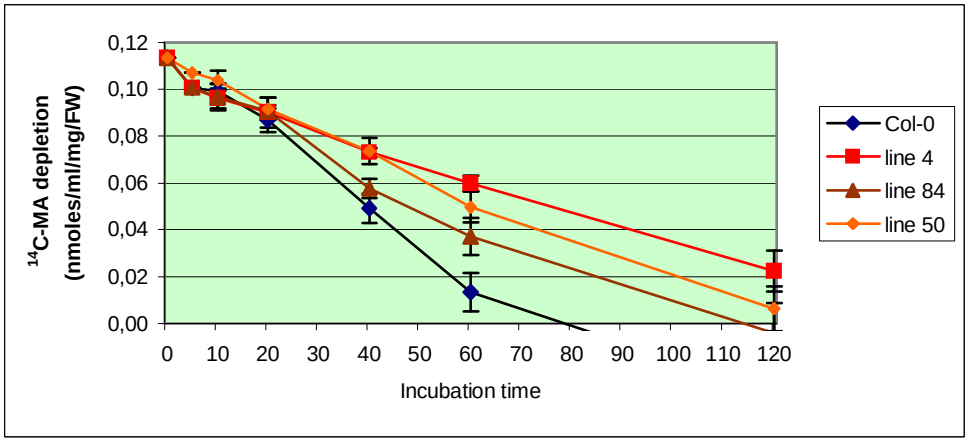

Fig. 5.3.4.2. Time course of ^{14}C-MA depletion from a 50 µM ^{14}C-MA solution for three *AMT1.1*RNAi-lines and *Col-0* (mean values of three replicates, bars indicate standard errors).

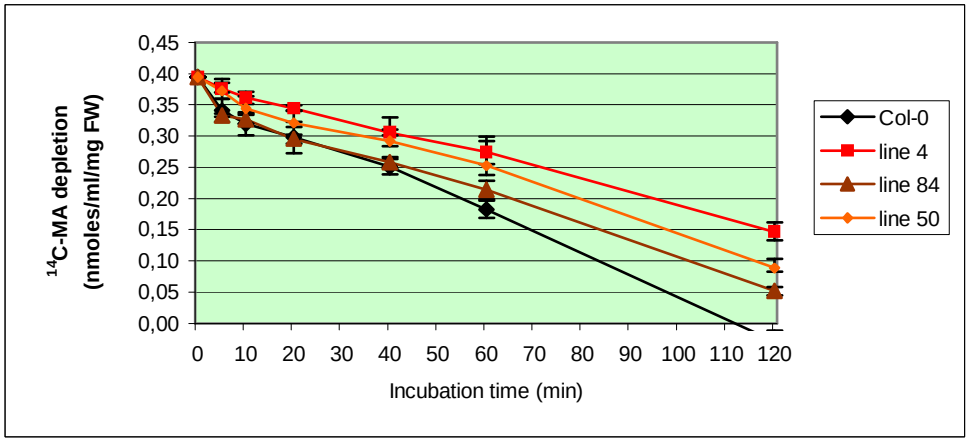

Fig. 5.3.4.3. Time course of ^{14}C-MA depletion from a 200 µM ^{14}C-MA solution for 3 *AMT1.1RNAi*-lines (mean values of three replicates) and *Col-0* (bars indicate standard errors).

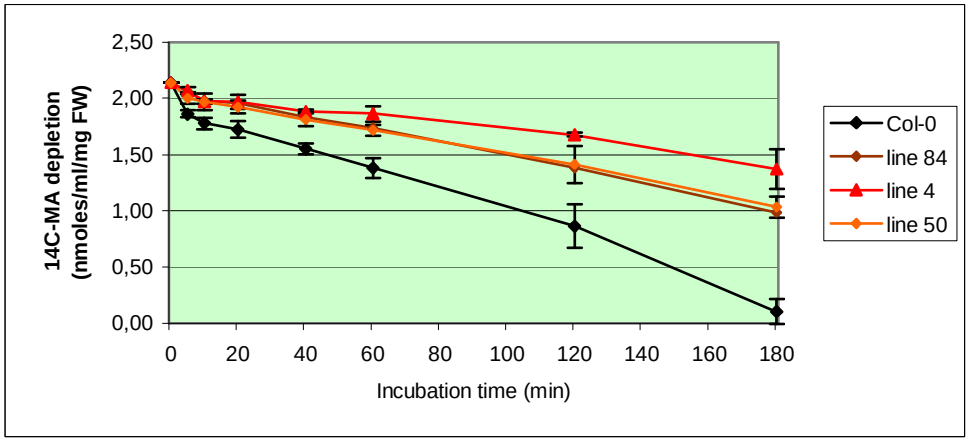

Fig. 5.3.4.4. Time course of ^{14}C-MA depletion from a 1 mM ^{14}C-MA solution for three *AMT1.1*RNAi-lines and *Col-0* (mean values of three replicates, bars indicate standard errors).

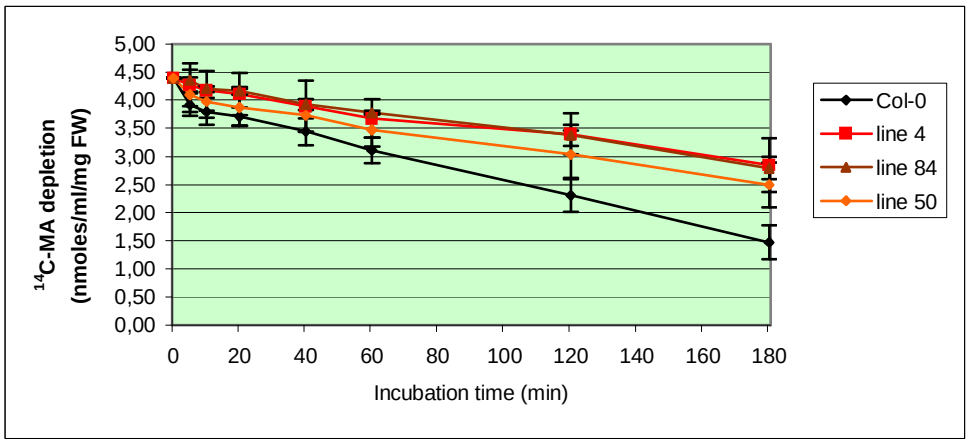

Fig. 5.3.4.5. Time course of ^{14}C-MA depletion from a 2 mM ^{14}C-MA solution for three *AMT1.1*RNAi-lines and *Col-0* (mean values of three replicates, bars indicate standard errors).

5.4. Quantification of *AtAMT* Transcript Levels in *AtAMT1.1RNAi* Lines at the T_4-Generation

Single-insert *AMT*1.1-RNAi line 4 showed the lowest MA uptake activity of the four RNAi lines analysed (5.3.). To determine the extent to which AMT transcript levels were reduced in this line compared to the WT, quantitative real-time PCR (qRT-PCR) was used. To obtain cDNA of whole plants, T_4-generation seedlings of line 4 and the WT control were grown in liquid culture medium for 7 days and subsequently harvested. To obtain root cDNA, line 4 and the WT control were grown for six weeks in full nutrient hydroponic medium and deprived of nitrogen for 24 hours before harvesting the roots. To obtain specific cDNA, line 4 and the WT control was grown for six weeks on 0-soil containing 10 µM NH_4 (II.2.4.2.). Transcript levels of all six *AMT* genes were measured by qRT-PCR using gene-specific primers (II.1.3.).

Compared to the WT, the transcript levels of several of the *AMT* genes were reduced substantially in whole plants of RNAi line 4 (Fig. 5.4.1.). *AtAMT1.1*, the source and primary target of the RNAi hairpin construct, showed a 50 % reduction in transcript levels in line 4 compared to the WT. Likewise, transcript levels of both, *AtAMT1.2* and *AtAMT1.3* were reduced by approximately 50 %, while *AtAMT1.4* and *AtAMT1.5* were not expressed at levels that could be reliably detected under these experimental conditions. Interestingly, *AtAMT2.1*, which is only distantly related to *AtAMT1.1*, still showed a moderate reduction (40 %) of mRNA levels.

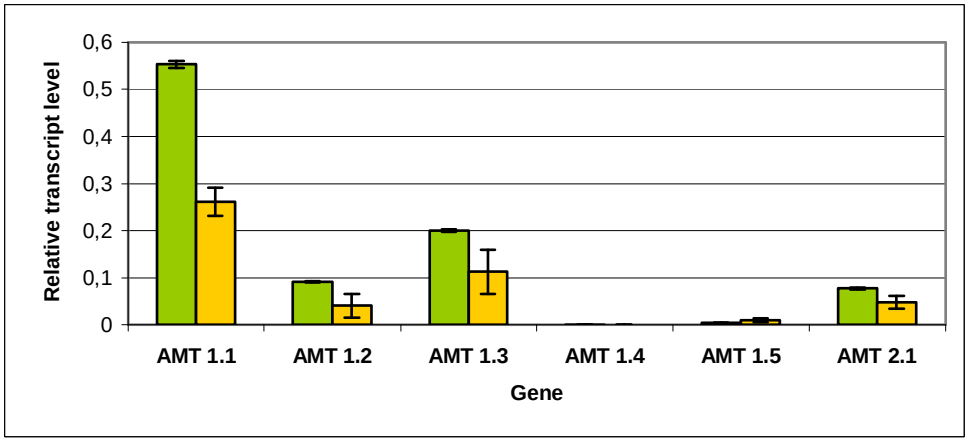

Fig. 5.4.1. *AtAMT* transcript levels relative to those of the housekeeping gene *UBQ-10* for Col-0 (green bars) and *AtAMT1.1-RNAi* line 4 (yellow bars). cDNA was isolated from whole plants grown in liquid culture for 7 days and then deprived of N for 24 hours (error bars represent standard errors of 3 replicates).

In roots, reduction in transcript levels was observed for all root-expressed *AtAMT1* genes in *AtAMT1.1-RNAi* line 4 investigated (Fig. 5.4.2). However, for *AtAMT2.1*, no reduction was detected. Transcript levels were reduced to 82 %, 79 % and 74 % of WT levels for the genes *AtAMT1.1, AtAMT1.2* and *AtAMT1.3*, respectively. *AtAMT1.5* showed the highest reduction in transcript levels to 43 % of WT levels (Fig. 5.4.2.).

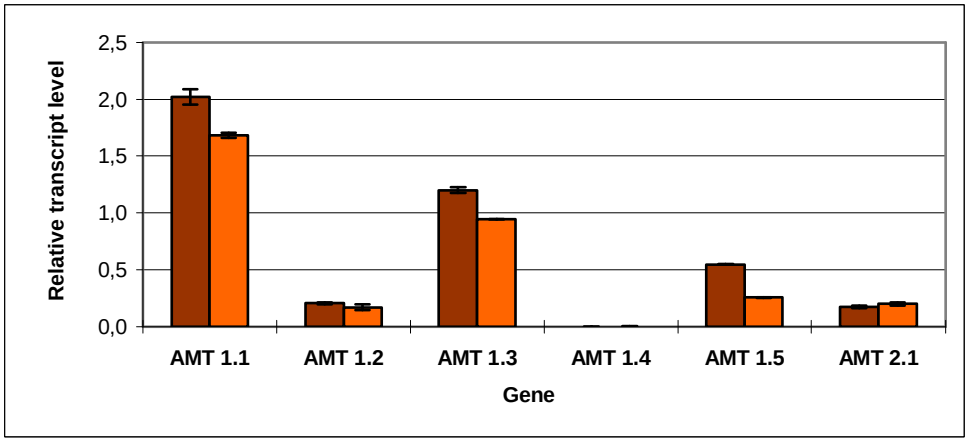

Fig. 5.4.2. Root specific *AtAMT* transcript levels relative to those of the housekeeping gene *UBQ-10* for Col-0 (dark bars) and *AtAMT1.1-RNAi* line 4 (light bars; error bars represent standard errors of three replicates).

In leaves, reduction in transcript levels were observed for all leaf-expressed *AtAMT* genes (Fig. 5.4.3). Transcript levels were reduced to 55 % and 43 % of WT levels for *AtAMT1.1* and *AtAMT1.2*, respectively. *AtAMT2.1* transcript levels showed a lower reduction to 62 % of WT levels.

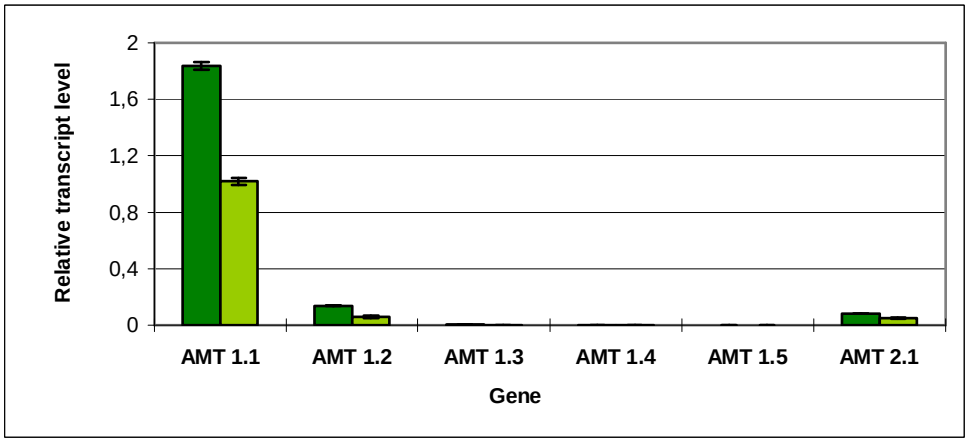

Fig. 5.4.3 Leaf specific *AtAMT* transcript levels relative to those of the housekeeping gene *UBQ-10* for Col-0 (dark bars) and *AtAMT1.1-RNAi* line 4 (light bars; error bars represent standard errors of three replicates).

5.5. Ammonia Uptake Kinetics of *AtAMT1.1RNAi* Lines

To supplement the ^{14}C-MA uptake kinetic studies with experiments in which the natural substrate of ammonium transporters was used, ammonium uptake kinetics were measured in experiments with the T_4-generation *AMT1.1*RNAi lines and Col-0.

Plants were grown in liquid culture as described in section II.2.4.1 for one week and then deprived of nitrogen for 24 hours. Seedlings were subsequently grouped into pools of approximately the same weight (± 2mg) and transferred to new 24-well micro titer plates. Each well contained 1ml fresh liquid culture medium lacking nitrogen. To initiate uptake experiments, ammonium was added to yield concentrations of ammonium of 50 µM, 100 µM and 200 µM and plates were incubated on a shaker at room temperature for 120 min in closed titer plates to avoid evaporation. Samples of 50 µl were taken after 5, 10, 20, 40, 60 and 120 minutes. The removed medium was replaced by the same volume of nitrogen free liquid culture medium. The ammonium concentration in each sample was determined using a spectrophotometric assay (II.2.5.3.).

Data from these experiments confirmed the data obtained by the ^{14}C-MA-uptake experiments with respect to an impairment of the *AMT1.1*RNAi-lines in ammonia uptake compared to the WT (Fig. 5.5.1.). As in the ^{14}C-MA uptake experiments performed with the T_4-generation, line 4 was the most severely impaired line in all experiments. The greatest differences to the WT were found after 20 minutes. After this time, at concentrations of 100 and 200 µM, the ammonia uptake was between 43 % and 78 % of the WT. After longer incubation times the differences to the WT became less. However, after 120 minutes incubation, line 4 had not taken up the same amount of ammonia as the WT, which was 12 % less at 50µM, 17 % less at 100 µM, and 30 % less at 200µM (Fig. 5.5.1.).

RNAi-lines 50 and 84 were also impaired in uptake compared to the WT but the differences became statistically significant only at 100 µM and 200 µM ammonium, after an incubation time of an hour. At 50 µM, line 4 was the only RNAi line that was significantly slower in uptake (Fig. 5.5.1.).

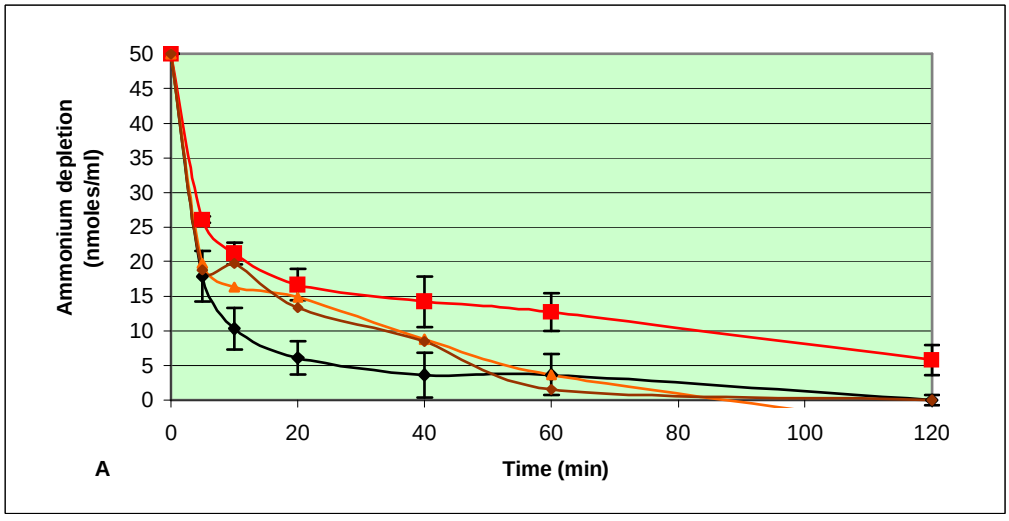

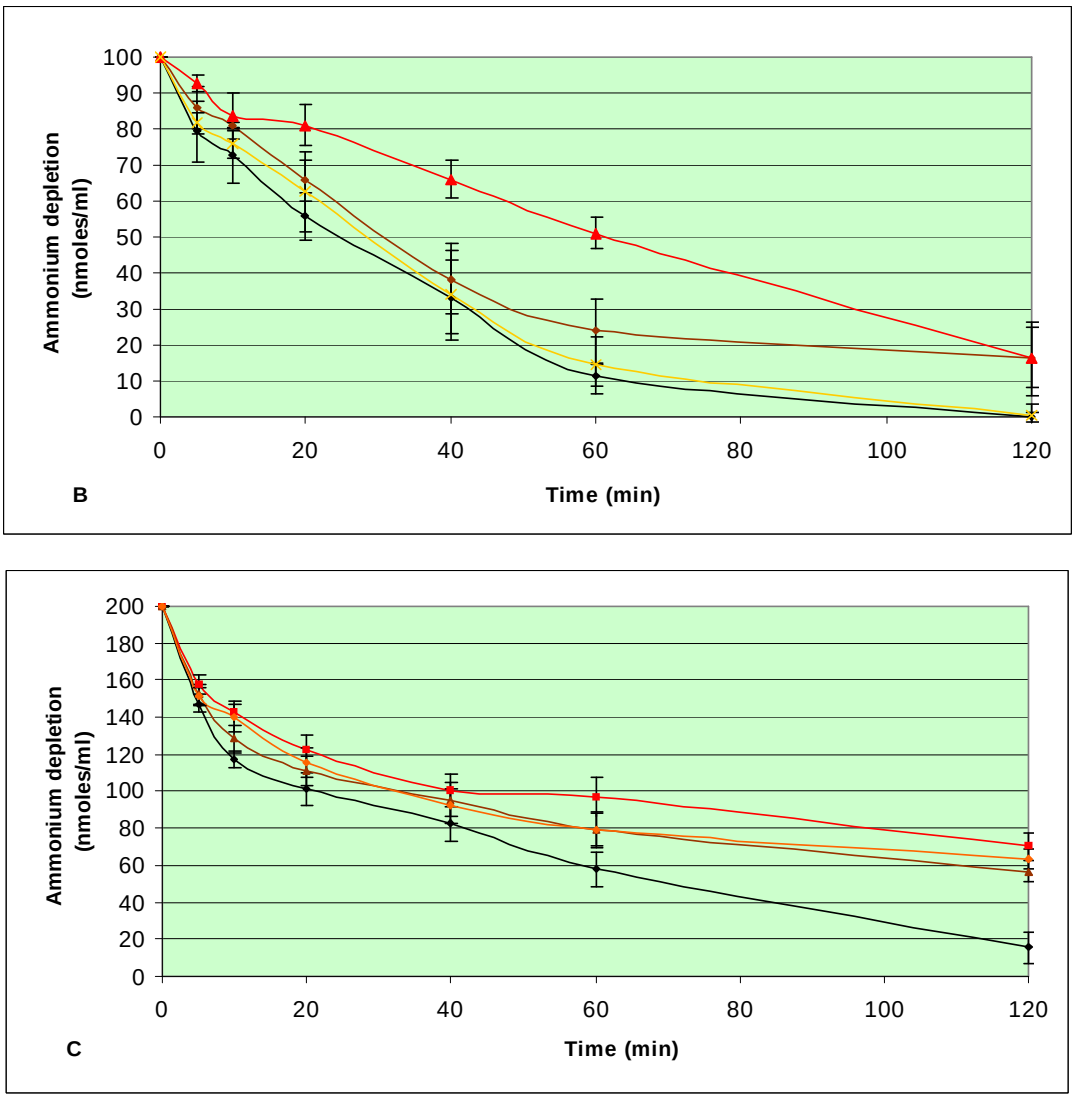

Fig. 5.5.1. Depletion curves of *AMT1.1*RNAi lines and the WT incubated at ammonia concentrations of 50 µM (a), 100 µM (b) and 200 µM (c) for 2 hours (WT-blue, RNAi4-red, RNAi50-orange and RNAi84-brown).

5.6. Developmental and Phenotypical Characterization of *AMT1.1*RNAi Plants

To analyse developmental and other phenotypical traits of the *AMT1.1RNAi* lines, 20 plants of the three RNAi lines 4, 50, and 84 and the WT were grown on soil under green house conditions (chapter 2.4.2. and Fig. 5.6.1.). The T_4-generation was used for detailed developmental characterisation.

Line 4 had many small plants in the T_2 and T_3-generations but some plants were wildtype like or appeared to be 'intermediate'as described in chapter 5.1. Line 50 had wildtype like plants in T_2- and T_3-generations but some plants developed to the 'oversized' phenotype described in chapter 5.1. Line 84 had many wildtype like plants in all generations but some remained smaller and were similar to the 'intermediate' phenotype. To put these observations onto a quantitative level, the three RNAi-lines were investigated with respect to various parameters throughout the whole life cycle of the T_4-generation. However, it was often noticed, that the descendants of individual parental plants of any line developed like the WT and had no differences in transcipt levels or ^{14}C-MA transport if compared to the WT. The decendants of these plants were not taken into further analysis. Therefore, only a few selected plants of the T_2- and T_3-generation were parental to the plant pools used for the physiological and developmental analysis.

Fig. 5.6.1. Phenotype of representative members of the three *AtAMT1.1*RNAi-lines and the WT after 4 weeks of growth on full soil in the green house. a) RNAi line 50, b)-RNAi line 4, c) RNAi line 84).

After 21 days of growth, the number of bolting and flowering plants were determined. Counting was repeated after 25, 27, 29, 31, and 34 days (Fig. 5.6.2). All three RNAi lines were delayed in bolting and flowering. After three weeks, when 90 % of wildtype plants were bolting and 60 % were flowering, none of the RNAi lines showed buds (Fig. 5.6.2). Four days later, all wildtype plants had flowered but half of line 50 and one quarter of line 84 plants were bolting and only 5 % of line 50 and 10 % of line 84 were flowering. At that time none of the RNAi line 4 plants showed buds. In the end, lines 50 and 84 were delayed by about 7 days in bolting and 10 days in flowering compared to the WT, while line 4 was delayed more than 2 weeks for bolting and flowering, compared to the WT.

When the flowering period of the WT was over (day 34, no emergence of new buds), plants were harvested and the above ground parts were weighted. The mean shoot weight of lines 50 and 84 was significantly

higher than that of the WT control (Fig. 5.6.3.), while that of RNAi line 4 was not significantly different to the WT weight.

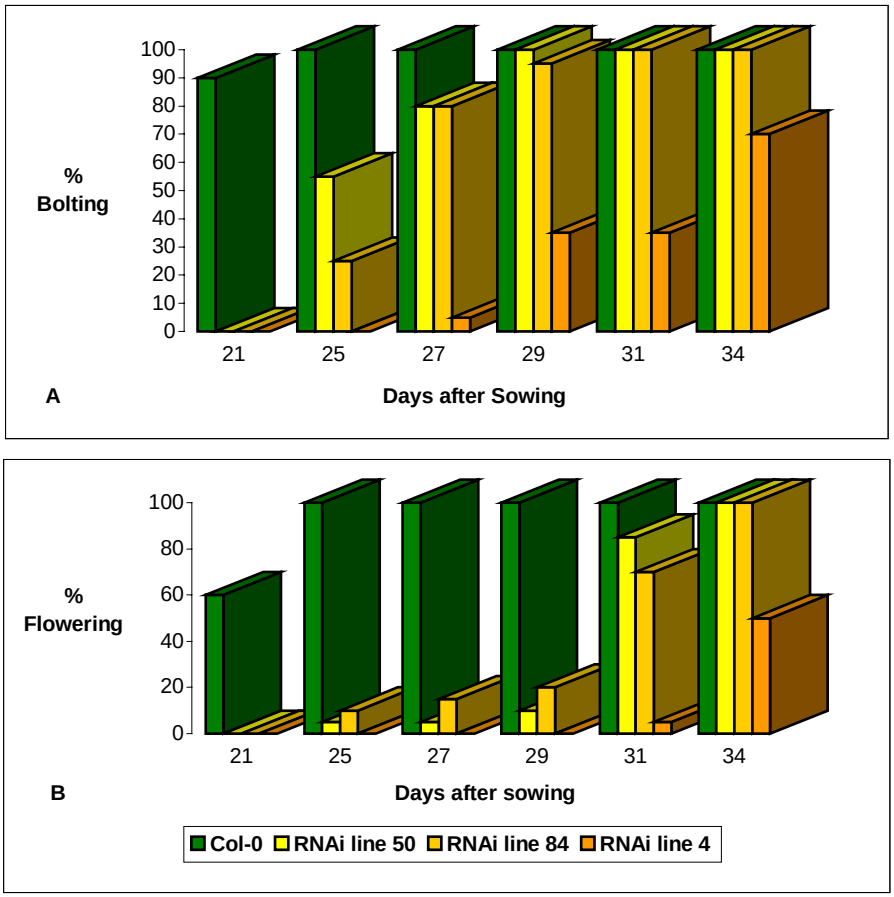

Fig. 5.6.2. Bolting and flowering phenotypes of *AMT1.1*RNAi lines and the corresponding WT.

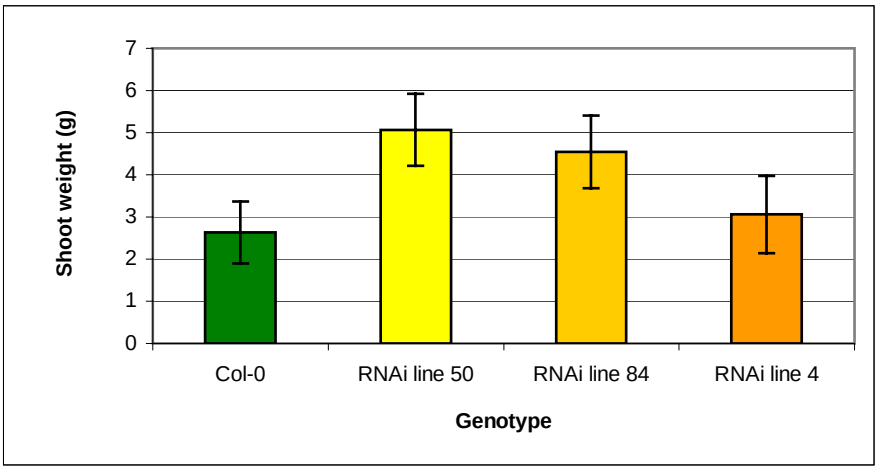

Fig. 5.6.3. Weight (g) of above ground parts of three *AMT1.1*RNAi lines and the corresponding WT after 34 days of growth (bars represent mean values of 20 plants, error bars indicate the standard error).

While flower development was being monitored, the rosette diameters of plants were also measured. Until day 25, the rosette diameters of the *AMT1.1*RNAi lines 4 and 84 were significantly smaller than the wildtype rosettes (Fig. 5.6.4.). RNAi line 50 was smaller on average but not significantly smaller than the WT (Fig. 5.6.4.).

To summarise, *AMT1.1*RNAi-lines grew slower than the WT and switched to the flowering phase at a later time. Thus, growth continued over a longer time in RNAi lines than in the WT, which led to an increase in biomass in the late stages of development. Additionally, at a time when most WT leaves were senescent, only a few leaves of RNAi plants were senescent, and this was restricted to the leaf margins. Furthermore, the RNAi lines showed a tendency to develop thicker inflorescence stems, although this was not a universal characteristic. Line 50 and 84 had thicker inflorescence stems which stood upright throughout development, whereas WT inflorescences bent down at the late stages of inflorescence growth.

RNAi line 50 continued to produce rosette leaves even after development had switched to generative growth. Thus, in late stages of development this line had more rosette leaves than the WT although most of the younger leaves remained small. However, this particular phenotype was not consistent in this line and was not observed among other RNAi lines.

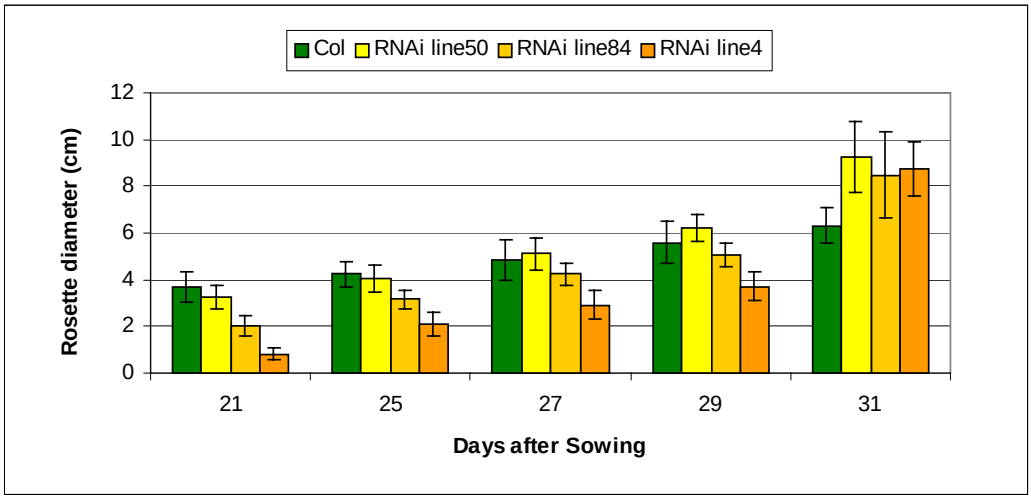

Fig. 5.6.4. Rosette diameter (cm) of three *AMT1.1*RNAi lines and the WT, at different time points of development (columns represent mean values of 20 plants, error bars show the standard error).

IV. Discussion

Summary

To discuss possible physiological functions of AMT proteins in *Arabidopsis thaliana* some characteristics of the abundance of ammonia in the soil and in plants, and the necessity of specialised NH_4^+ uptake, transport and retrieval have to be briefly recapitulated.

In most soils, NH_4^+ and NO_3^- are the predominant sources of inorganic nitrogen that are available for plant nutrition. Although the average NH_4^+ concentrations of soils are generally not above 40 µM and often are 100 to 1000 times lower than those of NO_3^- (Marschner, 1995), most plants preferentially take up NH_4^+ when both forms are present. In a recent study on tomato it was shown that 50 % of the nitrogen absorbed by plants was absorbed in the form of NH_4^+, although it represented only 10 % of the available nitrogen (Glass *et al*., 2002). NH_4^+ is more favorable as a nitrogen source for plants because unlike to NO_3^- it has not to be reduced prior to assimilation and thus requires less energy for assimilation (Bloom *et al*., 1992).

Nitrogen is often a limiting factor for plant growth due to its heterogenous distribution in the soil and to seasonal and diurnal changes in growth rates. In this context, plants have evolved numerous mechanisms that enable them to optimize nitrogen acquisition, which include the up and down regulation of nitrogen uptake under nitrogen limiting or excess conditions. Apart from high uptake rates in roots, high intracellular ammonium concentrations can also result from a rapid and quantitatively important internal breakdown of amino acids in roots and in leaves (Feng *et al*., 1998). In leaves, ammonium can originate during photorespiration and to a lesser extent during amino-acid transport and catabolism (Mattson *et al*., 1997, Pearson *et al*., 1998). Thus, plants need transport systems to mediate the uptake of external ammonium from the soil and to faciliate the retrieval of ammonia originating from cell metabolism (Coschigano *et al*., 1998). Additionally, for the plant families living in symbiosis with N_2-fixing bacteria, ammonium is the main source of nitrogen provided by bacteria to the plant (Udvardi and Day, 1997). Thus, NH_4^+ is a key component of N metabolism for all plants and can accumulate to varying concentrations in all compartments of the cell, including the cytosol, the vacuole, and the apoplast (Wells and Miller, 2000; Nielsen and Schjoerring, 1998).

Prior to this thesis, the functions of several AMTs were investigated in yeast, bacteria, and higher plants by gene expression studies and biochemical studies of transport properties in mutants and heterologous expression systems. Phylogenetic studies indicated the presence of six putative high-affinity transport systems (HATS) for NH_4^+ in *Arabidopsis* (five members of the AMT1 family and AMT2.). These transporters differ in their kinetic properties as well as their regulatory mechanisms. Among this family, AMT1.1, AMT1.2, AMT1.3, and AMT2.1 had been characterized in some detail in previous studies (Gazzarrini *et al*., 1999; Sohlenkamp *et al*. 2000). The determination of Km values prior to this thesis showed, that AtAMT1.1 (K_m value 10 to 20 µM, Kaiser *et al*., 2002; Sohlenkamp *et al*., 2002) and AtAMT1.3 (K_m 11 µM; Gazzarrini *et al*., 1999) display the highest affinity for ammonium, followed by AtAMT1.2 (K_m value 24 µM; Gazzarrini *et al*., 1999) and *AtAMT2.1* (K_m

value 22 µM, Sohlenkamp *et al*., 2002). In *Arabidopsis,* experimental evidence for the physiological function of NH_4^+ transporters *in vivo* was mainly derived from expression studies and $^{15}NH_4^+$ influx studies in roots (Gazzarrini *et al*., 1999). However, these methods were not sufficient to assign precise physiological functions to the individual transporters. Furthermore, AMT1.4 and AMT1.5 had not been studied prior to this thesis. Given this background, it was considered desirable to acquire a deeper knowledge of the physiological functions of the six *Arabidopsis* ammonium transporters. To this end, modern approaches such as the use of T-DNA insertional mutants and RNAi plants with reduced expression levels of *AMT* genes were employed. Phenotypical and developmental analysis such as growth tests on different media and ^{14}C-MA and NH_4^+ uptake studies with the isolated insertional mutants and RNAi lines were performed to deepen our knowledge of the individual functions of the six AMTs in *Arabidopsis*. In addition, double mutants of the insertional mutants were created as a first step to investigate the extent to which homologous genes could compensate for lost transporter functions.

These studies were supplemented by tissue specific expression profiles of the individual wildtype *AMT* genes obtained by quantitative real time PCR (qRT-PCR) and promoter-GUS expression.

1. Expression Analysis of *AtAMT* Genes in *Arabidopsis thaliana*

1.1. General Expression of *AMT* Genes in *Arabidopsis thaliana*

AtAMT1.1 is quantitatively the most highly expressed *AMT* gene in *Arabidopsis*. Transcript levels were at least three times higher than of any other *AMT* gene (Fig. 1.1.1.) and expression was found in roots, leaves, and flowers at high levels (Tab. 1.2.1.; Fig. 2.1.1.and 2.).

AtAMT1.3 is closely related to *AtAMT1.1* with 79 % similarity at the amino acid level, but it is expressed in roots only (Tab. 1.2.1.; Fig. 2.2.1.), where it showed the second highest transcript levels next to *AtAMT1.1* (Fig. 1.1.1.)

AtAMT1.5 is very closely related to AtAMT1.3 with approximately 90 % similarity on the amino acid level, and closely related to AtAMT1.1 with 80 % similarity. Expression in mature plants was restricted to roots (Fig. 1.2.1.), but strong expression was also observed in cotyledons of germinating seedlings (Fig.2.5.1.).

AtAMT1.2 is more distantly related to *AtAMT1.1* with 68 % amino acid similarity. It is highly expressed on whole plant level (Fig. 1.1.1.) and apart from roots (third highest expression, Fig. 1.2.1., Fig. 2.2.1.), *AtAMT1.2* was expressed in leaves (second highest, Fig. 1.2.2., Fig. 2.2.2.). *AtAMT1.4* is distantly related to *AtAMT1.1* (~70 % amino acid similarity) and the closest relative of AtAMT1.2. It is expressed at very low levels in leaves (Fig. 1.2.2) and at higher levels in flowers (Fig. 1.2.3.), where the expression was restricted to pollen (Fig. 2.4.1).

AtAMT2.1 is the most distantly related *AtAMT* gene with only 27 % amino acid similarity to *AtAMT1.1* (Sohlenkamp *et al*. 2002). It is expressed in roots (Fig. 1.2.1, Fig. 2.6.1.) and leaves (Fig. 1.2.2., Fig. 2.6.2.), where it had the fourth and third highest transcript levels, respectively.

1.2. Specific Expression and Possible Physiological Roles of AMTs in Roots

Previous RNA gel blot analyse showed that *AtAMT1.1* was transcribed in stems, leaves, and buds, whereas *AtAMT1.2* was mainly expressed in roots with faint signals in leaves, and *AtAMT1.3* expression was confined to roots (Gazzarrini *et al*., 1999).

In this thesis, qRT-PCR and promoter-GUS expression were used to obtain a comprehensive picture of the expression of all *AMT* genes in *Arabidopsis* in different nutritional states (see section 2. and 3.). As far as possible, the expression profiles compared with data from Affymetrix arrays contained in the CSB-database of the MPIMP, Golm (Steinhäuser *et al*., 2004; http://csbdb.mpimp-golm.mpg.de/). There was generally good agreement between results from qRT-PCR and Affymetrix data, both with respect to tissue-specifity of *AtAMT* gene expression, and relative transcript levels. For qRT-PCR, RNA was harvested from roots of six weeks old plants grown in a full nutrient hydroponic medium. *AtAMT1.1* was expressed in roots at high levels. *AtAMT1.2* was also expressed in roots but 4.5 times less than *AtAMT1.1*. Transcipts of *AtAMT1.3* were detected in roots at similar levels as *AtAMT1.1* (Fig. 1.2.1.). These findings support the RNA blot analysis of Gazzarrini *et al.,* 1999 and the tissue specific expression was also supported by the CSB-database (appendix, Tab.).

The qRT-PCR analysis showed that *AtAMT1.4* is not expressed in roots, while *AtAMT1.5* was expressed at very low level in roots under full nutrient conditions (Fig. 1.2.1.). *AtAMT2.1* expression was investigated for the first time by RNA blot analysis (Sohlenkamp *et al*., 2002). The qRT-PCR data of this thesis support the RNA blot analysis. *AtAMT2.1* was clearly expressed in roots but less than the other root expressed *AMTs*. These data were confirmed in the CSB-database (appendix, Tab.).

To verify the reported regulation of *AMT* genes by the nitrogen status of plants (Lauter *et al*., 1996, Gazzarrini *et al*., 1999, Rawat *et al*., 1999, Sohlenkamp *et al*., 2002) and to determine possible N-dependend regulation of other *AMT* genes, qRT-PCR experiments were performed with RNA extracted from hydroponically grown plants after 24h of N deprivation. In these experiments *AtAMT1.1* showed a strong increase of expression which was 4 times above the expression under full nutrient conditions (Fig. III1.2.1). This supported previous RNA gel blot analysis, which detected a 5-fold increase in *AtAMT1.1* mRNA relative to N-replete plants after 72 hours of N-deprivation (Gazzarrini *et al*., 1999). *AtAMT1.2* expression was not significally different after 24h of N deprivation (Fig. 1.2.1.), consistent with previous RNA gel blot analysis (Gazzarrini *et al*. 1999). *AtAMT1.3* expression increased 2.5 fold within 24 hours of nitrogen deprivation, which verifies previous RNA gel blot data that showed an approximately twofold increase after three days of N deprivation (Gazzarrini *et al*., 1999). The last root-expressed family member, *AtAMT1.5*, showed a unique expression pattern in roots. While expression was virtually undetectable when plants were grown in a full nutrient environment, *AtAMT1.5* was highly expressed when deprived of N for 24 hours. Transcipt levels rose more than 40 fold under these conditions and were as high as *AtAMT1.1* expression at full nutrient conditions. Furthermore, the induction of *AtAMT1.5* by N-deprivation was entirely restricted to roots (Fig. 1.2.1).

AtAMT2 expression increased in response to three days of N deprivation in an earlier study (Sohlenkamp *et a*l. 2002). This was not confirmed in the qRT-PCR experiments performed with root RNA extracts from plants that were deprived of N for only 24 hours. After one day of N deprivation, *AtAMT2.1* transcripts showed a tendency

to increase but this increase was not significant (Fig. 1.2.1.). In the earlier study, addition of nitrate to N-deprived plants resulted in a decrease in *AtAMT2* transcript levels in roots after 30 and 60 min, although levels did not fall to those observed in ammonium nitrate-grown plants (Sohlenkamp *et al*., 2002). Together with the qRT-PCR data, this indicates that *AtAMT2* is regulated by the general nitrogen status rather than ammonium per se.

In all *AMT1.1-GUS* plants, staining was strong in the primary as well as in the lateral roots but GUS staining was restricted to cortical cells only and was not observed in the pericycle, including the vascular tissue, in epidermal cells, the root tip, or in emerging lateral roots (Fig. 2.1.1.). Remarkably little *AMT1.1-GUS* staining was observed in the root hairs. The absence of *AtAMT1.1* expression in epidermal cells is somewhat at odds with the current view that the AMT1.1 protein is most responsible for ammonium uptake from the soil (see later in the text).

Promoter-GUS staining showed strong expression of *AtAMT1.3* in the lateral roots, with restriction to the elongation zone. In this part, it was expressed in the central cylinder as well as the cortex and additionally in root hairs (Fig. 2.3.1.). Additionally, in *AtAMT1.5-GUS* plants, staining was found in all parts of the root, i.e. the rizodermis, the cortex and the root hairs (Fig. 2.5.1.). These findings indicate, that AtAMT1.3 and AtAMT1.5 are important for ammonium uptake from the soil, possibly more so than AtAMT1.1. Root hairs increase the root surface considerably and it is likely that most ammonium is taken up by these specialized cells.

Regarding the GUS-staining pattern of AtAMT1.1, strong *AMT1.1*-GUS staining was observed in root cortical cells,which are also believed to be involved in uptake of soil ammonium that has entered the apoplastic continuum of root cell walls. Thus, it is possible that the function of the AtAMT1.1 protein lies in transport of the acquired ammonium from the rhizodermis cells and the apoplast into the cortex cells. Furthermore, it is possible that the region of the *AtAMT1.1* promoter used in this thesis did not include all the regulatory elements of the endogenous gene, and that the GUS staining pattern does not provide a complete picture of the expression domains of the gene. This, of course, is true for all of the *AMT*-promoter GUS-studies described here.

Nevertheless, the transcript levels obtained by the qRT-PCR experiments support the hypothesis that AtAMT1.3 and AtAMT1.5 are chiefly involved in the aquisition of external ammonium. Under nitrogen supplied conditions, the root expression level of *AtAMT1.3* is not different to the expression of *AtAMT1.1* (Fig. 1.2.1.). Under nitrogen deprived conditions, AtAMT1.1 transcript levels were much more induced than AtAMT1.3 transcripts, however. Under these conditions, the root hair-expressed *AtAMT1.5* was also very strongly induced. Together, *AtAMT1.3* and *-1.5* have approximately the same amount of transcript as *AtAMT1.1* (Tab. 1.2.1.), pointing to a complentary role of these two genes. An important indication for a possible role of AtAMT1.1 in the uptake of external ammonium has been the high affinity to ammonium (K_m = 8 µM; Gazzarrini *et al*., 1999). But this low K_m was not veryfied in later studies which reported similar affinities for AtAMT1.3 and AtAMT1.1 (Kaiser *et al*., 2002, Sohlenkamp *et al*., 2002). Further support for the hypothesis that AtAMT1.3 and AtAMT1.5 play an important role in root ammonium uptake comes from the observation that a knock out mutant of *AtAMT1.1* did not reduce

^{13}N-NH_4^+ influx in plants grown on normal soil, althoug uptake decreased by 20 to 30 % when plants were deprived of nitrogen for four days (Glass *et al*., 2001). Additionally, another study demonstrated that ammonium influx responded more rapidly to nitrogen resupply than *AtAMT1.1* mRNA levels (Rawat *et al*., 1999). This indicates that influx is either primarily mediated by other AtAMT proteins or that post transcriptional and/or post translational regulation plays an important role under such conditions.

Finally, the different pattern of *AtAMT1.3* compared to that of *AtAMT1.1* indicates different physiological roles. *AtAMT1.3* expression, which is restricted to roots, showed an increase during the light period, which might indicate a link to carbon provision to roots (Gazzarrini *et al*., 1999). During the day, photosynthesis driven carbohydrate synthesis takes place and increases the demand for nitrogen from the soil. This implies a link between the C and N metabolism (Lam and Coruzzi, 1998). The diurnal regulation of AtAMT1.3 points to a role for this transporter in ammonium uptake from the soil.

The Promoter-GUS analysis showed that *AtAMT2.1* was exclusively expressed in lateral roots and not in the primary roots. Here, GUS-staining was confined to the elongation zone where it was present in all tissues of the root, the cortex, the central cylinder and the root hairs. The root tips remained unstained as did older sections of the lateral roots. The expression in the root hairs and the root cortex (Fig. 2.6.1.) give reason to believe that this transporter is also involved in the acquisition of external ammonium. An argument for this function is that *AtAMT2.1* transcipt levels rise in the roots of plants starved of nitrogen, or they remain unchanged in shoots of the same plants (Sohlenkamp *et al*., 2002). This observed different regulation in roots and shoots could point to a function in ammonium acquisition from the rhizosphere. Additionally, *AtAMT2.1* has a comparable affinity for ammonium as several AMT1 family members. (K_m value 22 µM at pH 7.5; Sohlenkamp *et al*., 2002). However, despite the high affinity for ammonium, the capacity of AMT2 for ammonium transport is at least an order of magnitude lower than that of AtAMT1.1 at a pH below 7, when expressed in yeast. The *V*max of AtAMT2 increased with increasing external pH, whereas that of AtAMT1.1 decreased, so that at pH 7.5 the transport capacity of the two transporters appeared to be similar (Sohlenkamp *et al*., 2002). Possibly, AtAMT2.1 serves as a transporter that is able to acquire ammonium from basic soils where other transporters become less effective.

1.3. Expression and Possible Physiological Roles of AMTs in Leaves

Leaf ammonium is derived from import from the root via the xylem, and amino acid catabolism, especially during photorespiration. As a key component of nitrogen metabolism, ammonium accumulates in mM concentrations in the cytosol, the vacuole, and even in the apoplasm (Wells, 2000, Nielsen and Schjoerring, 1998). Thus, leaf cells require transport systems that mediate the initial uptake of xylem-derived NH_4^+ into the cells, for the retrieval of metabolically released ammonium, and for the transport from one compartiment to another (e.g when photorespiratory NH_3/NH_4^+ released from the mitochondria is to be retrieved by the plastidic glutamine synthase, it must be imported into the chloroplast; Coschigano *et al*., 1998; van Wiren *et al*., 2000). Detailed studies of the fluxes of NH_3 and NH_4^+ into leaf cells are limited and studies on intracellular NH_3/NH_4^+

fluxes are even scarcer. This makes it difficult to assign special functions to the leaf expressed ammonium transporters.

The qRT-PCR experiments showed that in plants grown under full nutrient conditions, *AtAMT1.1* was expressed at high levels (although only 1/3 of its level in roots), followed by *AtAMT1.2* which was 9 fold less expressed than *AtAMT1.1* (and 2/3 of the root expression; Fig. 1.2.2.). The qRT-PCR based leaf expression data is supported by the expression data of the CSB.database, which reports less *AtAMT1.1* and *AtAMT1.2* expression in leaves than in roots (http://csbdb.mpimp-golm.mpg.de/). Promoter-GUS staining showed the same expression pattern for both genes in leaves (Fig. 2.1.2.; 2.2.2.). *AtAMT1.1* driven GUS staining was very strong in sink as well as in source leaves. It was detected in all cells throughout the whole leaf (parenchymal, epidermal, and vascular cells) with highest intensity in the vessels. An identical pattern was observed in *AtAMT1.2* driven GUS staining. Although the staining was generally less intense it was stronger in the vascular than in parenchymal and epidermal cells. These results implicate both transport systems in NH_4^+ efflux/influx into/from the xylem across the mesophyll plasma membrane and in the movement of NH_4^+ from the leaf apoplastic solution into the leaf cells. This capability is of considerable importance for plants as ammonium concentrations in the xylem can rise to 2.6 mM under exclusive NH_4^+ (Cramer and Lewis, 1993). Expression in parenchymal leaf cells indicates that AtAMT1.1 and AtAMT1.2 mediate ammonium transport in these cells. Here, they are possibly involved in the retrieval of photorespiratory NH_3/NH_4^+ generated in the mitchondria or of NH_4^+ produced during nitrate reduction, phenylpropanoid metabolism, or amino acid catabolism. The latter process is of particular importance when proteins are broken down to amino acids (Mattsson and Schjoerring, 2003). Despite the importance of NH_4^+ as a central intermediate in leaf nitrogen metabolism, kinetic and molecular aspects of NH_4^+ transport in leaf cells have been investigated little. However, one study showed that ^{14}C-MA transport in leaves was mediated by a transport system rather than by diffusion across the plasma membrane (Raven and Farquhar, 1981). The transporters involved followed Michaelis–Menten kinetics at concentrations below 100 µM, as do *AtAMT1.1* and *AtAMT1.2*.

To analyse the response of gene expression to N deprivation, qRT-PCR experiments were performed with RNA of liquid culture grown plants after 24 h N deprivation (Fig. 1.2.2.). *AtAMT1.1* expression was 5 fold increased and *AtAMT1.2* expression 3.5 fold increased following this treatment. The induction of both genes was supported by other qRT-PCR experiments which were performed with RNA extracts of plants deprived of N for three days (Sohlenkamp, unpublished data). The increase of *AtAMT1.2* expression in response to N deprivation is remarkable compared with the response to the same conditions in roots where it was stably expressed under both conditions. This difference in regulation presumably reflectes different physiological imperatives in roots and leaves. *AtAMT1.2* expression is restricted to the central cylinder and, therefore, is possibly involved in loading of ammonium into the xylem. During nitrogen deprivation, less ammonium in the roots would be available for loading into the xylem, and an increase in the number of AMT proteins involved in xylem loading would not be necessary. However, in leaves there are other sources of ammonium than just the supply from the roots. In illuminated leaf cells, ammonium is released during photorespiration from the mitochondria in

large quantities (Leegood *et al.*, 1996) or in minor quantities in senescent tissues, when proteins are broken down to amino acids (Mattsson and Schjoerring, 2003). The leaf vacuole, which occupies more than 90 % of the parenchymal cells, has a large capacity for the storage of ammonium released during photorespiration (e.g. vacuolar ammonium concentrations in non-stressed plants range between 2 and 45 mM; Miller *et al.*, 2001). In darkness, transamination processes and the break down of storage proteins can be used as N sources in situations of N shortage. Thus, leaves are primary sources of ammonium during N deprivation. From this point of view, a leaf specific increase of *AMT* genes which are involved in the retrieval of ammonium released into the cytoplasm by the described processes and mediating the transport into the xylem would be advantageous for the plant in nitrogen limited situations. The root and leaf specific regulation of AtAMT1.2 possibly points towards such a function.

AtAMT1.1 has a high affinity for ammonium (Gazarrinni *et al.* 1999) and is the strongest expressed AtAMT in leaf mesophyll and vascular cells. It may have a prominent role in uptake of xylem-derived NH_4^+ via the leaf apoplast or the retrieval of photorespiratory NH_3/NH_4^+ escaping from the cytosol. The ubiquitous expression indicates a houshold function in leaves.

In the context of consistently expressed AMTs in leaves, it is interesting to discuss the leaf specific expression of *AtAMT1.5*. Promoter-GUS staining revealed that this transporter is strongly expressed in the cotelydons of germinating seedlings (Fig. 2.5.2.). Unfortunately, this expression could not be confirmed by the CSB.database because the *AtAMT1.5* gene identification number was identical to *AtAMT1.3* and thus, no data were obtained for *AtAMT1.5* gene expression (http://csbdb.mpimp-golm.mpg.de/). However, in the promoter-GUS experiments, both the parenchymal cells and veins were stained, with a slightly higher intensity in the latter (Fig. 2.5.2). The stained part of the cotyledon was sharply separated from the unstained cotyledon stem. This expression pattern was unique to *AtAMT1.5* among all *AtAMT* genes and it is very likely linked to the mobilization of storage proteins of the cotyledons. During germination, the rapidly growing *Arabidopsis* seedling is dependent on provision of nutrients stored in the cotyledons of the embryo. Storage proteins are broken down to amino acids and ammonium is released in these processes. AtAMT1.5 is likely to be involved in the retrieval of this ammonium. Considering the strong promoter-GUS staining in vascular tissues, AtAMT1.5 is possibly also involved in transport processes there.

Special promoter elements of *AtAMT1.5* could be responsible for the observed nitrogen controlled regulation. In yeast, the nitrogen mediated regulation of the *MEP* genes is mediated by two transcription factors of the GATA family (Marini *et al.*, 1997). Furthermore, in *Neurospora*, nitrate reductase expression is regulated by the two transcription factors NIT2 and NIT4 which bind to NIT specific sequences and also bind to GATA elements (Crawford and Arst, 1993). GATA factors bind to so-called GATA boxes in the promoter sequence which are, if present, usually represented several times in the promoter. In higher plants, GATA factors are involved in tissue specific regulation of gene expression (Gidoni *et al.*, 1989) and a NIT2 homologue has been described in tobacco (Daniele-Vedele and Caboche, 1993). Furthermore, NIT2 binding sequences were identified in the promoter of the nitrite reductase gene from spinach (Rastogi *et al.*, 1997). Meanwhile NIT2 homologues were

also isolated in *Arabidopsis* (Truong *et al.*, 1997). Since these data suggested a NIT2 and GATA factor involvement in the regulation of N metabolism in *Arabidopsis*, the promoter region of *AtAMT1.5* was analysed for these elements by using the promoter analysis programmes TESS (Higo *et al.*, 1999) and MEME (Bailey and Elkan, 1994). Seven GATA elements were found in the 1kb sequence that was fused to the *GUS* gene but no clustering of these elements was identified. Nevertheless, two elements almost identical to NIT2 elements were identified in this region (TESS).

Although *AtAMT1.4* leaf expression was not detected in the qRT-PCR experiments (Fig. 1.2.2.), promoter-GUS analysis showed a faint but distinct staining in the leaf veins but not in mesophyll or epidermal cells (Fig. 2.4.1.). This pattern was found in growing leaves as well as in fully grown leaves. Very faint leaf expression was also registered by Affymetrix chip data in the CSB.database (Appendix, Table 8). The restriction to the veins possibly indicates a specialisation for mediating NH_4^+ efflux/influx into or from the vascular system across the mesophyll plasma membrane. The subsequent transport of NH_4^+ from the leaf apoplast into the mesophyll cells or the retrieval of photorespiratory NH_3/NH_4^+, and reassimilation of NH_4^+ released during amino acid catabolism, is probably not one of the functions of AtAMT1.4. The fact that no transcripts were detected by qRT-PCR is consistent with a low and local concentration of *AtAMT1.4* expression in the relatively few cells surrounding the vascular bundles.

The qRT-PCR experiments showed that in plants grown under full nutrient conditions *AtAMT2.1* was expressed in leaves at low levels (Fig.1.2.2.). *AMT* transcript levels were three times lower in leaves than in roots under the same conditions. GUS-staining revealed a specific expression pattern for *AtAMT2.1*. It was only visible in growing leaves, and there only in the meristems of the leaf margins and the leaf veins (Fig. 2.6.2.). Occasionally, the mid rib also displayed GUS activity. However, no staining was detected in other parts of the leaves at any developmental stage. The restriction to meristems of growing leaves indicates that *AtAMt2.1* might fulfill a specialised function in this tissue, perhaps related to the high metabolic activity and the connected high demand for ammonium-nitrogen for assimilation during biosynthesis.

1. 4. Expression and Possible Physiological Roles of AMTs in Flowers

qRT-PCR experiments revealed that the leaf expressed *AMT* genes *AtAMT1.1*, *AtAMT1.2*, and *AtAMT2.1* are also expressed in flowers. These results were supported by the CSB database and AtAMT2.1 promoter-GUS analysis prior to this thesis (Appendix, Table 8). , Sohlenkamp *et al.* 2002). Additionally, *AtAMT1.4* was found to be expressed in flowers (Fig. 1.2.3.; 2.4.2.), which was also supported by the CSB database (Appendix, Table 8)

AtAMT1.1 was the most highly expressed *AtAMT* gene in this organ, followed by *AtAMT1.2* and *AtAMT2.1* with similarily low transcript levels. After N deprivation, *AtAMT1.1, AtAMT1.2,* and *AtAMT2.1* expression were not significantly altered to compared to full-N nutrition (Fig. 1.2.3.; Tab. 1.2.1.).

In the inflorescences, *AMT1.1::GUS* staining revealed a very distinct expression pattern. It was mainly visible throughout the sepals and the stems of mature siliques (Fig. 2.1.3.). However, the staining in the sepals got fainter during flower development when the flowers opened and stamens grew. The strongest GUS-staining of

sepals was visible in closed buds. Parallel to the decrease of the staining of the sepals, the staining began in the stems of the fertilized flowers. The older the siliques became, the stronger was the GUS staining. The stems of the matured siliques were stained homogenously with a stronger expression in the vascular tissue. In the ripening silique, GUS staining was hardly visible except for the veins.

The sole expression in the sepals and the exclusion of expression in the petals indicates that a major function of AtAMT1.1 is the recapture of photorespiratory NH_3/NH_4^+escaping from the cytosol. One physiological feature of *Arabidopsis* petals is that they do not perform photosynthesis. Green sepals obviously do and this is where *AtAMT1.1* expression was detected. Additionally, as sepals began to senescence, *AtAMT1.1* expression decreased. Thus, AtAMT1.1 appears to play roles in ammonium transport not only in roots (see earlier), but also in photosynthetic tissues, including sepals.

Due to the expression in the vascular tissue, AtAMT1.1 probably plays an additional role in mediating NH_4^+ efflux/influx into and/or from the xylem across the plasma membranes. Vascular expression of *AtAMT1.1*. was also found in the stems of growing siliques, where it was activated after fertilization of the flowers during the embryogenesis. At this developmental stage, the siliques probably have a relatively high demand of nitrogen, which could be met by uptake of ammonium from the xylem, via AtAMT1.1.

AtAMT1.2 expression in flowers was not detectable by GUS-staining. However, it is possible that it is expressed throughout the flower at levels too low to be detected in the GUS assay. The same appears to be true for *AtAMT2.1*. However, in a previous study of *AtAMT2.1* promoter activity (Sohlenkamp *et al*., 2002), GUS staining was observed in the vascular bundle of the sepals, petals and stamens. As revealed in the GUS-expression of illuminated vegetative leaves (Fig.2.5.2.), *AtAMT2.1* is likely to be involved in ammonium transport from the xylem in aerial organs.

AtAMT1.4 transcript levels were higher in flowers compared to leaves as determined by qRT-PCR (Tab.1.2.1.). These high levels were exclusively the result of expression in pollen. Promoter-GUS analysis showed that *AtAMT1.4* was solely expressed in the male gametophytes (Fig. 2.4.2.). Accordingly, the CSB.database reported highest relative transcript levels of *AtAMT1.4* in the stamens (Appendix, Table 8). No GUS staining was found in the vascular bundels or other tissues of the flowers. Considering the low expression in vegetative leaves, which was restricted to vascular bundles only, a possible function of AtAMT1.4 could be uptake of ammonium into the pollen. This ammonium would presumably be supplied by the xylem.

The results described in this thesis show that the six AtAMTs display a high degree of specifity in their tissue expression patterns. Therefore, it is likely that the degree of redundancy among the transporters is less than postulated previously. Based on the variety of expression domains, the AtAMTs appear to have undergone specializations of function within the same tissues as well as in different plant organs. To summarize the possible functions which were inferred from the quantitative and tissue specific expression patterns it can be noted that AtAMT1.1 is likely to be a 'work horse' for cellular ammonium transport and reassimilation. A major role is probably the recapture of photorespiratory NH_3/NH_4^+escaping from the cytosol. In roots, it is likely to transport NH_4^+ from the apoplast into cortical cells.

AtAMT1.3 and AtAMT1.5 appear to be specialised for the acquisition of external NH_4^+ from the soil. Furthermore, AtAMT1.5 probably plays an additional role in the reassimilation of NH_3/NH_4^+ released during the breakdown of storage proteins in the cotyledons of germinating seedlings.

AtAMT1.2 is expressed in the central cylinder of the roots, and in leaves in parenchymal and vascular cells where it shares the same expression pattern as AtAMT1.1. Thus, it is difficult to distinguish a specialisation between both transporters. However the root and flower specific expression patterns of these two genes are different and may indicate divergent functions in these organs.

AtAMT1.4 shows a very distinct expression that is restricted to the vascular bundles of leaves and to pollen only, where it is likely to be involved in the uptake of NH_4^+ into cells.

The AtAMT2.1 expression pattern is confined to vascular bundels and meristematic active tissues in leaves, where ammonium concentrations can reach very high levels (Cramer and Lewis, 1993). Thus, it might be specialised in ammonium transport in ammonium rich environments where the functions of other transporters are limited. The root hair expression ascribes an additional role in NH_3/NH_4^+ acquisition.

However, firm conclusions about the functional specialisation of individual AtAMTs are not possible from qRT-PCR data and Promoter-GUS expression analysis. To obtain more secure knowledge of possible specialisations and redundancies of the ammonium transporters, physiological, biochemical, and phenotypical studies with single and double knock-out mutants of the individual *AMT*-genes were required. For that reason homozygous T-DNA insertional mutants of the *AtAMT* genes were isolated.

2. Analysis of the *AMT* T-DNA Insertion Lines

2.1. *AMT* T-DNA Insertion Lines: Initial Analysis

Analysis of insertion sites revealed that the T-DNA had inserted either in the 5'-UTR or further upstream in the promoter region of an *AtAMT* gene in four lines (Fig. 4.1.1.).

In *SyAMT1.1* the T-DNA inserted into the 5'-UTR very close to the ATG (-24 bp). In *SyAMT1.2* the T-DNA inserted at the beginning of the 5'-UTR (-57 bp). *SyAMT1.4* and *SyAMT2.1* carried the T-DNA 33bp and 100bp upstream of the 5'-UTR or -75 bp and –151 bp upstream of the coding sequence, respectively. The remaining two *AMT* genes, *AtAMT1.3* and *AtAMT1.5*, were not represented by T-DNA insertion lines in any T-DNA library. Because most of the protein encoding genes of *Arabidopsis* were represented in a T-DNA library at the time when the inquiry was performed, this was surprising because both genes are not situated in the proximity of centromers. A further surprise was the exclusive insertion of the T-DNA upstream of the coding sequences in all isolated lines.

Previous studies (Azpiroz-Leehan and Feldmann, 1997; Parinov *et al*., 1999; Galbiati *et al*., 2000; Szabados et al., 2002) indicated, that T-DNA-based mutagenesis agents insert randomly into the genome is consistent with insertion via illegitimate recombination (Tinland, 1996). Although DNA integration bias has been observed for

yeast, animals, and plants, no bias in *Agrobacterium* T-DNA integration was reported in most previous studies (Alonso *et al*. 2003; Brunaud *et al*. 2002; Craig 1997; Szabados *et al*. 2002).

However, very recent studies revealed that T-DNA does favor distinct regions of the chromosomes for insertion in *Arabidopsis* (Pan *et al*., 2005; Schneeberger *et al*., 2005). On the chromosomal level, insertion frequencies indicated that T-DNA integration is suppressed near centromeres and rDNA loci, progressively increases towards telomeres, and is highly correlated with gene density. At the gene level, T-DNA insertions show a statistically significant preference for integration within genes and their immediate environments, the UTRs. Here, T-DNA had a striking preference toward the upstream region starting from approximately 100 bp upstream of the start codon. The increased insertion frequencies in 5'-upstream regions compared to coding sequences were positively correlated with gene expression activity and DNA sequence composition (Pan *et al*., 2005; Schneeberger *et al*., 2005). Insertion preferences in the 5'-flanking regions of genes had been observed earlier in other organisms such as yeast, where Ty1 and Ty3 retroelements are targeted preferentially into regions adjacent to RNA polymerase III, and in *Drosophila* where P-elements show preferential insertion in the 5'-UTR regions of genes (Liao *et al*., 2000; Parinov *et al*., 1999; Raina *et al*., 2002). In maize, Ac and Mutator elements target preferencially 5'-UTRs, which can account for over 80% of the insertion events recovered at the *glossy 8* locus (Dietrich *et al*., 2002). However, the underlying mechanism for directing insertion to the 5'-regions of genes is not well understood, even though the molecular biology of the T-DNA transfer to the plant nucleus has been studied extensively (Gelvin, 2000; Tzfira and Citovsky 2002). The preference for T-DNA insertion in 5'- upstream regions of genes strongly correlates with the gene expression level and particularly with the compositional features of RNA polymerase II promoter regions. The maximum insertion frequency position was located at around –150 bp and the minimum insertion frequency observed was located at around +100 bp relative to the start codon of the coding sequence (Schneeberger *et al*., 2005). Furthermore, this study clearly showed that insertion preference is not uniformly high in noncoding sequences but is highest close to the start codon and reduced to a level similar to that of the coding sequence about 1000 bp upstream the translated region. It was shown that genes with a high average expression show significantly higher rates of T-DNA insertion at –400, –100, and 0 bp upstream of the start of transcription compared to genes with low average gene expression levels (Schneeberger *et al*., 2005). This could be a consequence of changes in the DNA structure associated with the increased accessibility of these regions due to the binding of transcription regulatory proteins (Dietrich *et al*. 2002; Muller and Varmus 1994; Vigdal *et al*. 2002). The high rate of transcription initiation of highly expressed genes may provide more access to recombination proteins in the 5'-upstream region.

Considering the recent studies on T-DNA integration into the *Arabidopsis* genome, it is not too surprising that the T-DNA in all four isolated knock-out lines inserted upstream of the coding sequence. The promoter regions of these genes are likely to be related and the mechanisms that direct the T-DNA to the insertion sites can act similarily. The absence of T-DNA insertions into *AtAMT1.3* and *AtAMT1.5* in current insertion populations may reflect, at least in parts, the bias for T-DNA integrations into expressed genes and the selection process of T-

DNA mutants. *AtAMT1.3* is expressed at relatively low levels and *AtAMT1.5* is not expressed under normal greenhouse growth conditions, which would make them less prone to the machinery of insertion.

2.2. Effects of the T-DNA Integration on *AtAMT*-Gene Expression

AMT transcript levels were determined for the affected genes in each of the *AtAMT* T-DNA lines. Although no T-DNA had integrated into the coding sequence, the relatively high transcription of each of the genes in the mutants was astonishing (Fig.4.3.1.). The right border of the closest insertion was –24 bp from the start codon (*SyAMT1.1*) while furthest removed T-DNA was at bp –151 (*SyAtAMT2.1*). Apparently, none of these insertions affected greatly normal promoter recognition by the polymerase II holoenzyme (Pol II). In eukaryotes, Pol II recognition sites are usually situated about 100 bp upstream of the transcription start, but crucial DNA binding sequences might also be closer to the ATG (Triezenberg, 1995). Furthermore, the binding of the Pol II-holoenzyme is also mediated by transcription factors which interact with the components of the Pol II-holoenzyme and enhancer elements of the DNA. These can be positioned a long distance up- or downstream of the promoter and could act over the T-DNA sequence. Additionally, DNA-gyrase, which opens up the DNA to faciliate binding of the transcription complex, can effect remote sequence elements, and can support the binding of Pol II over long distances in regions containing multiple genes. In *E.coli*, a six basepair long consensus sequence which lies -10 to -35 nucleotides upstream of the start codon suffices for recognition by RNA polymerase, and for binding of the transcription complex a region of only about –10 bp is crucial.

Of particular interest in this context is the recent isolation of an additional *AtAMT1.1* T-DNA insertion mutant in which the right border of the T-DNA was inserted 6 bp upstream of the start codon of *AtAMT1;1* (Glass and Kaiser, 2002). RNA blot analysis showed no *AtAMT1.1* RNA in this mutant. This indicates that the region from –6 to –24 bp must be crucial for the recognition of the Pol II (-24catcttcttctctaaactc-6).

2.3. Phenotypical and Developmental Effects of the *AMT*-T-DNA Integrations

To determine whether T-DNA integration into *AMT* genes had any effect on developmental or physiological traits, growth tests on different media and ^{14}C-MA uptake studies with the insertional mutants were performed in parallel with *AtAMT* transcipt analyis (section 4.2., 4.3., 4.4.). Vegetative development and the generative period was analysed with respect to various parameters, as described in section 4.

In root growth assays, none of the T-DNA lines revealed statistically significant differences compared to the WT. Similarily, analysis of root NH_4^+ and NO_3^- and glutamine in a complete *AtAMT1.1* knock-out line also revealed only minor, statistically not significant differences between the mutant and wild-type lines, regardless of the N status (Glass and Kaiser, 2002). These results are not surprising, in view of the minor effects of the T-DNA insertions on *AMT* gene expression, and the likelihood that several AMT proteins, including AtAMT1.3 and AtAMT1.5 (see above) work together to transport ammonium in roots.

The growth of the rosette leaves of the T-DNA insertion lines on well fertilized soil was not statistically different to the WT. On average, the leaves showed the same length and shape. Further growth tests were performed

with developing inflorescences of plants grown on ammonium rich and poor soils. It was considered that a reduction of functional transcripts caused by the T-DNA insertion into the promoters of leaf and flower expressed genes could have lead to insufficient ammonium reassimilation or intercellular transport in these tissues. These effects could potentially lead to reduced growth or retardation in development, which could become apparent at normal nutritional conditions or during shortages of ammonia. It was shown that *SyAMT2.1* was severely retarded in bolting (Tab. 4.3.2.1.). This reduction of growth speed in several *SyAMT2.1* plants was remarkable because promoter-GUS analysis showed that this transporter is primarily expressed in the meristems of growing leaves. A reduction of AtAMT2.1 transport capacity may negatively influence leaf growth.

SyAMT1.1 showed a less extreme retardation in bolting. However, it was increased on ammonium limited soil. A similar effect was also observable at the begin of flowering for both lines (Tab. 4.3.2.1.). It is possible that these effects were caused by tissue-specific changes in *AMT* expression in these mutants during those stages of development. Unfortunately, due to time constraints, AMT transcript levels in these mutants were not measured for these specific tissues/stages of development.

Concerning inflorescence length, no line was statistically different to the WT control at any time point. At the end of the vegetative period, the total seed weight was determined. Again, no significant differences were found.

2.4. ^{14}C-MA Uptake of the T-DNA Insertion Lines

To analyse the ammonia uptake kinetics of the T-DNA-insertion lines ^{14}C-MA uptake studies were performed. After an incubation time of ten minutes, no line differed significantly in ^{14}C-MA content from the WT controls (Fig. 4.4.1.and 2.).

To summarise the analyse of T-DNA mutants, it can be concluded that promoter disruption by the T-DNA insertions was not sufficient to assess the specific functions of the individual genes.

Homozygous combinations of the T-DNA tagged genes were generated through the crossing of double mutants into the F_2-generation. In this generation, no visible phenotypes were detected among the isolated homozygous double mutants on fertilized and N poor soils and it was considered that the lack of phenotypes and the remaining transcription of the leaky promoters did not justify the effort of further analysis.

3. Analysis of the *AMT1.1*RNAi Lines

As an alternative to gene knock out by T-DNA insertion, RNA silencing of the *AtAMT* genes was attempted by expression of *AtAMT1.1*-RNAi hairpin (hp) constructs. RNAi silencing refers to a series of events that lead to the targeted degradation of cellular mRNA and thus, to silencing of the corresponding gene if the introduced gene and the target gene shares homologies of at least 21 identical nucleotieds (section 5.1). The *AtAMT1* gene family consists of closely related members with over 75 % DNA sequence identity (Tab. 1.1., Fig. 5.2.). It was shown that expression of an hpRNA construct of the *AtAMT1.1* gene sequence was able to reduce the transcript levels of the genes of the *AtAMT* genes (Tab. 5.4.1.). Thus, the RNAi plants provided a means to investigate the effects of transcript reduction of a whole *AMT* family on a molecular, physiological, and developmental level and are able to reveal possible functions of AMTs in plants and the importance of ammonium transport for plant development.

Whereas an RNA silencing-like mechanism was first described in plants in 1990 in transgenic petunia (Napoli *et al*., 1990; van der Krol *et al*., 1990), until the discovery that dsRNA was more effective in silencing gene expression than single stranded antisense RNA (Fire *et al*., 1998; Montgomery *et al*., 1998; Waterhouse *et al*., 1998), RNAi was not used as a method for targeted gene silencing. This makes RNAi a relatively new method for the investigation of gene functions and at the beginning of this thesis relatively little was known about the long term effects of RNAi silencing and the inheritage of the silencing mechanism in plants. However, it was reported that in plants the induced RNA silencing mechanism can be stably maintained for several months (Voinnet *et al*., 1998), whereas in *Caenorhabditis*, RNA silencing is inheritable (Fire *et al*., 1998).

3.1. Quantification of *AtAMT* Transcript Levels in *AtAMT1.1RNAi* Lines

To test the functionality of the *AMT1.1*-hpRNA construct in the transformed plants, leaves of BASTA resistant T_2-plants with wildtype like and dwarfed phenotypes were harvested (line2 to line 4). The transcript levels of the leaf expressed *AMT* genes *AtAMT1.1, AtAMT1.2* and *AtAMT2.1* were measured by qRT-PCR using gene specific primers (II.1.3.). It was shown that the mRNA levels of these genes were reduced in all lines investigated. The *AMT1.1*-hpRNA construct silenced most efficiently the *AtAMT1.1* gene. Its mRNA levels were reduced by 77% and 55 % in the three lines investigated (Tab. 5.2.). The efficiency was slightly higher than that of a recent study on RNAi silencing efficiency which reported ~50 % reduction for hpRNAi constructs (Smith *et al*., 2000). However, these constructs contained not an intron based spacer loop (Tab. II.1.4.) but a GUS spacer loop which negatively affects the efficiency of the RNAi effect (Waterhouse *et al*. 2000). The transcript levels of the other leaf expressed *AtAMT1* genes were also reduced (Tab. 1.4.). This finding, that other genes than *AtAMT1.1* were also affected by the RNAi silencing mechansim confirmed previous studies that extended homology between the introduced gene and target genes are not required for initiation of RNAi silencing and that the homology required to initiate RNA silencing can be relatively short (Voinnet *et al*., 1998). DNA sequence comparisons of the *AtAMT* genes showed over 75 % identities on the nucleotide level between *AtAMT1* genes (Tab. 1.1., Fig. 5.2.a). However, the reduced efficiency of the *AMT1.1*-hpRNA construct to silence less close related genes also

confirmed, that silencing becomes less effective as homology between RNAi construct and target declines (Thomas *et al*., 2001).

With these data of the T2-generation, the *AMT1.1*-hpRNA construct was considered functional and the selected lines were transferred into further generations. In the T4-generation, *AtAMT* gene transcript levels of whole plants, roots, and shoots of RNAi line 4 were analysed in qRT-PCR. This line was selected for an intensive transcript analysis because it showed the most stable decrease of ^{14}C-MA influx throughout all generations (section 5.3.) and also showed the most severe phenotypes among the cultivated RNAi lines (section 5.6.). Therefore, it was considered that the RNAi silencing effects were stable in this line and representative for the effects of the *AtAMT1.1*-RNAi hairpin construct. On the whole plant level, transcript levels of the *AtAMT1* genes were generally reduced in the *AtAMT1.1RNAi* line compared to the wildtype (Fig. 5.4.1.). As already observed in the T_2-generation, *AtAMT1.1* mRNA quantities were stronger reduced than the mRNA quantities of the other *AtAMT* genes (Fig. 5.4.1.). *AtAMT1.1* mRNA levels were 5.7 fold more reduced than *AtAMT1.2* levels and 3.4 times more reduced than *AtAMT1.2* levels (Tab. 5.4.1.). *AtAMT2.1,* which is very distantly related to *AtAMT1.1* had 10 times less reduced mRNA levels than *AtAMT1.1*. (Tab. 5.4.1).

That *AtAMT2.1* transcript levels were reduced at all by the *AtAMT1.1*-RNAi hp construct was surprising because an alignment of the *AtAMT1.1* and *AtAMT2.1* sequences showed, that *AtAMT2.1* has no 21 bp long sequence identities. Instead, it contains numerous up to 8 bp long stretches which are identical to *AtAMT1.1*. These are seperated by single or more nucleotide substitutions (Fig. 5.2.b.). This may indicate, that the required length of identical sequences to initiate RNA silencing can be shorter than 21 bp.

In roots, reduction in transcript levels was observed for the root expressed genes *AtAMT1.1, AtAMT1.3*, and *AtAMT1.5* in *AtAMT1.1-RNAi* line4 (Fig. 5.4.2.). However, the relative transcript levels of *AtAMT1.1* were reduced only 1.3 times more than *AtAMT1.3* and 1.2 times more than *AtAMT1.5* (Tab. 5.4.1.). The little difference in the silencing efficiency between these genes might be explained by the close relationship to *AtAMT1.1* (Fig. 1.). These genes share over 76% identities on the nucleotide level (Tab. 1.1.).

In leaves, silencing was observed for *AtAMT1.1 and AtAMT1.2*. Silencing was efficient in both genes, but *AtAMT1.1* transcripts were more reduced than *AtAMT1.2*. transcripts (Fig. 5.4.3.). The lower efficiency in the silencing of *AtAMT1.2* is likely due to the remote relation of these genes (Fig. 1.).

Supplementary it can be noted that *AtAMT1.1* mRNA levels were in general more reduced by the *AtAMT1.1* hp construct than other *AtAMT* genes on whole plant level. However, the root expressed *AtAMT1.3* and *AtAMT1.5* genes, which are the closest relatives, are reduced by almost the same amount (Fig. 5.4.2.). This is probably due to their high degree of identities on the DNA level. Furthermore, the cell specific expression of these genes is also slightly different in roots (section 3.1., 3.3., and 3.5.), and this possibly contributes to a more efficient gene silencing in cells where the siRNAs find less or no *AtAMT1.1* mRNA. *AtAMT1.2* transcripts are not significantly reduced in roots compared to wildtype levels, but showed a reduction of transcripts to 44 % of the WT (Fig. 5.4.3.). *AtAMT1.1* transcripts were quantitatively 10 times more reduced than *AtAMT1.2*, but were only reduced to 55 % of its wildtype levels. The relatively high silencing effect on *AtAMT1.2* mRNA levels in leaves is

at odds with the low silencing efficiency in roots. However, cell specific expression of *AtAMT1.2* in leaves indicates a higher expression along the leaf veins than in parenchymal cells (section 3.2.). This difference in the cell specific expression to *AtAMT1.1* might have an additional effect on silencing efficiencies. However, a similar effect is not seen in roots.

3.2. Analysis of the Ammonium Uptake Kinetics of the *AMT1.1RNAi* Lines

To verifiy the functionality of the *AMT1.1*-hpRNA construct on a physiological level, BASTA resistant T1-plants with a wildtype like and a dwarfed phenotype were selected (named line1 to line 4) and the descendants of these T_1-plants were submitted to ^{14}C-MA uptake experiments in the T_2 (Fig. 4.2.1.1). These experiments showed a severe reduction of ^{14}C-MA influx which ranged between 16 % and 27 % of WT levels after 10 minutes incubtion. After 20 min incubation, the reduction became less in relation to the WT and ranged beween 21 % and 50 % of WT levels (Tab. 4.3.1.). This increase in influx during the last minutes of incubation is probably caused by an accumulation of MA in the plant organs in the absence of further metabolism. This level would be reached more quickly in the WT because of the faster uptake. These results complement the qRT-PCR analysis of AtAMT transcipts in the *AMT1.1RNAi* lines which showed a reduction of *AtAMT* transcript level compared to the WT (5.2.) and indicate that the RNAi construct was functional in the selected lines. However, lower uptake could have resulted from poor growth caused by pleiotropic effects unrelated to a reduction of *AtAMT* transcripts. But germination and growth of the seedlings was comparable to the WT and when the sterile culture medium was not replaced by fresh medium after 7 days, the WT plants reduced growth and eventually became senescent instead of the *AMT1.1RNAi* lines (Fig. 5.3.1.). This indicated an earlier N deprivation of the WT plants which is likely due to faster ammonium uptake and subsequent metabolic consumption.

The same experiment was repeated at the T_3-generation. However, only homozygous single insert lines were isolated for the experiments of the T_3- and later generations (except line2). The use of homozygous single insert lines avoided segregation of the RNAi constructs in later generations which would complicate the analysis of the RNAi effects. Due to the selection of single insert lines, only two lines which were used in the T_2-experiment were used again in the T_3-generation. ^{14}C-MA influx into *AtAMT1.1*RNAilines was less reduced in the T_3-generation compared to the T_2-generation. After 10 min incubation in 50µM ^{14}C-MA, influx was reduced by between 76 % to 24 % compared to the WT (Tab. 5.3.2.1.). This indicated, that the RNAi construct lost inhibitory activity from one generation to the next.

To verify the results obtained by the ^{14}C-MA uptake experiments using an independent approach, plants of the T_3-generation of the RNAi lines 1, 2, 3 and 4 were submitted to a ^{15}N-ammonium uptake experiment. After 20 minutes incubation, influx in all RNAi lines was lower than the WT by between 53 % and 22 % (Fig. 5.3.2.2.). This reduction was less than in the T2-generation, where ^{14}C-MA influx in RNAi lines was between 79 % and 50 % lower than the WT after 20 minutes. This again indicated that the *AMT1.1*-hpRNA construct impaired the MA influx in the analysed lines but that it lost some activity from one generation to the next.

The decline in RNAi silencing efficiency continued into the T_4-generation. For example, MA influx into line 4 increased from the T_2 to the T_4 generation by three fold. Likewise, lines 50 and 84 exhibited increased MA influx capacity between the T_3 and the T_4 by 2 fold and 3.5 fold, respectively (Fig. 5.3.3.).

It is interesting to compare the effects of *AtAMT1.1*RNAi on MA uptake with those of the *AMT1.1* T-DNA insertion on ^{13}N-ammonium influx (Glass *et al*., 2002). In the *AMT1.1* T-DNA line, high-affinity $^{13}NH_4^+$ influx was decreased by only ~30% compared with WT plants after 10 minutes incubation at 50 µM (Glass *et al*., 2002). In contrast, the most impaired RNAi line of the T_1-generation showed a decrease of ~84 % ^{14}C-MA after 10 minutes incubation (Tab. 5.3.1.). Thus, although transcript levels were not completely reduced in any single AtAMT gene in the RNAi lines (Tab. 5.2.), the overall effect on uptake was more dramatic in the RNAi lines. This comparison indicates that AMT transporters other than *AtAMT1.1* contribute significantly to ammonium uptake in *Arabidopsis*.

To further supplement the ^{14}C-MA uptake studies, the transport kinetics for ammonia per se were measured in uptake experiments using the T_4-generation of *AMT1.1*RNAi lines and *Col-o* (Fig. 5.5.1.). These experiments confirmed the results of the ^{14}C-MA uptake studies. Ammonia influx was decreased in the T_4 compared with the WT plants at generally the same levels as ^{14}C-MA influx at the T_4. For ammonia, the decrease ranged between 28 % and 16 % after 10 minutes at 50 µM ammonium in this generation, while the reduction in ^{14}C-MA ranged between 52 % and 14 % (Fig. 5.5.1).

3.3. Growth Analysis of the *AtAMT1.1*RNAi Lines

Many BASTA resistant plants had wildtype appearance but some plants had a phenotype different to the WT (5.6.). In the still segregating populations some of the phenotypes and intermediates were possibly due to stochastic epigenetic effects caused by the insertion events and not by the RNAi activity. Of cultivated lines some plants passed down similar phenotypes to the following not segregating generations. The unstability of phenotypes was probably caused by the nature of the silencing mechanism of RNAi which is, unlike a gene mutation, a biochemical process which is mediated by enzymes synthethized by individual plants. Here, sources of high natural variation exist. It was reported that the RNAi effect is often transient (Vaistij *et al*., 2002; Anandalakshmi *et al*., 2000; Voinnet *et al*., 1999), Correspondingly, in the experiments performed, it was occasionally observed, that from one generation to the next the *AtAMT* gene transcripts rose to WT levels, reductions in ^{14}C-MA uptake became undetectable, and BASTA resistance ceased, which was probably largely due to the loss of the RNAi effect.

The RNAi lines 4, 50 and 84 showed relatively stable physiological as well as morphological phenotypes which were still visible in the T_4-generation. Plants had a reduced size and contained small rosette leaves or showed a continous production of rosette leaves even throughout the flowering period which led to a densely filled but small rosette. Line 50 had relatively large rosette leaves which grew bigger than the wildtype leaves. Since it

was difficult to assign a stable and specific phenotype to the RNAi effect, a statistical approach was taken, in which the growth of 40 plants of each of these line and the WT was followed throughout development.

Vegetative and inflorescence growth, and the number of bolting and flowering plants were determined. It was found that bolting as well as flowering was retarded statistically significant in all analysed RNAi lines compared to wildtype plants. Because these retardations of development were visible in all 3 lines investigated, it is supposed that they are caused by the RNAi effect on the mRNA levels of the *AMTs*. Due to the RNAi effect, the plants acquired ammonium less efficiently from the soil (5.3.) and the internal ammonium transport is presumably impaired. Both probably slows down growth as less nitrogen is available for the plant metabolism in time, compared to wildtype plants. The slower growth may have caused the RNAi plants to enter into the flowering period later. This hypothesis is supported by two observations. Firstly, RNAi plants grown on 10 µM ammonium containing soil flowered later than RNAi plants grown on normal fertilized soil (Fig. 5.6.2.) and secondly, the WT control plants also flowered later on 10 µM containing soil than on normally fertilized soil (Fig.5.6.2.). This indicates that the available ammonium influences not only growth but also flowering time under constant conditions.

Furthermore, the rosette diameters of the plants were measured during development. During the first three weeks, the rosette diameters of the *AMT1.1*RNAi lines remained significantly smaller than the WT rosettes Fig. 5.6.4.). After 28 days, when the WT stopped flowering and began to senescent, the investigated RNAi lines were still growing and flowering. At this time, the rosette diameters of the RNAi lines were larger and the above ground plant parts had a heigher dry weight than the WT (Fig. 5.6.3.). The increase in dry weight of the shoots was probably caused by the prolonged vegetative period of the RNAi plants. Thus, they produced more rosette leaves which contributed most to the increase in weight. Since the plants acquired less ammonium per time (5.3.) they grew slower. But due to the continous fertilizing, they never were deprived of N and could grow continously. Since the WT stopped the vegetative growth earlier, the RNAi plants eventually produced more leaves. Surprisingly, some RNAi plants did not stop vegetative growth during the flowering period. They kept producing rosette leaves during flowering but these leaves did not reach the wildtype size. However, the weight of the small RNAi line 4 plants was not statistically significant higher (Fig. 5.6.3.). These plants might have acquired not enough ammonium to make up the shortages during the prolonged growth. This is supported by the observations that the plants of line 4 appeared to be sicker and had a high lethality after 4 weeks.

Line 50 produced rosette leaves which were larger than WT leaves (Fig. 5.6.4.). This was interesting because the leaves of the *amt1*;*1*:*T-DNA* line were found to be distinctly more succulent than those of the wild type (Glass *et al*., 2002). This phenotype of RNAi plants and the *amt1*;*1*:*T-DNA* plants might be related. No other discernible developmental phenotype was evident in the *amt1*;*1*:*T-DNA* plants and they germinated, bolted, and set flower as did wild-type plants (Glass *et al*., 2002). This indicates, that the reduction of transcript levels of *AtAMT1.1* alone probably has not caused the described phenotypes.

Possibly, the reduced mRNA levels of *AtAMT1.3* and *AtAMT1.5* (Tab. 5.4.1.) are additionally responsible for the slow growth because the expression data of these genes (section 2. and 3.) indicate a function in the acquisition of external ammonium. In a recent study of a *AtAMT2.1*RNAi mutant, which had lost *AtAMT2.1* transcripts almost completely (Sohlenkamp 2001, unpublished) no nitrogen-dependent growth differences to wildtype plants were observed. This indicates that the observed reduction of *AtAMT2.1* in the RNAi lines has possibly not caused the described phenotypes. However, in this *AtAMT2.1*RNAi mutant, the *AtAMT1* gene expression was not analysed and it is unknown if the transcript levels of these genes were also affected. *AtAMT1.4* is not expressed in roots and at low levels in leaves and it is unlikely that a reduction of AtAMT1.4 transcrips is able to cause an observable growth reduction. Together with the functional *amt1*;*1*:*T-DNA* and the *AtAMT2.1*RNAi plants which gave no growth phenotype, the circle of possible candidates, responsible for the described phenotypes, has become narrow and points to AtAMT1.3 and AtAMT1.5 as prime candidates for nitrogen dependent phenotypes. Functional knockout mutants of these genes should proove this hypothesis and make it promising targets for future reverse genetics.

References

Alonso JM, Stepanova AN, Leisse TJ, Kim CJ, Chen H, Shinn P, Stevenson DK, Zimmerman J, Barajas P, Cheuk R, *et al.* (2003) Genome-wide insertional mutagenesis of *Arabidopsis thaliana*. *Science* **301**: 653–657

Altschul S.F., W. Gish, W. Miller, E.W. Myers, D.J. Lipman (1990) Basic local alignment search tool *J. Mol. Biol*. **215** 403-410.

Anandalakshmi, R., Marathe, R., Ge, X., Herr, J.M. Jr., Mau, C., Mallory, A., Pruss, G., Bowman, L. and Vance, V.B. (2000). A Calmodulin-related protein that suppresses post transcriptional gene silencing in plants. *Science* **290**: 142–144.

Asmussen MA, Gilliland LU, Meagher RB (1998) Detection of deleterious genotypes in multigenerational studies. II. Theoretical and experimental dynamics with selfing and selection. *Genetics*, **149**: 727-737.

Azpiroz-Leehan R, Feldmann KA (1997) T-DNA insertion mutagenesis in *Arabidopsis*: going back and forth. *Trends Genet* **13**: 152–156

Bailey TL, Elkan C (1994) Fitting a mixture model by expectation maximization to discover motifs in biopolymers. *Proceedings of the Second International Conference on Intelligent Systems for Molecular Biology*. AAAI Press, Menlo Park, CA: 28–36

Bechtold N, Pelletier G (1998) In planta *Agrobacterium*-mediated transformation of adult *Arabidopsis thaliana* plants by vacuum infiltration. *Methods Mol Biol* **82**: 259–266

Bertl, J.D. Reid, H. Sentenac, C.L. Slayman (1997) The spTRK gene encodes a potassium-specific transport protein TKHp in Schizosaccharomyces pombeJ. J Membr Biol. **159**(1):95-

Blackwel R.D., A.J.S. Murray, P.L. Lea, A.C. Kendall, N.P. Hall, J.C. Turner, R.M. Wallsgrove (1988) *Photosynth. Res*. **16** 155-176.

Bloom A. J., Sukrapanna S.S., Warner R.L. (1992) Root growth as a function of ammonium and nitrate in the root zone. *Plant Physiol*. **99** 1294-1301.

Bloom A.J., ISI Atlas of Science (1988) *Anim. Plant Sci*. **1** 55-59.

Bloom AJ, Sukrapanna SS, Warner RL (1992) Root respiration associated with ammonium and nitrate absorption and assimilation by barley. *Plant Physiol* 1992, **99** 1294-1301.

Brent N. Kaiser, Suman R. Rawat, M. Yaeesh Siddiqi, Josette Masle, and Anthony D.M. Glass (2002) Functional Analysis of an *Arabidopsis* T-DNA "Knockout" of the High-Affinity NH4 Transporter AtAMT1;1 *Plant Physiology*, 2002,. **130**,1263–1275

Britto D.T., Kronzucker H.J.. (2001) Constancy of nitrogen turnover kinetics in the plant cell: Insights into the integration of subcellular N fluxes. *Planta* **213** 175–181.

Britto D.T., Siddiqi M.Y., Glass A.D.M., Kronzucker H.J. (2001) Futile membrane ion cycling: a new cellular hypothesis to explain ammonium toxicity in plants*. Proceedings of National Academy of Sciences*, USA **98** 4255–4258.

Brunaud V, Balzergue S, Dubreucq B, Aubourg S, Samson F, Chauvin S, Bechtold N, Cruaud C, DeRose R, Pelletier G, *et al.* (2002) T-DNA integration into the *Arabidopsis* genome depends on sequences of preinsertion sites. *EMBO Rep*. **3**: 1152–1157

Bustin S.A., (2000), Absolute quantification of mRNA using real-time reverse transcription polymerase chain reaction assays. *Journal of Molecular Endocrinology* **25**, 169-193

Chalker D, Sandmeyer S (1992) Ty3 integrates within the region of RNA polymerase III transcription initiation. *Genes and De*velopment **6**:117–128

Sohlenkamp C., Wood C.C., Roeb G.W., and Udvardi M.K. (2002) Characterisation of *Arabidopsis AtAMT2*, a High-Affinity Ammonium Transporter of the Plasma Membrane1. *Plant Physiology*, **130**, pp. 1788–1796

Clough *et al*. (1998) Floral Dip: a simplified method for *Agrobacterium* mediated tranformation of *Arabidopsis thaliana. Plant J*. **16**, 735-753.

Cooper HD, Clarkson DT. (1989) Cycling of amino-nitrogen and other nutrients between shoots and roots in cereals—a possible mechanism integrating shoot and root in the gene expression. *Journal of integrative plant biology* **2**: 291–299.

Coschigano KT, Melo-Oliveira R, Lim J, Coruzzi GM (1998) *Arabidopsis* gls mutants and distinct Fd-GOGAT genes: implications for photorespiration and primary nitrogen assimilation. *Plant Cell*, **10** 741-752

Derewenda Z.S. (1995) The occurrence of C-H...O hydrogen bonds in proteins. *J. Molec. Biol*. **252** 248

Devine S, Boeke J (1996) Integration of the yeast retrotransposon Ty1 is targeted to regions upstream of genes transcribed by RNA polymerase III. *Genes and Development* **10**: 620–633

Dietrich CR, Cui F, Packila ML, Li J, Ashlock DA, Nikolau BJ, Schnable PS (2002) Maize Mu transposons are targeted to the 5′ untranslated region of the *gl8* gene and sequences flanking Mu target-site duplications exhibit nonrandom nucleotide composition throughout the genome. *Genetics* 160:697–716

F.R. Lauter, O. Ninnemann, M. Bucher, J.W. Riesmeier, W.B. Frommer (1996) Preferential expression of an ammonium transporter and two putative nitrate transporters in toot haires of tomato. *Proc. Natl. Acad. Sci. USA* **93** 8139-8144.

Feldmann *et al*., (1989); A dwarf mutant of *Arabidopsis* generated by T-DNA insertion mutagenesis. *Science* **243** 1351-1354

Felsenfeld G, Boyes J, Chung J, Clark D, Studitsky V (1996) Chromatin structure and gene expression. *Proc Natl Acad Sci USA* **93**: 9384–9388

Feng J, Volk RJ, Jackson WA (1998) Source and magnitude of ammonium generation in maize roots**.** *Plant Physiol*, **118** 835-841

Fire, A., Xu, S., Montgomery, M.K., Kostas, S.A., Driver, S.E. and Mello C.C. (1998) Potent and specific genetic interference by double-stranded RNA in *Caenorhabditis elegans*. *Nature* **391**: 806–811.

Forde, B.G. and Clarkson D.T. (1999). Nitrate and ammonium nutrition of plants: physiological and molecular perspectives. *Adv. Bot. Res*. **30**: 1–90.

Galbiati M, Moreno MA, Nadzan G, Zourelidou M, Dellaporta SL (2000) Large-scale T-DNA mutagenesis in *Arabidopsis* for functional genomic analysis. *Funct Integr Genomics* **1**: 25–34

Gaymard F, Pilot G, Lacombe B, Bouchez D, Bruneau D, Boucherez J, Michaux-Ferriere N, Thibaud JB, Sentenac H: Identification and disruption of a plant shaker-like outward channel involved in K+ release into the xylem sap. *Cell* 1998, **94**: 647-655.

Gazzarrini S., Lejay L., Gojon A., Ninnemann O., Frommer WB, von Wiren, N., (1999) Three functional transporters for constitutive, diurnally regulated, and starvation induced uptake of ammonium into Arabidopsis roots. *Plant Cell* **11:** 937–947

Gelvin SB (2000) *Agrobacterium* and plant genes involved in T-DNA transfer and integration. In: RLB Jones, Hans J Delmer, Deborah P (eds) Annual review of plant physiology and plant molecular biology. *Annual Reviews*, Palo Alto, Calif., pp 223–256

Gilliland LU, McKinney EC, Asmussen MA, Meagher RB (1998) Detection of deleterious genotypes in multigenerational studies. I. Disruptions in individual *Arabidopsis* actin genes. *Genetics*, **149** 717-725.

Glass *et al*., *Journal of Experimental Botany* (2002) Inorganic Nitrogen Assimilation Special Issue 53 **370** 855–864

Glass, A.D.M., Erner, Y., Kronzucker, H.J., Schjoerring, J.K., Siddiqi, M.Y. and Wang, M.Y. (1997) Ammonium fluxes into plant roots: energetics, kinetics and regulation. Z. *Pflanzenernaehr. Bodenk*. **160**, 261–268.

Marschner, (1995) Mineral Nutrition of Higher Plants, *Academic Press, Cambridge* **2**

Haardt M., E. Bremer (1996) Use of phoA and lacZ fusions to study the membrane topology of ProW, a component of the osmoregulated ProU transport system of Escherichia coli. *J. Bacteriol*. **178** 5370-5381.

Hanahan, D. (1983) Studies on transformation of bacteria with plasmids. *J.Mol.Biol*. **166**, 557-580

Hanstein S, Felle HH (1999) The in¯uence of atmospheric NH3 on the apoplæstic pH of green leaves: a non-invasive approach with pH-sensitive microelectrodes. *New Phytologist* **143** 333-338.

Howitt, S.M. and Udvardi, M.K. (2000). Structure, function and regulation of ammonium transporters in plants. *Biochim. Biophys. Acta* **1465**: 152–170.

Ireland R.J., P.J.Lea, in: B.J. Singh (1999) Plant Amino Acids, Marcel Dekker, New York, 49-110.

Macdu J.H., Jackson S.B. (1991) The impact of atmospheric ammonia and temperature on growth and **preferences** for ammonium or nitrate uptake by. barley in relation to root temperature *J. Exp. Bot*. **42** 521-530.

Kaiser B.N., P.M. Finnegan, S.D. Tyerman, L.F. Whitehead, F.J. Bergersen, D.A. Day, Udvardi M.K. (1998), Characterization of an ammonium transport protein from the peribacteroid membrane of soybean nodules.*Science* **281** 1202-1206.

Kaiser BN, Rawat SR, Siddiqi MY, Masle J, Glass ADM. (2002) Functional analysis of an Arabidopsis T-DNA `Knockout' of the high-affnity NH^+_4 transporter AtAMT1;1. *Plant Physiology* **130** 1263-1275.

Karimi M., Inze D., Depicker A. (2000) GatewayTM vectors for Agrobacterium-mediated plant tranformation Trends in Plant *Science*. **7**

Khadhemi S., O'Connell J., Remis J. and Stroud M. (2004) Mechanism of Ammonium Transport by Amt/MEP/Rh:Structure of AmtB at 1.35 Angström. *Science* **305** 1587-1594.

Knepper M.A., Packer R., Good D., (1989) Ammonium transport in the kidney. *Physiol. Rev*. **69** 179

Koncz C, Nemeth K, Redei GP, Schell J (1992) T-DNA insertional mutagenesis in *Arabidopsis. Plant Mol Biol* **20**: 963–976

Kronzucker H.J., J.K. Schjoerring, Y. Erner, G.J.D. Kirk, M.Y. Siddiqi, A.D.M. Glass (1998) Dynamic interactions between root NH4+ influx and long-distance N translocation in rice: Insights into feedback processes. *Plant Cell Physiol*. **39** 1287-1293.

Kronzucker H.J., M.Y. Siddiqi, A.D.M. Glass (1995) Compartmentation and flux characteristics of nitrate in sprucePlanta **196** 691-698.

Kronzucker HJ, Siddiqi MY, Glass ADM (1996) Kinetics of NH4 influx in spruce. Plant Physiol **110:** 773–779

Lam HM, Coschigano K, Schultz C, Melo-Olivira R, Tjaden G, Oliveira I, Ngai N, Hsieh MH, Coruzzi G (1995) Use of *Arabidopsis* mutants and genes to study amide amino acid biosynthesis. *Plant Cell* **7** 887-898

Lam HM, Hsieh MH, Coruzzi G (1998) Reciprocal regulation of distinct asparagine synthetase genes by light and metabolites in *Arabidopsis thaliana***.** *Plant J* **16** 345-353.

Lam, H.-M., Coschigano, I.C., Oliveira, R., Melo-Oliveira, R. and Coruzzi, G.M. (1996). The molecular genetics of nitrogen assimilation into amino acids in higher plants. Annu. Rev. Plant Physiol. Plant Mol. Biol. **47**: 569–593.

Lauter FR, Ninnemann O, Bucher M, Riesmeier JW, Frommer WB (1996) Preferential expression of an ammonium transporter and of two putative nitrate transporters in root hairs of tomato. *Proc Natl Acad Sci USA* **93** 8139-8144.

Lee R.B., K.A. Rudge (1986) Effects of nitrogen deficiency on the absorption of nitrate and ammonium by barley plants**.** Ann. Bot. **57** 471-486.

Leegood RC, Lea PJ, Hausler RE. (1996). Use of barley mutants to study the control of photorespiratory metabolism. *Biochemical Society Transactions* **24**, 757-761.

Lehninger and Albert (2001) Lehninger principles of biochemistry **3**, 820-823

Lehrach, H., Diamond, D., Wozney, J.M. and Bötcker, H. (1977) RNA molecular weight determinations by gel electrophoresis under denaturing conditions, a critical reexamniation. *Biochemistry* **16**, 4743-4751.

Liboz, T., Bardet, C. and Lescure, B. (1990) The four members of the gene family encoding the Arabidospis thaliana translation elongation factor EF-1 alpha are actively transcribed. *Plant Mol. Biol*. **14**, 107-110.

Liu LH, Ludewig U, Gassert B, Frommer WB, von Wireen N (2003) Urea transport by nitrogen-regulated tonoplast intrinsic proteins in Arabidopsis. *Plant Physiology* **133** 1220-1228.

Loque D., von Wiren N. (2004) Regulatory levels for the transport of ammonium in plant roots *Journal of Experimental Botany* **55** No. 401, 1293-1305

Lorentz, M.C. and Heitmann, J. (1998) The MEP2 ammonium permease regulates pseudhyphal differentiation in Saccharomyces cerevisiae. *EMBO J.* **17**, 1236-1247.

Fried M.F., F. Zsoldos F., Vose P.B., Shatokhin I.L., (1965) Characterising the NO_3^- and NH_4^+ uptake process of rice roots by use of 15N labeled NH_4NO_3 *Physiol. Plant*. **18** (1965) 313-320.

M.L. Montesinos, P.A. Muro, A. Herrero, E. Flores (1998) Ammonium/methylammonium permeases of a cyanobacterium *J. Biol. Chem*. **273** 31463-31470.

Mäck G., R. Tischner *(1994) J. Plant Physiol.* ***144*** *351-357.*

Marini A.M, Vissers S, Urrestarazu A., Andre B. (1994) Cloning and expression of the MEP1 gene encoding an ammonium transporter in *Saccharomyces cerevisiae*. *EMBO* **13** 3456-3463.

Marini A.M., B.S. Soussi, S. Vissers, B. Andre (1997) A family of ammonium transporters in *Saccharomyces cerevisiae Mol. Cell. Biol*. **17** 4282-4293.

Marini, A.M., Matassi G, Raynal V, Andre B, Cartron JP, Cherif-Zahar B. (2000) The human Rhesus-associated RhAG protein and a kidney homologue promote ammonium transport in yeast *Nature Genetics* **26**, 341

Marschner HL (1995) *Mineral Nutrition in Higher Plants*. London: Academic Press

Mattsson M, Häusler RE, Leegood RC, Lea PJ, Schjoerring JK (1997) Leaf-atmosphere NH_3 exchange in barley mutants with reduced activities of glutamine synthetase**.** *Plant Physiol*, **114** 1307-1312.

Mattsson M, Schjoerring JK. (2002) Dynamic and steady-state responses of inorganic nitrogen pools and NH3 exchange in leaves of Lolium perenne and Bromus erectus to changes in root nitrogen supply. *Plant Physiology* **128** 742-750.

Mattsson M, Schjoerring JK. (2003) Senescence-induced changes in apoplastic and bulk tissue ammonia concentrations of ryegrass leaves. *New Phytologist* **160** 489-499.

McKinney EC, Ali N, Traut A, Feldmann KA, Belostotsky DA, McDowell JM, Meagher RB (1995) Sequence-based identification of T-DNA insertion mutations in *Arabidopsis*: actin mutants act2-1 and act4-1. *Plant J*, **8**: 613-622.

McManus, M.T. & Sharp, P.A. (2002) Gene silencing in mammals by small interfering RNAs. *Nature Rev. Genet*. **3**, 737-747

Miller AJ, Cookson SJ, Smith SJ, Wells DM. (2001) The use of microelectrodes to investigate compartmentation and the transport of metabolized inorganic ions in plants. *Journal of Experimental Botany* **52** 541-549.

Montgomery, M.K., Xu, S.-Q. and Fire, A. (1998) RNA as a target of double-stranded RNA-mediated genetic interference in *Caenorhabditis elegans. Proc. Natl. Acad. Sci*. **95**: 15502–15507.

Morrison TB, Weis JJ & Wittwer CT (1998), Quantification of low-copy transcripts by continuous SYBR Green I monitoring durng amplification. *Biotechniques* **24** 954-962

Muller H, Varmus H (1994) DNA bending creates favored sites for retroviral integration: an explanation for preferred insertion sites in nucleosomes. *EMBO J* **13**: 4704–4714

Napoli, C., Lemieux, C. and Jorgensen, R.A. (1990) Introduction of a chimeric chalcone synthase gene into Petunia results in reversible co-suppression of homologous genes in trans.
Nature **418**, 244 - 251 (2002);

Nicolas Bouché and David Bouchez (2001) *Arabidopsis* gene knockout: phenotypes wanted *Current Opinion in Plant Biology*, **4** 111–117

Nielsen KH, Schjoerring JK (1998) Regulation of apoplastic NH4 + concentration in leaves of oilseed rape. *Plant Physiol*, **118** 1361-1368

O. Ninnemann O., J.C. Jauniaux, W.B. Frommer, (1994)Identification of a high affinity ammonium transporter in plants *EMBO J.* 3464-3471.

P. Susi, M. Hohkuri1, T. Wahlroos1,2 and N.J. Kilby (2004), Characteristics of RNA silencing in plants: similarities and differences across kingdoms. *Plant Molecular Biology* **00**: 1–18

Palkova, Z., Janderova, B., Gabriel, J., Zikanova, B., Pospisek, M., and Forstova, J. (1997). Ammonia mediates communication between yeast colonies. *Nature* **390** 532–536.

Pan X., Li Y., and Stein L. (2005) Site Preferences of Insertional Mutagenesis Agents in Arabidopsis *Plant Physiology* **137** 168–175

Parinov S, Sevugan M, Ye D, YangW-C, Kumaran M, Sundaresan V (1999) Analysis of flanking sequences from Dissociation insertion lines: a database for reverse genetics in *Arabidopsis. Plant Cell* **11**: 2263–2270

Parinov S, Sundaresan V: Functional genomics in *Arabidopsis*: large-scale insertional mutagenesis complements the genome sequencing project. *Curr Opin Biotechnol* 2000, **11**:157-161.

Park J.H., Saier M.H. (1996) Phylogenetic characterisation of the MIP family of transmembrane channel proteins *J. Membr. Biol*. **153** 171

Parker RM, Barnes NM (1999) mRNA: detection by *in situ* and northern hybridization. *Methods in Molecular Biology* **106** 247-283

Paul AL, Ferl RJ (1998) Permeabilized *Arabidopsis* protoplasts provide new insight into the chromatin structure of plant alcohol dehydrogenase genes. *Dev Genet* **22**: 7–16

Pearson J, Clough ECM, Woodall J, Havill DC, Zhang XH (1998) Ammonia emission to the atmosphere from leaves of wild plants and *Hordeum vulgare* treated with methionine sulfoximine. *New Phytol*, **138** 37-48.

R.M. Siewe, B. Weil, A. Burkovski, B.J. Eikmanns, M. Eikmanns, R. Kramer (1996) Functional and genetic characterization of the (methyl)ammonium uptake carrier of *Coryebacterium glutamicum J. Biol. Chem.* **271** 5398-5403.

Raina S, Mahalingam R, Chen F, Fedoroff N (2002) A collection of sequenced and mapped Ds transposon insertion sites in *Arabidopsis thaliana. Plant Mol Biol* **50**: 93–110

Raven J.R., G.D. Farquhar (1981) Methylammonium transport in *Phaseolus vulgaris* leaf slices. Plant Physiol. **67** 859-863.

Rawat S.R., S.N. Silim, H.J. Kronzucker, M.Y. Siddiqi, A.D.M. Glass, (1999) *AtAMT1* gene expression and NH4+ uptake in roots of *Arabidopsis thaliana*: evidence for regulation by root glutamine levels. *Plant J.* 143-152.

Richard G. Schneeberger Ke Zhang, Tatiana Tatarinova, Max Troukhan, Shing F. Kwok, Josh Drais, Kevin Klinger, Francis Orejudos, Kimberly Macy, Amit Bhakta, James Burns, Gopal Subramanian, Jonathan Donson, Richard Flavell and Kenneth A. Feldmann (online publication march 2005) *Agrobacterium* T-DNA integration in *Arabidopsis* is correlated with DNA sequence compositions that occur frequently in gene promoter regions *Functional & Integrative Genomics*

Ross-Macdonald P, Coelho PS, Roemer T, Agarwal S, Kumar A, Jansen R, Cheung KH, Sheehan A, Symoniatis D, Umansky L et al.(1999) Large-scale analysis of the yeast genome by transposon tagging and gene disruption. *Nature*, **402**: 413-418.

Schjoerring, J.K., Finnemann, J., Husted, S., Mattson, M., Nielson, K.H. and Pearson, N. (1999). Regulation of ammonium distribution in plants. In: G. Gissel-Nielsen and A. Jensen (Eds) *Plant*

Nutrition: Molecular Biology and Genetics, Kluwer Academic Publishers, Dordrecht, The Netherlands, pp. 69–82.

Sentenac H., N. Bonneaud, M. Minet, F. Lacroute, J.-M. Salmon, F. Gaymard, C. Sessions A, Burke E, Presting G, Aux G, McElver J, Patton D, Dietrich B, Ho P, Bacwaden J, Ko C, *et al.* (2002) The high-throughput *Arabidopsis* reverse genetics system. *Plant Cell* **14**: 2985–2994

Shelden, M.C., Dong B., de Bruxelles, G.L., Trevaskis, B.,Whelan, J., Ryan, P.R., Howitt, S.M., Udvardi, M.K. (2001) *Arabidopsis* ammonium transporters, *AtAMT1;1* and *AtAMT1;3*, have different biochemical properties and functional roles. *Plant and Soil* **231**: 151–160.

Simon-Rosin U., Wood C.C., Udvardi M.K. (2003) Molecular and cellular characterisation of LjAMT2;1, an ammonium transporter from the model legume *Lotus japonicus*. *Plant Mol Biol* **51:** 99–108

Smith F.A., Raven J.A. (1979) Plant members of a family of sulfate transporters reveal functional subtypes. Annu. *Rev. Plant Physiol*. **30** 289-311.

Smith, N.A. *et al*. (2000) Gene Expression: total silencing by intron-spliced hairpin RNAs. *Nature* **407**, 319-320

Sohlenkamp C., M. Shelden, S. Howitt, M. Udvardi (2000) Characterisation of *Arabidopsis AtAMT2,* a novel ammonium transporter in plants. *FEBS Lett*. **467** 273-278.

Soupene E., Inwood W., Kustu S. (2004) Lack of the Rhesus protein Rh1 impairs growth of the green alga *Chlamydomonas reinhardtii* at high CO2 *Proc. Natl. Acad. Sci*. **101** 7787

Soupene E, L. He, D. Yan, S. Kustu (1998) Ammonia acquisition in enteric bacteria: physiological role of the ammonium/methylammonium transport B protein. *Proc. Natl. Acad. Sci. USA* **95** 7030-7034.

Steinhauser D, Usadel B, Luedemann A, Thimm O, Kopka J. (2004) CSB.DB: a comprehensive systems-biology database. *Bioinformatics*. **20** (18): 3647-51

Stewart G.R., A.F. Mann, P.A. Fentem 1980, in: B.J. *The Biochemistry of Plants*, vol. **5**, Amino Acids and Derivatives, Academic Press, New York, , 271-327.

Stitt, M. (1999) Nitrate regulation of metabolism and growth. *Curr. Opin. Plant Biol*. **2**, 178-186.

Szabados L, Kovacs I, Oberschall A, Abraham E, Kerekes I, Zsigmond L, Nagy R, Alvarado M, Krasovskaja I, Gal M, *et al* (2002) Distribution of 1000 sequenced T-DNA tags in the Arabidopsis genome. *Plant Journal* **32**: 233–242

Tatusova T., Madden T. L. (1999), Blast 2 sequences - a new tool for comparing protein and nucleotide sequences, *FEMS Microbiol Lett*, (1999) **174**:247-250

Thatcher JW, Shaw JM, Dickinson WJ (1995) Marginal fitness contributions of nonessential genes in yeast. *Proc Natl Acad Sci USA* 1998, **95**: 253-257.

Thijs G., Moreau Y., De Smet F., Mathys J., Lescot M., Rombauts S., Rouzé P., De Moor B., Marchal K., (2002). INCLUSive: INtegrated Clustering, Upstream sequence retrieval and motif Sampling, *Bioinformatics*, **18**(2), 331-332.

Thomas, C.L., Jones, L., Baulcombe, D.C. and Maule, A.J. (2001). Size constraints for targeting post-transcriptional gene silencing and for RNA-directed methylation in *Nicotiana benthamiana* using a potato virus X vector. *Plant J*. **25**: 417–425.

Thompson WF, Flavell RB (1988) DNase I sensitivity of ribosomal RNA genes in chromatin and nucleolar dominance in wheat. *J Mol Biol* **204**: 535–548

Tilman, D., Fargione, J., Wolff, B., D'Antonio, C., Dobson, A., Hworth, R., Schlesinger, W.H. and Swackhammer, D. (2001) Forecasting agriculturally driven global environmental change. Science **292**, 281-284.

Timothy L. Bailey and Charles Elkan (1994) Fitting a mixture model by expectation maximization to discover motifs in biopolymers, *Proceedings of the Second International Conference on Intelligent Systems for Molecular Biology*, 28-36, AAAI Press, Menlo Park, California

Tinland B (1996) The integration of T-DNA into plant genomes. *Trends Plant Sciences* **1**: 178–183 Tinland B. *Trends Plant Sci* **1** 178–183

Tzfira T, Vaidya M, Citovsky V (2001) VIP1, an *Arabidopsis* protein that interacts with Agrobacterium VirE2, is involved in VirE2 nuclear import and *Agrobacterium* infectivity. *EMBO J* **20**:3596–3607

Udvardi MK, Day DA (1997) Metabolite transport across symbiotic membranes of legume nodules. *Annu Rev Plant Physiol Plant Mol Biol*, **48** 493-523.

Vaistij, F.E., Jones, L. and Baulcombe, D.C. (2002). Spreading of RNA targeting and DNA methylation in RNA silencing requires transcription of the target gene and a putative RNA dependent RNA polymerase. *Plant Cell* **14**: 857–867.

Vale, F.R., Volk, R.J. and Jackson, W.A. (1988) Simultaneous influx of ammonium and potassium into maize roots: kinetics and interactions. *Plants* **173**, 424-431.

Vidmar JJ, Zhuo D, Siddiqi MY, Schjoerring JK, Touraine B, Glass ADM. (2000). Regulation of HvNRT2 expression and high-affinity nitrate influx in roots of Hordeum vulgare by ammonium and amino acids. *Plant Physiology* **123**, 307–318.

Vigdal TJ, Kaufman CD, Izsvak Z, Voytas DF, Ivics Z (2002) Common physical properties of DNA affecting target site selection of sleeping beauty and other Tc1/mariner transposable elements. *J Mol Biol* **323**: 441–452

Voinnet, O., Pinto, Y.M. and Baulcombe, D.C. (1999). Suppresion of gene silencing: a general strategy used by diverse DNA and RNA viruses on plants. *Proc. Natl. Acad. Sci*. **96**: 14147–14152.

Voinnet, O., Vain, P., Angell, S. and Baulcombe, D.C. (1998) Systemic spread of sequence-specific transgene RNA degradation in plants is initiated by localized introduction of ectopic promoterless DNA. *Cell* **95**: 177–187.

von Wiren N., A. Bergfeld, O. Ninnemann, W.B. Frommer, Sequence anouncement *Plant Mol. Biol*. **35** (1997) 681.

von Wiren, N., Gazzarini, S., Gojon, A. and Frommer, W.B. (2000). The molecular physiology of ammonium uptake and retrieval. Curr. Opin. Plant Biol. **3**: 254–261.

von Wiren, N., Lauter, F.R., Ninnemann, O., Gillissen, B., Walch-Liu P., Engels, C., Jost, W. and Frommer W.B. (2000). Differential regulation of three functional ammonium transporter genes by nitrogen in root hairs and by light in leaves of tomato. Plant J. **21**: 167–175.

vonWiren N., S. Gazzarrini, W.B. Frommer (1997) Regulation of mineral nitrogen uptake in plants *Plant Soil* **196** 191-199.

Walch-Liu P, Neumann G, Bangerth F, Engels C (2000) Rapid effects of nitrogen form on leaf morphogenesis in tobacco. *J Exp Bot* **51:** 227–237

Wallsgrove RM, Turner JC, Hall NP, Kendally AC, Bright SWJ (1987) Barley mutants lacking chloroplast glutamine synthetase- biochemical and genetic analysis. *Plant Phys*. **83** 155-158.

Wang M.Y., A.D.M. Glass, J.E. Sha, L.V. Kochian (1994) Ammonium uptake by rice roots. III. Electrophysiology Plant Physiol. **104** 899-906.

Wang T & Brown MJ (1999) mRNA quantification by real time TaqMan polymerase chain reaction: validation and comparison with RNase protection. *Analytical Biochemistry* **269** 198-201

Wang, M.Y:, Siddiqi, M.Y., Ruth, T.J. and Glass, A.D. (1993) Ammonium uptake by rice roots. II. Kinetics of 13NH4+ influx across the plasmalemma. Plant Physiol. **103**, 1259-1267.

Waterhouse, P.M, Graham, M.W., Wang, M.B. (1998) Virus resistance and gene silencing in plants can be icduced by simultaneous expression of sense and antisense RNA, *PNAS* **95**, 13959-13964

Waterhouse, P.M., Wang, M.B. & Lough, T. (2001) Gene silencing s an adaptive defence against viruses. *Nature* **411**, 834-842

Weintraub H (1983) A dominant role for DNA secondary structure in forming hypersensitive structures in chromatin. *Cell* **32**: 1191–1203

Weis JH, Tan SS, Martin BK & Wittwer CT (1992) Detection of rare mRNAs via quantitative RT-PCR. *Trends in Genetics* **8** 263-264

Wells D, Miller AJ (2000) Intracellular measurement of ammonium in *Chara corallina* using ion-selective microelectrodes**.** *Plant Soil*,

Winkler RG, Frank MR, Galbraith DW, Feyereisen R, Feldmann KA (1998) Systematic reverse genetics of transfer-DNA-tagged lines of *Arabidopsis*. Isolation of mutations in the cytochrome P450 gene superfamily. *Plant Physiol*, **118**: 743-750.

Wong H-K, Chan H-K, Coruzzi G.M., Lam H-M (2004) Correlation of *ASN2* Gene Expression with Ammonium Metabolism in *Arabidopsis. Plant Physiology*, **134:** 332–338

Yamaya T., A. Oaks (1987) Synthesis of glutamate by mitochondria—an anaplerotic function for glutamate dehydrogenase.Physiol. Plant. **70** 749-756.

Yamaya T., A. Oaks, H. Matsumoto (1984) Characteristics of glutamate dehydrogenase in mitochondria prepared from corn shoots. Plant Physiol. **76** 1009-1013.

Yin Z.-H., W.M. Kaiser, U. Heber, J.A. Raven (1996) Acquisition. and assimilation of gaseous ammonia as revealed by intecellular Planta **200** 380-387.

Zhuo D, Okamoto M, Vidmar JJ, Glass ADM. (1999). Regulation of a putative high-affinity nitrate transporter (Nrt2;1At) in roots of *Arabidopsis thaliana. The Plant Journal* **17**, 563–568.

Table of Abbreviations

˚C	degrees centigrade
µE	micro Einstein
µg	microgram
µl	micro litre
µmol	micromole
Amp	ampicillin
AMT	Ammoniumtransporter
AS	Asparagine Synthetase
BAC	Bacterial Artificial Chromosome
BASTA	Handelsname für die chemischen Verbindungen der Glufosinate
Bp	base pair
BSA	Bovine serum albumin
cDNA	complementary DNA
dCTP	Deoxycytosine triphosphate
DNA	Desoxyribonucleic Acid
dNTPs	2'-deoxynucleoside triphosphate
EDTA	Ethylendiamine tetraacetic acid
EST	Expressed Sequence Tag
GDH	Glutamate Dehydrogenase
GFP	Green Fluorescent Protein
Gln	Glutamate
GOGAT	Glutamine Oxoglutarate Aminotransferase
GS	Glutamine Synthetase
GS1	Cytosolic isoform of GS
GS2	Plastidic isoform of GS
GUS	ß-Glucuronisidase
h	hour
HATS	High-Affinity Transport System
HPLC	High Performance Liquid Chromatography
IPTG	isopropyl-beta-D-thiogalactopyranoside
Kan	kanamycin
K_M	Michaelis constant; substrate concentration at 1/2 V_{max}
LATS	Low-Affinity Transport System
LB	Luria-Bertani medium
MA	Methylammonium
MEP	Methylammonium Permease
MES	2-(N-Morpholino)ethanesuflonic acid
mM	millimoles
MS	Murashige and Skoog
N	Nitrogen
NiR	Nitrite Reductase
nm	nanometer
NR	Nitrate Reductase
OD600	Optical density at 600 nm
PCR	Polymerase Chain Reaction
PTGS	Posttransciptional Gene Silencing
qRT-PCR	quantitative Real Time PCR
Rif	Rifampicin
RNA	Ribonucleic Acid
RNAi	RNA interference
Rpm	rounds per minute
T-DNA	Transfer-DNA
U	unit
v/v	volume per volume
V_{max}	maximum velocity
WT	Wildtype
x-gal	5-brom-4-chloro-3-indolyl-beta-D-galactopyranoside

Appendix

Tab. 1 qRT-PCR data for cDNA derived from root mRNA (root + indicates plants were grown on hydroponic medium containing nitrogen (1.7.2.); root – indicates plants were deprived of nitrogen for 24 h.)

cDNA	primer	Ct-value	PCR eff(+1)	MW UBQ-10	DCTr	(1+E)e-dCTr
root +	AMT 1.1	20,395292	2,032	19,491	0,904	0,527
root +	AMT 1.1	20,407621	2,030	19,491	0,917	0,523
root +	AMT 1.1	20,420277	2,012	19,491	0,929	0,522
root +	AMT 1.2	22,878006	1,849	19,491	3,387	0,125
root +	AMT 1.2	22,899164	1,852	19,491	3,408	0,122
root +	AMT 1.2	23,056198	1,906	19,491	3,565	0,100
root +	AMT 1.3	20,607876	1,982	19,491	1,117	0,466
root +	AMT 1.3	20,54362	2,033	19,491	1,053	0,474
root +	AMT 1.3	20,674643	1,908	19,491	1,184	0,465
root +	AMT 1.4	40	1,378	19,491	20,509	0,001
root +	AMT 1.4	38,441833	1,352	19,491	18,951	0,003
root +	AMT 1.4	40	1,259	19,491	20,509	0,009
root +	AMT 1.5	27,044752	1,814	19,491	7,554	0,011
root +	AMT 1.5	26,819208	1,821	19,491	7,328	0,012
root +	AMT 1.5	26,996859	1,818	19,491	7,506	0,011
root +	AMT 2.1	23,362284	1,816	19,491	3,871	0,099
root +	AMT 2.1	23,34417	1,858	19,491	3,853	0,092
root +	AMT 2.1	23,50138	1,819	19,491	4,010	0,091
root +	UBQ-10	19,590698	1,761	19,491		
root +	UBQ-10	19,453096	1,742			
root +	UBQ-10	19,428953	1,745			
root -	AMT 1.1	19,425705	1,996	20,579	-1,153	2,219
root -	AMT 1.1	19,399426	1,861	20,579	-1,180	2,081
root -	AMT 1.1	19,397682	1,853	20,579	-1,181	2,073
root -	AMT 1.2	23,163067	1,834	20,579	2,584	0,209
root -	AMT 1.2	23,268642	1,868	20,579	2,690	0,186
root -	AMT 1.2	23,257957	1,870	20,579	2,679	0,187
root -	AMT 1.3	20,346754	2,041	20,579	-0,232	1,180
root -	AMT 1.3	20,386826	1,998	20,579	-0,192	1,142
root -	AMT 1.3	20,329145	2,016	20,579	-0,250	1,191
root -	AMT 1.4	34,14827	1,590	20,579	13,569	0,002
root -	AMT 1.4	34,353523	1,584	20,579	13,775	0,002
root -	AMT 1.4	35,36224	1,555	20,579	14,783	0,001
root -	AMT 1.5	21,601412	1,978	20,579	1,022	0,498
root -	AMT 1.5	21,567762	1,959	20,579	0,989	0,514
root -	AMT 1.5	21,59664	1,966	20,579	1,018	0,503
root -	AMT 2.1	23,379232	1,863	20,579	2,800	0,175
root -	AMT 2.1	23,395182	1,888	20,579	2,816	0,167
root -	AMT 2.1	23,63743	1,883	20,579	3,058	0,144
root -	UBQ-10	20,55424	1,863	20,579		
root -	UBQ-10	20,565277	1,782			
root -	UBQ-10	20,617493	1,781			

Tab. 2 qRT-PCR data for cDNA derived from leaf mRNA (for soils see 1.8.).

cDNA	Primer	Ct	MW UBQ-10	gene-ubq	2E-dcT	MW	StabwN
WT full soil	AMT1.1	20,139238	18,6720283	1,46720967	0,36168115	0,363	0,007300454
WT full soil	AMT1.1	20,168303	18,6720283	1,49627467	0,35446752		
WT full soil	AMT1.1	20,097704	18,6720283	1,42567567	0,37224499		
WT full soil	AMT1.2	23,340446	18,6720283	4,66841767	0,03932478	0,039	0,000333606
WT full soil	AMT1.2	23,370731	18,6720283	4,69870267	0,03850788		
WT full soil	AMT1.2	23,354843	18,6720283	4,68281467	0,0389343		
WT full soil	AMT1.3	28,32922	18,6720283	9,65719167	0,0012385	0,001	0,000109069
WT full soil	AMT1.3	28,48237	18,6720283	9,81034167	0,00111376		
WT full soil	AMT1.3	28,679487	18,6720283	10,0074587	0,00097153		
WT full soil	AMT 1.4	28,400675	18,6720283	9,72864667	0,00117865	0,001	0,000161669
WT full soil	AMT 1.4	28,917442	18,6720283	10,2454137	0,0008238		
WT full soil	AMT 1.4	28,431835	18,6720283	9,75980667	0,00115347		
WT full soil	AMT 1.5	Undetermined	18,6720283	#WERT!	#WERT!	#WERT!	#WERT!
WT full soil	AMT 1.5	Undetermined	18,6720283	#WERT!	#WERT!		
WT full soil	AMT 1.5	38,911335	18,6720283	20,2393067	8,0791E-07		
WT full soil	AMT 2.1	24,154886	18,6720283	5,48285767	0,02236121	0,022	8,50273E-05
WT full soil	AMT 2.1	24,15802	18,6720283	5,48599167	0,02231269		
WT full soil	AMT 2.1	24,167826	18,6720283	5,49579767	0,02216155		
WT full soil	UBQ-10	18,595686	18,6720283		1		
WT full soil	UBQ-10	18,691006			1		
WT full soil	UBQ-10	18,729393			1		
WT full soil	nix	Undetermined			1		
WT null-Erde	AMT1.1	20,602753	21,4950123	-0,89225933	1,85608056	1,837	0,025482125
WT null-Erde	AMT1.1	20,646372	21,4950123	-0,84864033	1,80080296		
WT null-Erde	AMT1.1	20,604723	21,4950123	-0,89028933	1,85354782		
WT null-Erde	AMT1.2	24,288834	21,4950123	2,79382167	0,14420352	0,138	0,004334144
WT null-Erde	AMT1.2	24,362352	21,4950123	2,86733967	0,13703918		
WT null-Erde	AMT1.2	24,39647	21,4950123	2,90145767	0,13383639		
WT null-Erde	AMT1.3	28,554327	21,4950123	7,05931467	0,00749781	0,008	0,000521273
WT null-Erde	AMT1.3	28,679667	21,4950123	7,18465467	0,0068739		
WT null-Erde	AMT1.3	28,433882	21,4950123	6,93886967	0,00815065		
WT null-Erde	AMT 1.4	29,496967	21,4950123	8,00195467	0,00390096	0,004	0,000104045
WT null-Erde	AMT 1.4	29,409607	21,4950123	7,91459467	0,00414448		
WT null-Erde	AMT 1.4	29,429462	21,4950123	7,93444967	0,00408783		
WT null-Erde	AMT 1.5	Undetermined	21,4950123	#WERT!	#WERT!	#WERT!	#WERT!
WT null-Erde	AMT 1.5	Undetermined	21,4950123	#WERT!	#WERT!		
WT null-Erde	AMT 1.5	Undetermined	21,4950123	#WERT!	#WERT!		
WT null-Erde	AMT 2.1	25,07713	21,4950123	3,58211767	0,08349782	0,083	0,000453249
WT null-Erde	AMT 2.1	25,069227	21,4950123	3,57421467	0,08395647		
WT null-Erde	AMT 2.1	25,08834	21,4950123	3,59332767	0,08285154		
WT null-Erde	UBQ-10	21,484299	21,4950123				
WT null-Erde	UBQ-10	21,479961					
WT null-Erde	UBQ-10	21,520777					
WT null-Erde	nix	Undetermined					

Tab. 3 qRT-PCR data for cDNA derived from flower mRNA (for soils see 1.8.).

cDNA	primer	Ct-value	MW-ubq	gene-ubq	primer eff	(1+E)e-dCTr	Mittelwert	StabwN
flower +	AMT 1.1	25,90000	25,19844	0,70156	1,78481	0,66603	0,69833	0,05198
flower +	AMT 1.1	25,90936	25,19844	0,71092	1,80440	0,65731		
flower +	AMT 1.1	25,65086	25,19844	0,45242	1,77344	0,77167		
flower +	AMT 1.2	28,60291	25,19844	3,40447	1,80595	0,13368	0,13060	0,01027

flower +	AMT 1.2	28,86454	25,19844	3,66610	1,70518	0,14135		
flower +	AMT 1.2	28,94527	25,19844	3,74683	1,77385	0,11677		
flower +	AMT 1.3	34,02913	25,19844	8,83069	1,77566	0,00628	0,00625	0,00181
flower +	AMT 1.3	32,97554	25,19844	7,77710	1,84751	0,00845		
flower +	AMT 1.3	34,90084	25,19844	9,70240	1,76577	0,00402		
flower +	AMT 1.4	30,07076	25,19844	4,87232	1,86876	0,04752	0,03979	0,00766
flower +	AMT 1.4	31,00384	25,19844	5,80540	1,83628	0,02936		
flower +	AMT 1.4	30,43646	25,19844	5,23803	1,82746	0,04250		
flower +	AMT 1.5	40,00000	25,19844	14,80156	1,43207	0,00491	0,02539	0,02947
flower +	AMT 1.5	40,00000	25,19844	14,80156	1,20029	0,06706		
flower +	AMT 1.5	40,00000	25,19844	14,80156	1,44767	0,00419		
flower +	AMT 2.1	28,18605	25,19844	2,98761	1,83538	0,16296	0,16309	0,00902
flower +	AMT 2.1	28,15212	25,19844	2,95368	1,80699	0,17420		
flower +	AMT 2.1	28,34041	25,19844	3,14198	1,82097	0,15210		
flower +	UBQ-10	25,09488	25,19844	-0,10356	1,67471	1,05485	0,35162	0,49726
flower +	UBQ-10	25,21380		25,21380	1,67182	0,00000		
flower +	UBQ-10	25,28664		25,28664	1,67138	0,00000		
flower -	AMT 1.1	21,16888	20,78352	0,38536	1,94467	0,77391	0,79370	0,02467
flower -	AMT 1.1	21,15614	20,78352	0,37261	1,95664	0,77872		
flower -	AMT 1.1	21,06624	20,78352	0,28272	1,94552	0,82849		
flower -	AMT 1.2	24,56814	20,78352	3,78462	1,84919	0,09763	0,10071	0,01452
flower -	AMT 1.2	24,77688	20,78352	3,99336	1,85572	0,08467		
flower -	AMT 1.2	24,38297	20,78352	3,59945	1,80297	0,11983		
flower -	AMT 1.3	30,32359	20,78352	9,54007	1,76672	0,00439	0,00425	0,00025
flower -	AMT 1.3	30,26209	20,78352	9,47856	1,76998	0,00446		
flower -	AMT 1.3	30,05990	20,78352	9,27638	1,81870	0,00389		
flower -	AMT 1.4	26,21408	20,78352	5,43055	1,87076	0,03333	0,03385	0,00038
flower -	AMT 1.4	26,17302	20,78352	5,38950	1,87285	0,03399		
flower -	AMT 1.4	26,19069	20,78352	5,40717	1,86659	0,03423		
flower -	AMT 1.5	40,00000	20,78352	19,21648	1,31422	0,00524	0,02938	0,02227
flower -	AMT 1.5	35,76257	20,78352	14,97904	1,28293	0,02395		
flower -	AMT 1.5	40,00000	20,78352	19,21648	1,15872	0,05896		
flower -	AMT 2.1	24,16229	20,78352	3,37876	1,89234	0,11590	0,12400	0,01001
flower -	AMT 2.1	24,18392	20,78352	3,40039	1,87478	0,11800		
flower -	AMT 2.1	24,04150	20,78352	3,25798	1,83610	0,13811		
flower -	UBQ-10	20,74728	20,78352	-0,03624	1,70723	1,01957	1,01957	0,00000
flower -	UBQ-10	20,77394			1,76163			
flower -	UBQ-10	20,82934			1,84606			

Tab. 4 qRT-PCR data for cDNA derived from SyAMT lines and the WT

cDNA	Primer	Ct	MW ubq-10	gene-ubq	2E-dcT	MW	StabwN
syng 1.1	AMT 1.1	18,80000	17,43333	1,36667	0,38779	0,42113	0,02361
syng 1.1	AMT 1.1	18,63000	17,43333	1,19667	0,43628		
syng 1.1	AMT 1.1	18,62000	17,43333	1,18667	0,43932		
syng 1.1	UBQ-10	17,18000	17,43333	-0,25333	1,19196	1,19196	
syng 1.1	UBQ-10	17,44000					
syng 1.1	UBQ-10	17,68000					
syng 1.2	AMT 1.2	22,87000	18,85667	4,01333	0,06193	0,06453	0,00745
syng 1.2	AMT 1.2	22,60000	18,85667	3,74333	0,07467		
syng 1.2	AMT 1.2	22,99000	18,85667	4,13333	0,05698		
syng 1.2	UBQ-10	18,14000	18,85667	-0,71667	1,64338	1,64338	0,00000
syng 1.2	UBQ-10	18,51000					
syng 1.2	UBQ-10	19,92000					
syng1.4	AMT 1.4	24,39000	15,12333	9,26667	0,00162	0,00123	0,00028

syng 1.4	AMT 1.4	25,02000	15,12333	9,89667	0,00105		
syng 1.4	AMT 1.4	25,04500	15,12333	9,92167	0,00103		
syng 1.4	UBQ-10	15,21000	15,12333	0,08667	0,94170	0,94170	0,00000
syng 1.4	UBQ-10	15,09000					
syng 1.4	UBQ-10	15,07000					
syng 2.1	AMT 2.1	19,52000	15,97333	3,54667	0,08558	0,08346	0,00826
syng 2.1	AMT 2.1	19,41000	15,97333	3,43667	0,09235		
syng 2.1	AMT 2.1	19,76000	15,97333	3,78667	0,07246		
syng 2.1	UBQ-10	16,16000	15,97333	0,18667	0,87863	0,87863	0,00000
syng 2.1	UBQ-10	15,88000					
syng 2.1	UBQ-10	15,88000					
Col-0	AMT 1.1	19,05000	18,10667	0,94333	0,52003	0,59625	0,15781
Col-0	AMT 1.1	19,25000	18,10667	1,14333	0,45271		
Col-0	AMT 1.1	18,40000	18,10667	0,29333	0,81601		
Col-0	AMT 1.2	21,95000	18,10667	3,84333	0,06967	0,07207	0,00410
Col-0	AMT 1.2	21,79000	18,10667	3,68333	0,07784		
Col-0	AMT 1.2	21,97000	18,10667	3,86333	0,06871		
Col-0	AMT 1.4	27,17000	18,10667	9,06333	0,00187	0,00141	0,00032
Col-0	AMT 1.4	27,82000	18,10667	9,71333	0,00119		
Col-0	AMT 1.4	27,84000	18,10667	9,73333	0,00117		
Col-0	AMT 2.1	21,69000	18,10667	3,58333	0,08343	0,08362	0,00027
Col-0	AMT 2.1	21,69000	18,10667	3,58333	0,08343		
Col-0	AMT 2.1	21,68000	18,10667	3,57333	0,08401		
Col-0	UBQ-10	18,31000	18,10667	0,20333	0,86854	0,86854	0,00000
Col-0	UBQ-10	17,86000					
Col-0	UBQ-10	18,15000					

Tab. 5 qRT-PCR data for cDNA derived from RNAi line4 plants and wildtype plants grown for seven days in liquid culture and deprived of N for 24 h.

Sample Name	primer	Ct	MW ubq-10	gene-ubq	2E-dCt	MW delta-Ct	StabwN
WT	AMT 1.1	19,268763	18,438545	0,830218	0,562444	0,553261	0,007476
WT	AMT 1.1	19,292652	18,438545	0,854107	0,553208		
WT	AMT 1.1	19,316515	18,438545	0,877970	0,544132		
WT	AMT 1.2	21,867561	18,438545	3,429016	0,092846	0,091926	0,000839
WT	AMT 1.2	21,878944	18,438545	3,440399	0,092116		
WT	AMT 1.2	21,899446	18,438545	3,460901	0,090817		
WT	AMT 1.3	20,772913	18,438545	2,334368	0,198283	0,199874	0,002313
WT	AMT 1.3	20,773558	18,438545	2,335013	0,198194		
WT	AMT 1.3	20,737963	18,438545	2,299418	0,203145		
WT	AMT 1.4	28,119240	18,438545	9,680695	0,001218	0,001174	0,000056
WT	AMT 1.4	28,273012	18,438545	9,834467	0,001095		
WT	AMT 1.4	28,131250	18,438545	9,692705	0,001208		
WT	AMT 1.5	26,332165	18,438545	7,893620	0,004205	0,004437	0,000177
WT	AMT 1.5	26,244160	18,438545	7,805615	0,004470		
WT	AMT 1.5	26,191587	18,438545	7,753042	0,004636		
WT	AMT 2.1	22,104530	18,438545	3,665985	0,078782	0,077599	0,001361
WT	AMT 2.1	22,162260	18,438545	3,723715	0,075692		
WT	AMT 2.1	22,112990	18,438545	3,674445	0,078322		
WT	UBQ-10	18,471272	18,438545				
WT	UBQ-10	18,407490					
WT	UBQ-10	18,436872					
RNAi4	AMT 1.1	19,133469	17,116667	2,016802	0,247105	0,261538	0,029043
RNAi4	AMT 1.1	18,843777	17,116667	1,727110	0,302056		
RNAi4	AMT 1.1	19,203157	17,116667	2,086490	0,235453		

RNAi4	AMT 1.2	20,833469	17,116667	3,716802	0,076056	0,040708	0,025061
RNAi4	AMT 1.2	22,423414	17,116667	5,306747	0,025264		
RNAi4	AMT 1.2	22,703627	17,116667	5,586960	0,020805		
RNAi4	AMT 1.3	21,430418	17,116667	4,313751	0,050284	0,112899	0,046676
RNAi4	AMT 1.3	20,103899	17,116667	2,987232	0,126111		
RNAi4	AMT 1.3	19,739912	17,116667	2,623245	0,162302		
RNAi4	AMT 1.4	28,320000	17,116667	11,203333	0,000424	0,000470	0,000148
RNAi4	AMT 1.4	28,740000	17,116667	11,623333	0,000317		
RNAi4	AMT 1.4	27,660000	17,116667	10,543333	0,000670		
RNAi4	AMT 1.5	23,160000	17,116667	6,043333	0,015163	0,009964	0,003797
RNAi4	AMT 1.5	24,450000	17,116667	7,333333	0,006201		
RNAi4	AMT 1.5	23,990000	17,116667	6,873333	0,008529		
RNAi4	AMT 2.1	21,015036	17,116667	3,898369	0,067062	0,048183	0,013354
RNAi4	AMT 2.1	21,823694	17,116667	4,707027	0,038286		
RNAi4	AMT 2.1	21,789576	17,116667	4,672909	0,039203		
RNAi4	UBQ-10	17,180000	17,116667				
RNAi4	UBQ-10	17,010000					
RNAi4	UBQ-10	17,160000					
RNAi4	water control	40,000000					
RNAi4	water control	40,000000					
RNAi4	water control	40,000000					

Tab. 6 RT-PCR data for cDNA derived from roots of RNAi line4 plants and wildtype plants grown for 21 days in hydropnic culture and deprived of N for 24 h.

	primer	**Ct**	**PCR eff**	**MW ubq**	**gene-ubq**	**(1+E)e-dCt**	**MW**	**StabwN**
Col-0	AMT 1.1	19,7519	1,996	20,8358	-1,083872	2,115	2,020	0,06751
Col-0	AMT 1.1	19,7438	1,861	20,8358	-1,092039	1,971		
Col-0	AMT 1.1	19,7344	1,853	20,8358	-1,101446	1,973		
Col-0	AMT 1.2	23,3194	1,834	20,8358	2,483608	0,222	0,207	0,01041
Col-0	AMT 1.2	23,4212	1,868	20,8358	2,58537	0,199		
Col-0	AMT 1.2	23,4017	1,870	20,8358	2,565857	0,201		
Col-0	AMT 1.3	20,5634	2,041	20,8358	-0,272373	1,214	1,201	0,02221
Col-0	AMT 1.3	20,6099	1,998	20,8358	-0,225885	1,169		
Col-0	AMT 1.3	20,5546	2,016	20,8358	-0,281225	1,218		
Col-0	AMT 1.4	34,2489	1,590	20,8358	13,413094	0,002	0,002	0,0002
Col-0	AMT 1.4	34,4817	1,584	20,8358	13,645924	0,002		
Col-0	AMT 1.4	35,5248	1,555	20,8358	14,688973	0,002		
Col-0	AMT 1.5	21,7324	1,978	20,8358	0,896635	0,543	0,545	0,00303
Col-0	AMT 1.5	21,7264	1,959	20,8358	0,890635	0,550		
Col-0	AMT 1.5	21,7369	1,966	20,8358	0,901066	0,544		
Col-0	AMT 2.1	23,5281	1,863	20,8358	2,692328	0,187	0,174	0,01209
Col-0	AMT 2.1	23,552	1,888	20,8358	2,71616	0,178		
Col-0	AMT 2.1	23,7491	1,883	20,8358	2,91327	0,158		
Col-0	UBQ-10	20,8105	1,863	20,8358	-0,025259	1,016	1,016	0
Col-0	UBQ-10	20,8335	1,782					
Col-0	UBQ-10	20,8634	1,781					
RNAi line4	AMT 1.1	19,0978	1,949	19,85116	-0,753359	1,653	1,682	0,02048
RNAi line4	AMT 1.1	19,0588	1,943	19,85116	-0,792408	1,693		
RNAi line4	AMT 1.1	19,0617	1,958	19,85116	-0,789467	1,700		
RNAi line4	AMT 1.2	22,6522	1,794	19,85116	2,801048	0,195	0,171	0,02389
RNAi line4	AMT 1.2	22,6616	1,842	19,85116	2,810421	0,180		
RNAi line4	AMT 1.2	22,8374	1,940	19,85116	2,986271	0,138		
RNAi line4	AMT 1.3	19,9369	1,984	19,85116	0,085716	0,943	0,945	0,0031
RNAi line4	AMT 1.3	19,9277	1,973	19,85116	0,0765	0,949		
RNAi line4	AMT 1.3	19,9363	2,004	19,85116	0,085117	0,943		

RNAi line4 AMT 1.4	33,6227	1,582	19,85116	13,771574	0,002	0,002	0,0004
RNAi line4 AMT 1.4	32,9699	1,574	19,85116	13,118723	0,003		
RNAi line4 AMT 1.4	34,8201	1,531	19,85116	14,968889	0,002		
RNAi line4 AMT 1.5	21,9511	1,907	19,85116	2,099905	0,258	0,257	0,00239
RNAi line4 AMT 1.5	21,897	1,931	19,85116	2,045841	0,260		
RNAi line4 AMT 1.5	21,8862	1,960	19,85116	2,035032	0,254		
RNAi line4 AMT 2.1	22,3425	1,834	19,85116	2,491384	0,221	0,202	0,01513
RNAi line4 AMT 2.1	22,3127	1,921	19,85116	2,461498	0,201		
RNAi line4 AMT 2.1	22,2994	1,998	19,85116	2,448276	0,184		
RNAi line4 UBQ-10	19,8584	1,763	19,85116	0,007231	0,996	0,996	0
RNAi line4 UBQ-10	19,7543	1,842					
RNAi line4 UBQ-10	19,9408	1,754					

Tab. 7 RT-PCR data for cDNA derived from leaves of RNAi line4 plants and wildtype plants grown for 21 days in hydropnic culture and deprived of N for 24 h.

cDNA	**primer**	**Ct**	**MW ubq**	**gene-ubq**	**2E-dCt**	**MW**
WT null-Erde	AMT1.1	20,602753	21,495012	-0,892259	1,85608	1,8368
WT null-Erde	AMT1.1	20,646372	21,495012	-0,84864	1,8008	
WT null-Erde	AMT1.1	20,604723	21,495012	-0,890289	1,85355	
WT null-Erde	AMT1.2	24,288834	21,495012	2,7938217	0,1442	0,1384
WT null-Erde	AMT1.2	24,362352	21,495012	2,8673397	0,13704	
WT null-Erde	AMT1.2	24,39647	21,495012	2,9014577	0,13384	
WT null-Erde	AMT1.3	28,554327	21,495012	7,0593147	0,0075	0,0075
WT null-Erde	AMT1.3	28,679667	21,495012	7,1846547	0,00687	
WT null-Erde	AMT1.3	28,433882	21,495012	6,9388697	0,00815	
WT null-Erde	AMT 1.4	29,496967	21,495012	8,0019547	0,0039	0,004
WT null-Erde	AMT 1.4	29,409607	21,495012	7,9145947	0,00414	
WT null-Erde	AMT 1.4	29,429462	21,495012	7,9344497	0,00409	
WT null-Erde	AMT 1.5	Undetermined	21,495012	#WERT!	#WERT!	######
WT null-Erde	AMT 1.5	Undetermined	21,495012	#WERT!	#WERT!	
WT null-Erde	AMT 1.5	Undetermined	21,495012	#WERT!	#WERT!	
WT null-Erde	AMT 2.1	25,07713	21,495012	3,5821177	0,0835	0,0834
WT null-Erde	AMT 2.1	25,069227	21,495012	3,5742147	0,08396	
WT null-Erde	AMT 2.1	25,08834	21,495012	3,5933277	0,08285	
WT null-Erde	UBQ-10	21,484299	21,495012	-0,010713	1,00745	1,0025
WT null-Erde	UBQ-10	21,479961			1	
WT null-Erde	UBQ-10	21,520777			1	
WT null-Erde	nix	Undetermined			1	
RNAi 4 null-Erde	AMT1.1	21,537445	21,556625	-0,01918	1,01338	1,0184
RNAi 4 null-Erde	AMT1.1	21,569305	21,556625	0,0126803	0,99125	
RNAi 4 null-Erde	AMT1.1	21,485647	21,556625	-0,070978	1,05043	
RNAi 4 null-Erde	AMT1.2	25,798545	21,556625	4,2419203	0,05285	0,0603
RNAi 4 null-Erde	AMT1.2	25,642786	21,556625	4,0861613	0,05888	
RNAi 4 null-Erde	AMT1.2	25,412772	21,556625	3,8561473	0,06905	
RNAi 4 null-Erde	AMT1.3	30,449387	21,556625	8,8927623	0,0021	0,0021
RNAi 4 null-Erde	AMT1.3	30,230127	21,556625	8,6735023	0,00245	
RNAi 4 null-Erde	AMT1.3	30,689492	21,556625	9,1328673	0,00178	
RNAi 4 null-Erde	AMT 1.4	30,033468	21,556625	8,4768433	0,00281	0,0028
RNAi 4 null-Erde	AMT 1.4	30,315142	21,556625	8,7585173	0,00231	
RNAi 4 null-Erde	AMT 1.4	29,824484	21,556625	8,2678593	0,00324	
RNAi 4 null-Erde	AMT 1.5	Undetermined	21,556625	#WERT!	#WERT!	######
RNAi 4 null-Erde	AMT 1.5	Undetermined	21,556625	#WERT!	#WERT!	
RNAi 4 null-Erde	AMT 1.5	Undetermined	21,556625	#WERT!	#WERT!	
RNAi 4 null-Erde	AMT 2.1	25,682085	21,556625	4,1254603	0,05729	0,0518

RNAi 4 null-Erde	AMT 2.1	25,780449	21,556625	4,2238243	0,05352	
RNAi 4 null-Erde	AMT 2.1	26,040623	21,556625	4,4839983	0,04469	
RNAi 4 null-Erde	UBQ-10	21,563913	21,556625	0,0072883	0,99496	0,995
RNAi 4 null-Erde	UBQ-10	21,566986				
RNAi 4 null-Erde	UBQ-10	21,538975				
RNAi 4 full soil	nix	Undetermined				
Wasser	AMT1.1	33,700443				
Wasser	AMT1.1	Undetermined				
Wasser	AMT1.1	Undetermined				
Wasser	AMT1.2	Undetermined				
Wasser	AMT1.2	Undetermined				
Wasser	AMT1.2	Undetermined				
Wasser	AMT1.3	Undetermined				
Wasser	AMT1.3	Undetermined				
Wasser	AMT1.3	Undetermined				
Wasser	AMT 1.4	Undetermined				
Wasser	AMT 1.4	Undetermined				
Wasser	AMT 1.4	Undetermined				
Wasser	AMT 1.5	Undetermined				
Wasser	AMT 1.5	Undetermined				
Wasser	AMT 1.5	Undetermined				
Wasser	AMT 2.1	32,418076				
Wasser	AMT 2.1	Undetermined				
Wasser	AMT 2.1	Undetermined				
Wasser	UBQ-10	Undetermined				
Wasser	UBQ-10	Undetermined				
Wasser	UBQ-10	Undetermined				

Tab. 8: Expression data of Affymetrix chips obtained for the AtAMT genes at the CSB-database

Sample	At4g13510	At1g64780	At3g24300	At4g28700	At3g24290	At2g38290
cotyledons	381	151	0	1	0	112
hypocotyl	58	20	8	2	8	64
roots	175	157	203	2	203	69
shoot apex	114	32	3	1	3	80
leaves 1 + 2	221	93	0	2	0	59
veg. shoot apex	54	40	8	1	8	63
"seedling, green parts"	279	362	0	1	0	52
roots	172	90	172	1	172	78
"rosette leaf #4, 1cm"	182	43	0	1	0	86
rosette leaf # 2	553	99	1	1	1	159
rosette leaf # 4	600	99	1	1	1	189
rosette leaf # 6	669	70	0	1	0	204
rosette leaf # 8	656	51	0	0	0	167
rosette leaf # 10	628	34	0	1	0	190
rosette leaf # 12	634	23	1	1	1	157
"leaf 7, petiol"	343	7	0	0	0	158
"leaf 7, proximal half"	749	43	0	1	0	217
"leaf 7, distal half"	743	60	0	1	0	213
flowers stage 9	219	213	1	12	1	101
flowers st 10/11	240	240	0	32	0	84
flowers st 12	159	80	0	30	0	87
"flowers st 12,sepals"	333	144	0	2	0	107
"flowers st 12,petals"	82	1	0	2	0	30
"flowers st 12, stamens"	75	13	0	123	0	14
"flowers st 12,carpels"	104	4	0	2	0	118
flowers st 15	302	43	0	1	0	105

"flowers st 15,pedicels"	351	25	0	1	0	80
"flowers st 15,sepals"	480	111	0	0	0	160
"flowers stage 15, petals"	100	3	0	1	0	38
"flowers st 15,stamen"	123	1	1	1	1	34
"flowers st 15,carpels"	161	11	1	1	1	104
mature pollen	22	2	1	91	1	11
"siliques, w/seeds st 2"	144	15	3	1	3	53
"siliques, w/seeds st 3"	150	32	0	2	0	41
"siliques, w/seeds st 4"	102	63	4	1	4	29
"siliques, w/ seeds stage 5"	108	36	3	1	3	32
"seeds,st 6, w/o siliques"	35	1	0	1	0	11
"seeds,st 7, w/o siliques"	49	2	0	0	0	17
"seeds, st 8, w/o siliques"	50	1	1	1	1	10
"seeds, st 9,w/o siliques"	85	1	0	1	0	23
"seeds, st 10,w/o siliques"	82	1	0	1	0	22
veg rosette	125	157	6	0	6	44
veg rosette	120	46	1	1	1	80
veg rosette	121	19	2	1	2	81
leaf	174	59	1	2	1	70
root	533	520	379	1	379	115
flower	178	143	0	73	0	92
root	557	601	249	2	249	84
"seedling, green parts"	482	73	2	1	2	228
root	524	432	378	4	378	100

Tab. 9: 14C-MA uptake data for 10 and 50µM, uptake experiments performed with WT and RNAi lines,

10µM				50 µM			
cpm at start: 13269	time (min)	FW	CPM	13391	time (min)	FW	CPM
Col-0	5	44	11744	Col-0	5	41,7	11120
Col-0	5	42	10204	Col-0	5	40,1	11423
Col-0	5	46	10704	Col-0	5	42,2	11335
line 4	5	48	11301	line 4	5	45,7	12084
line 4	5	44	11495	line 4	5	43,4	12561
line 4	5	41	12312	line 4	5	47,3	12615
line 84-3	5	45	11078	line 84	5	41,2	12171
line 84-3	5	47	11773	line 84	5	43,3	11319
line 84-3	5	44	12067	line 84	5	45,4	12050
line 50 s	5	48	11715	line 50	5	42,1	12736
line 50 s	5	43	11589	line 50	5	46,3	12743
line 50 s	5	46	10740	line 50	5	43,1	12721
Col-0	10	44	11343	Col-0	10	41,7	11133
Col-0	10	42	10216	Col-0	10	40,1	11802
Col-0	10	46	9968	Col-0	10	42,2	11138
line 4	10	48	11137	line 4	10	45,7	11421
line 4	10	44	11587	line 4	10	43,4	12590
line 4	10	41	12048	line 4	10	47,3	12149
line 84	10	45	10721	line 84	10	41,2	11404
line 84	10	47	11443	line 84	10	43,3	11296
line 84	10	44	11581	line 84	10	45,4	12097
line 50	10	48	11089	line 50	10	42,1	12416
line 50	10	43	10753	line 50	10	46,3	12435
line 50	10	46	10690	line 50	10	43,1	12784

Col-0	20	44	9914	Col-0	20	41,7	9656
Col-0	20	42	8307	Col-0	20	40,1	10977
Col-0	20	46	8087	Col-0	20	42,2	10430
line 4	20	48	10955	line 4	20	45,7	11872
line 4	20	44	11247	line 4	20	43,4	11477
line 4	20	41	12049	line 4	20	47,3	11852
line 84	20	45	10535	line 84	20	41,2	11401
line 84	20	47	11016	line 84	20	43,3	10967
line 84	20	44	11207	line 84	20	45,4	11427
line 50	20	48	10154	line 50	20	42,1	11577
line 50	20	43	9294	line 50	20	46,3	11153
line 50	20	46	9918	line 50	20	43,1	11765
Col-0	40	44	5852	Col-0	40	41,7	7335
Col-0	40	42	4218	Col-0	40	40,1	7706
Col-0	40	46	3968	Col-0	40	42,2	5829
line 4	40	48	10350	line 4	40	45,7	10577
line 4	40	44	9907	line 4	40	43,4	10451
line 4	40	41	11681	line 4	40	47,3	10220
line 84	40	45	6276	line 84	40	41,2	9127
line 84	40	47	9244	line 84	40	43,3	7515
line 84	40	44	9062	line 84	40	45,4	7926
line 50	40	48	8851	line 50	40	42,1	10853
line 50	40	43	5650	line 50	40	46,3	9889
line 50	40	46	6992	line 50	40	43,1	9737
Col-0	60	44	4872	Col-0	60	41,7	3695
Col-0	60	42	3580	Col-0	60	40,1	5219
Col-0	60	46	1818	Col-0	60	42,2	2406
line 4	60	48	9308	line 4	60	45,7	10029
line 4	60	44	7998	line 4	60	43,4	10278
line 4	60	41	9868	line 4	60	47,3	8361
line 84	60	45	4381	line 84	60	41,2	8004
line 84	60	47	7848	line 84	60	43,3	6860
line 84	60	44	7071	line 84	60	45,4	4788
line 50	60	48	6831	line 50	60	42,1	9322
line 50	60	43	3521	line 50	60	46,3	8210
line 50	60	46	4247	line 50	60	43,1	6851
Col-0	120	44	1226	Col-0	120	41,7	854
Col-0	120	42	568	Col-0	120	40,1	2537
Col-0	120	46	514	Col-0	120	42,2	529
line 4	120	48	5402	line 4	120	45,7	7010
line 4	120	44	4435	line 4	120	43,4	7890
line 4	120	41	5520	line 4	120	47,3	7091
line 84	120	45	1478	line 84	120	41,2	5576
line 84	120	47	3125	line 84	120	43,3	3773
line 84	120	44	3191	line 84	120	45,4	2954
line 50	120	48	1607	line 50	120	42,1	6327
line 50	120	43	737	line 50	120	46,3	4456
line 50	120	46	723	line 50	120	43,1	5192

Tab. 10: 14C-MA uptake data for 200 µM and 1 mM; uptake experiments performed with WT and RNAi lines

	200µM MA	**Start CPM: 6641**		1 mM MA	Start CPM:	**12843**
	time (min)	fresh weight (mg)	14C CPM	time (min)	fresh weight (mg)	14C CPM
Col-0	5	49,6	6136	5	45	11022
Col-0	5	48,3	5452	5	46,8	11113
Col-0	5	53,1	5791	5	46,3	11412
line 4	5	51,6	6229	5	45,9	12345
line 4	5	46,3	6183	5	48,9	12162
line 4	5	47,1	5923	5	43,7	12555
line 84-3	5	54,9	6118	5	46,5	12448
line 84-3	5	52	5907	5	45,4	12514
line 84-3	5	53,7	6047	5	46,2	12311
line 50	5	49,6	5983	5	44,6	12048
line 50	5	44,8	5877	5	45,3	11709
line 50	5	48,5	6056	5	47,7	12194
Col-0	10	49,6	5891	10	45	10936
Col-0	10	48,3	5140	10	46,8	10651
Col-0	10	53,1	5565	10	46,3	11035
line 4	10	51,6	6205	10	45,9	12423
line 4	10	46,3	5932	10	48,9	11625
line 4	10	47,1	5823	10	43,7	12199
line 84-3	10	54,9	6112	10	46,5	12304
line 84-3	10	52	6002	10	45,4	11889
line 84-3	10	53,7	5881	10	46,2	11929
line 50	10	49,6	5387	10	44,6	12210
line 50	10	44,8	5564	10	45,3	11718
line 50	10	48,5	5913	10	47,7	11935
Col-0	20	49,6	5861	20	45	11291
Col-0	20	48,3	4981	20	46,8	10653
Col-0	20	53,1	5209	20	46,3	10824
line 4	20	51,6	6247	20	45,9	12432
line 4	20	46,3	5776	20	48,9	11900
line 4	20	47,1	5714	20	43,7	12583
line 84-3	20	54,9	5881	20	46,5	12295
line 84-3	20	52	5545	20	45,4	12708
line 84-3	20	53,7	5470	20	46,2	12113
line 50	20	49,6	5837	20	44,6	12187
line 50	20	44,8	5433	20	45,3	11806
line 50	20	48,5	5110	20	47,7	12148
Col-0	40	49,6	5119	40	45	10807
Col-0	40	48,3	4840	40	46,8	10484
Col-0	40	53,1	4886	40	46,3	10671
line 4	40	51,6	6096	40	45,9	12227
line 4	40	46,3	5378	40	48,9	12392
line 4	40	47,1	5553	40	43,7	12346
line 84-3	40	54,9	5645	40	46,5	12859
line 84-3	40	52	5253	40	45,4	12476
line 84-3	40	53,7	5154	40	46,2	12505
line 50	40	49,6	5502	40	44,6	11959
line 50	40	44,8	5831	40	45,3	12430
line 50	40	48,5	4778	40	47,7	12075
Col-0	60	49,6	3971	60	45	10904

Col-0	60	48,3	4382	60	46,8	9953
Col-0	60	53,1	4233	60	46,3	10248
line 4	60	51,6	6108	60	45,9	12517
line 4	60	46,3	4957	60	48,9	11775
line 4	60	47,1	5588	60	43,7	13096
line 84-3	60	54,9	5359	60	46,5	13080
line 84-3	60	52	4892	60	45,4	13654
line 84-3	60	53,7	4607	60	46,2	12935
line 50	60	49,6	5063	60	44,6	12143
line 50	60	44,8	5842	60	45,3	12481
line 50	60	48,5	4436	60	47,7	12354
Col-0	120	49,6	1399	120	45	9526
Col-0	120	48,3	1965	120	46,8	8122
Col-0	120	53,1	2060	120	46,3	10905
line 4	120	51,6	4885	120	45,9	12135
line 4	120	46,3	4784	120	48,9	11385
line 4	120	47,1	4292	120	43,7	14111
line 84-3	120	54,9	3277	120	46,5	14579
line 84-3	120	52	3041	120	45,4	14182
line 84-3	120	53,7	3318	120	46,2	14265
line 50	120	49,6	4050	120	44,6	13693
line 50	120	44,8	3354	120	45,3	12582
line 50	120	48,5	3696	120	47,7	11879
				180	45	6974
				180	46,8	6638
				180	46,3	8193
				180	45,9	13797
				180	48,9	10851
				180	43,7	12692
				180	46,5	14471
				180	45,4	16014
				180	46,2	13729
				180	44,6	13326
				180	45,3	12401
				180	47,7	12466

Tab. 11: 14C-MA uptake data for 2 mM, uptake experiments performed with WT and RNAi lines (Start CPM: 13240).

	time (min)	FW	CPM	min	FW	CPM
Col-0	5	45	11022	60	45	10904
Col-0	5	46,8	11113	60	46,8	9953
Col-0	5	46,3	11412	60	46,3	10248
line 4	5	45,9	12345	60	45,9	12517
line 4	5	48,9	12162	60	48,9	11775
line 4	5	43,7	12555	60	43,7	13096
line 84-3	5	46,5	12448	60	46,5	13080
line 84-3	5	45,4	12514	60	45,4	13654
line 84-3	5	46,2	12311	60	46,2	12935
line 50 s	5	44,6	12048	60	44,6	12143
line 50 s	5	45,3	11709	60	45,3	12481

line 50 s	5	47,7	12194	60	47,7	12354
Col-0	10	45	10936	180	45	6974
Col-0	10	46,8	10651	180	46,8	6638
Col-0	10	46,3	11035	180	46,3	8193
line 4	10	45,9	12423	180	45,9	13797
line 4	10	48,9	11625	180	48,9	10851
line 4	10	43,7	12199	180	43,7	12692
line 84	10	46,5	12304	180	46,5	14471
line 84	10	45,4	11889	180	45,4	16014
line 84	10	46,2	11929	180	46,2	13729
line 50	10	44,6	12210	180	44,6	13326
line 50	10	45,3	11718	180	45,3	12401
line 50	10	47,7	11935	180	47,7	12466
Col-0	20	45	11291	120	45	9526
Col-0	20	46,8	10653	120	46,8	8122
Col-0	20	46,3	10824	120	46,3	10905
line 4	20	45,9	12432	120	45,9	12135
line 4	20	48,9	11900	120	48,9	11385
line 4	20	43,7	12583	120	43,7	14111
line 84	20	46,5	12295	120	46,5	14579
line 84	20	45,4	12708	120	45,4	14182
line 84	20	46,2	12113	120	46,2	14265
line 50	20	44,6	12187	120	44,6	13693
line 50	20	45,3	11806	120	45,3	12582
line 50	20	47,7	12148	120	47,7	11879
Col-0	40	45	10807			
Col-0	40	46,8	10484			
Col-0	40	46,3	10671			
line 4	40	45,9	12227			
line 4	40	48,9	12392			
line 4	40	43,7	12346			
line 84	40	46,5	12859			
line 84	40	45,4	12476			
line 84	40	46,2	12505			
line 50	40	44,6	11959			
line 50	40	45,3	12430			
line 50	40	47,7	12075			

Danksagung

Ich möchte mich bei Dr. Michael Udvardi für die Überlassung des Themas dieser Arbeit bedanken und möchte ihm weiterhin ausdrücklich für die Ratschläge, die in diese Arbeit eingeflossen sind, danken.

Weiterhin möchte ich Craig Wood für die Betreuung während unserer Zeit am MPI in Golm danken und für die darüber hinausgehende Unterstützung während seiner Zeit am CSIRO in Australien. Seine Hilfsbereitschaft, Hinweise und sein Optimismus haben immer geholfen.

Ebenso möchte ich Lothar Willmitzer für die Betreuung meiner Arbeit danken und dafür, dass er immer ein offenes Ohr für die Sorgen und Nöte einer Doktorarbeit hat, und im gleichen Maß Geduld wie Verständnis.

Zuletzt möchte ich den Gärtnern und insbesondere Torsten Schulze für die Versorgung und Betreuung meiner vielen mutanten und wilden Pflanzen danken, und dass er mich nie gefragt hat, warum schon wieder neue Linien ausgesäht werden. RNAi ist oft nicht vorhersehbar, besonders in der 3. Generation. In diesem Zusammenhang möchte ich auch Maria für ihre Hilfe im Labor danken. Mit ihren Fähigkeiten und ihrer Begabung schaffte sie es, ein Jahr auf ein paar Wochen zu verkürzen.

Und dann danke ich natürlich auch allen anderen hier am MPI für die gute Stimmung und die vielen kleinen Hilfen und Gesten. Die Atmosphäre war immer gut, auch wenn man den Blick dafür manchmal verliert.